Modelling global fresh surface water temperature

Tessa Eikelboom
MSc Thesis Physical Geography
May 2010
Supervisors: Dr. L.P.H. van Beek and Prof. Dr. Ir. M.F.P. Bierkens

Universiteit Utrecht

Department of Physical Geography
Faculty of Geosciences
Utrecht University

ABSTRACT

A change in fresh surface water temperature influences biological and chemical parameters such as oxygen and nutrient availability, but also has major effects on hydrological and physical processes which include transport, sediment concentration, ice formation and ice melt. The thermal profile of fresh surface waters depends on meteorological and morphological characteristics. Climate change influences the water and energy budget and thereby also the thermal structure of fresh surface waters. The oceans temperature is influenced by the inflow of rivers and streams. The variations in fresh surface water temperatures are only known for a scarce amount of long term temperature records. The understanding of changes in thermal processes by modelling the variations in temperature over time is therefore very useful to simulate the global effect of climate change on water temperatures.

A physical based model was validated with regional daily and global monthly water temperature data of fresh surface water which includes both rivers and lakes. The basic assumption for the PCR-GLOBWB model is the assumption that the fresh surface water temperature is the net result of all incoming en outgoing fluxes. The global hydrological model PCR-GLOBWB contains a water and heat budget. The heat balance is solved using the following terms: short-wave insolation, long-wave atmospheric radiation, water-surface backscatter, evaporation, air/water conduction and can be simplified into lateral and advective energy. The water budget exists of precipitation, surface and subsurface runoff, ice thickness, evaporation, discharge and groundwater flow.

Lakes are different from rivers due to stratification. Therefore a stand-alone lake model (Flake) that only uses lake depth, transparency, wind fetch and meteorological data to simulate lake mixing, is validated with four major lakes in North America.

The global performance of the physical model for both lakes and rivers was analysed for the climatology over the year and for 267 stations located in different climates around the world with global monthly data for the period 1973-2002. A timeseries analysis was done with daily data for 15 stations in North America. The results of temperature simulation for fresh surface lakes suggest that the FLake model and the model PCR-GLOBWB perform equally. Indeed, the FLake model suggests a high performance for medium sized lakes and the advantages of FLake are that it needs just few parameters that can be derived relatively easy and it also requires very few calculation time to run the model. It is expected that coupling of the two models will improve the model results for lakes and rivers downstream of lakes.

The results of temperature simulation for fresh surface lakes suggest that both the FLake model and the model PCR-GLOBWB perform well. When comparing the two models, PCR-GLOBWB in general over- and underestimates the peaks in summer and in winter, whereas FLake underestimates the maximum summer temperatures. The advantages of FLake are that it needs just few parameters that can be derived relatively easy and it also requires very few calculation time to run the model. The FLake model suggests a high performance for medium sized lakes and. Coupling of the two models combines the advective energy fluxes and mixing processes and is therefore theoretically preferred.

Based on the monthly data, the results for the yearly pattern are statistically very reliable and suggest a high predictability of the model. When concentrating on climates, it is more difficult to simulate the colder regions. The model performs poorest for these regions, but on the other hand performs very well for warmer climates like the tropical forests. The same result applies to the largest rivers, where the temperature and discharge of colder rivers like the Amur, Ob and the Lena are underestimated.

Next to the monthly pattern, also a comparison to daily data reveals reliable results. The stations with daily observed temperatures that are located in North America were very different in size and this was also reflected in the results. Several stations along the same river show different results, but the overall result shows that the daily pattern of the observations were reflected in the simulations.

The model can be improved with a calibration that especially focuses on the colder regions. The model results give the possibility to apply a climate scenario to predict future fresh water temperatures globally or for a specific region like the inflowing rivers of the Arctic Ocean.

The differences between water and air temperature over the year and for different climates show where and when transport of heat by rivers is important. The mapped locations confirm the need for a hydrological model for water temperature as it is not sufficient to assume that the fresh surface waters have the same temperature as the air temperature. This research shows how a physical model can be used to model the complex relations between water and atmosphere. The model can be used for a wide range of analyses and the results can be used for a broad range of disciplines.

ACKNOWLEDGEMENT

This master research on modelling fresh water surface temperatures is part of the master study Physical Geography. The research is undertaken at the department Physical Geography at the Utrecht University and is supervised by dr. L.P.H. van Beek and Prof dr. Ir. M.F.P. Bierkens. This is done in collaboration with research done by M. v. Vliet, PhD student at Wageningen University on the impact of climate change and its induced changes in river flow on surface water temperatures, and associated consequences for freshwater ecosystems and public utilities, which is part of the FP6 Water and Global Change (WATCH) EU project.

TABLE OF CONTENTS

Abstract 2

Acknowledgement 3

Table of contents 4

List of Tables 7

List of Figures 8

List of Maps 9

1. Introduction 10

1.1 Background 10

1.2 Problem description 10

1.3 Research objectives 10

1.4 Study Area 11

1.5 Structure report 11

2. Literature overview 12

2.1 Introduction 12

2.2 Fresh surface waters 13

2.2.1 Rivers 13

2.2.2 Lakes 14

2. 3 Water Temperature Models 16

2.3.1 Introduction 16

2.3.2 Lake models 16

2.3.3 FLake model 17

Model description 17

The Concept of Self-Similarity of the Temperature Profile 17

Model parameters 19

Sensitivity analysis 19

2.3.4 River models 21

2.3.5 PCR-GLOBWB 22

Model description 22

Model parameters 23

3. Method 24
3.1 Introduction 24
3.2 Model validation 24
3.3 Data 26
3.3.1 Data quality 27
3.4 Description study area 28
3.4.1 Description lakes 28
3.5.2 Description rivers 29
3.5 Parameters 31
3.5.1 Depth 31
3.5.2 Wind fetch 31
3.5.3 Transparency 31
3.5.4 Meteorological data 34
4. Results 35
4.1 Introduction 35
4.2 Discharge 35
4.3 Comparison of results PCR-GLOBWB and FLake for the Great Lakes 37
4.3 Climatology GEMS stations for different months 39
4.4 Climatology of GEMS stations for different climates 40
4.5 Statistics for largest rivers 42
4.6 Daily data of USGS stations 43
4.7 Difference between water and air temperature 48
5. Discussion 51
6. Conclusion 52
Literature 53
Appendix IA 55
Appendix IB 59
Appendix IIA 60
Appendix IIB 61
Appendix III 62
Appendix IV 66

Appendix V 71

Appendix VI 76

Appendix VII 78

Appendix VIII 80

LIST OF TABLES

Table 1 World's largest rivers (in terms of discharge) (Dingman, 1994)..... 14

Table 2 World's largest lakes (Dingman, 1994)..... 14

Table 3 Overview of lake models..... 16

Table 4 Overview of stream temperature models (modified from: Norton and Bradford, 2009)..... 21

Table 5 Datacheck of GEMS statistics..... 27

Table 6 Long term river data for the period 1975-2004..... 29

Table 7 Statistics of GEMS mean averge discharge..... 36

Table 8 Statistics of the Great Lakes for FLake and PCR-GLOBWB..... 38

Table 9 Results FLake simulation and observation of four lakes..... 39

Table 10 Statistics of GEMS mean average temperature..... 40

Table 11 Statistics of GEMS average temperature for different climates..... 40

Table 12 The relative drainage area error and statistics for largest rivers for the average temperature and average discharge..... 42

Table 13 Coverage, Drainage error, Spearman correlation (ρ) and statistics of USGS stations..... 43

LIST OF FIGURES

Figure 1 Global pools and fluxes of water on Earth, showing the magnitude of groundwater storage relative to other major water storages and fluxes (Alley et al., 2002). 13

Figure 2 River heat exchange processes (Caissie, 2006). 13

Figure 3 Sketch illustrating possible mixing mechanisms operating in a lake subject to a sudden wind stress (Spigel and Imberger, 1987). 15

Figure 4 Schematic representation of the temperature profile in the upper mixed layer and in the thermocline (Mironov, 2008). 18

Figure 5 Schematic representation of the temperature profile in the mixed layer, in the thermocline, and in the thermally active layer of bottom sediments (Mironov, 2008)..... 18

Figure 6 Development of average surface temperature for increasing extinction coefficient, lake depth, wind fetch and change in air temperature..... 20

Figure 7 Model concept: on the left, the soil compartment, divided in the two upper soil stores and the third groundwater store and their corresponding drainage components of direct runoff (QDR), interflow (QSf) and base flow (QBf). In the centre, the resulting discharge along the channel (QChannel) with lateral in- and outflow and local gains and losses are depicted, on the right the energy balance for the fresh water surface and the possible formation of ice (Van Beek, 2008)..... 22

Figure 8 Map of the Great Lakes Basin (Natural resources Canada, 2003). 28

Figure 9 Boxplot of the extinction coefficient for different mixing types.....33

Figure 10 Boxplot of the extinction coefficient for different climates.....33

Figure 11 Relation mean lake depth and extinction coefficient on a logaritmic scale (n=211) 34

Figure 12 Simulated and observed discharge for January and August. Each symbol reflects a different climate..... 36

Figure 13 Relation simulated and observed temperature for the great lakes over 1960-1990 with FLake (left) and with PCR-GLOBWB (Right) (x=simulated temperature in degrees celcius and y=observed temperature in degrees celcius).....37

Figure 14 Simulated and observed water temperature for January and August. Each symbol reflects a different climate 38

Figure 15 Relation between simulated and observed temperature for all GEMS stations for the period 1975-2004..... 39

Figure 16 Boxplot of the Relative standard error for different climates.....40

Figure 17 Simulated and observed water temperature for January and August. Each symbol reflects a different climate.....41

Figure 18 Relation simulated and observed temperature for the USGS stations for 1975-2002 (x=simulated tempreature (degrees Celcius, y=observed temperature (degrees Celcius)).....45

Figure 19 Residuals for the USGS rivers (x=simulated temperature in degrees Celcius, y=observed-simulated temperature).....47

Figure 20 Difference between water and air temperature for each month for all GEMS stations split up over the different climates.....48

LIST OF MAPS

Map 1 Global fresh surface waters (Lehner and Döll, 2004) 11

Map 2 Lakes of the ILEC database. 28

Map 3 GEMS stations 29

Map 4 Locations with long-term river data in Northern America. 30

Map 5 Transparency 32

Map 6 Δavg (degrees celcius) and tavg (kelvin) for winter and summer 1975 and 2000 49

Map 7 Negative difference between water and air temperature in summer 50

Map 8 Positive difference between water and air temperature in summer 50

Map 9 River temperature anomalies relative to their surrounding in August 2000 in kelvin 50

Map 10 Heat transport in the river Nile in January 2000 in kelvin 50

1. INTRODUCTION

1.1 BACKGROUND

Water temperature has a strong influence on many physical and chemical characteristics of water, which include vapour pressure, surface tension, density and viscosity, the solubility of oxygen and other gases, sediment concentration and transportation, chemical reaction rates and the presence or absence of pathogens. For ecology the geographical distribution, growth and metabolism, food and feeding habits, reproduction and life histories, movements and migrations, behaviour and tolerance to parasites, diseases and pollution are affected by the thermal regime (Webb, 1996). A change in water temperature of surface waters can influence water quality factors such as pH, Nitrogen, Phosphor, Phytoplankton and Zooplankton, Dissolved oxygen and Chloride (Rounds *et al.*, 1999).
There is consensus about the increase in air temperature over the last years due to climate change. In this research the relative effect of this warming of the air temperature on the water temperature is investigated. It is expected that there is a different effect on upstream water that is fed by melt water and downstream water that is heated by the sun. Due to global warming more melt water will feed the surface waters. Melt water has a temperature of around the freezing point. The attribution of this cold water leads to lower water temperatures in upstream regions, whereas downstream the increase in air temperature and solar radiation leads to heating of the surface waters. Also a difference between surface waters is expected. Rivers react differently to climate change than lakes. The surface water layer of a lake is heated easily, whereas the deep water of a lake responds slowly to climate variability. Next, there is the temporal variation like seasonal effects and interannual variability. Spatial variability can be caused by differences in properties like topography, morphology, vegetation and human impact.
The fresh surface water temperature can be derived by integrating the different energy contributors of the contributing water fluxes into the surface water of interest: groundwater, precipitation, (surface) runoff, tributaries, discharge from upstream and the interaction with the atmosphere.

1.2 PROBLEM DESCRIPTION

Climate change affects water temperature, but the amount and variation in changes of fresh surface water temperature (ΔT) over time (and space) that has effects on ecology, marine sea ice and chemical processes is unknown. Differences and variations in fresh surface water temperatures can be explained by different variables related to advective energy like radiation (location on earth, time of the year), topography, and the regional climate (temperature, precipitation, evaporation etc.). Other influencing factors that are not considered in the model are land use, morphology (stream velocity), sun exposure and the effect of shading by vegetation. Various sources explain that water temperature is not the same as air temperature. It is therefore relevant to use the available records to model global fresh surface water temperatures when modelling the aquatic ecological effects of climate change instead of assuming the air temperature.
Fresh surface water temperature can be seen as a measure of the amount of heat energy per unit volume of water changing either the amount of heat entering the stream, river (or lake) or the amount of water, and has the potential to alter stream temperature.

1.3 RESEARCH OBJECTIVES

The aim of this research was the simulation of temporal variations in global fresh water surface temperature by modelling the temperature to predict variability in space and time. Hydrological processes differ for both rivers and lakes. Therefore the aim was to validate an existing global hydrological model (PCR-GLOBWB) and a so called 'lake module'. The goal of validating a lake module was to explore how the prediction of downstream fresh surface water temperatures by including the thermal behaviour of lakes improves the simulations. Also lakes cover a major part of the total fresh surface waters. By taking into account the changes in the thermal profile of a lake over the seasons and changes in temperature with depth over time will contribute to an overall improved estimation of fresh surface water temperatures.
As the main objective of the study was to develop a deterministic fresh surface water temperature model to predict fresh surface water temperatures the following specific and test objectives were pursued: i) to collect long scale global data of rivers and lakes , ii) to evaluate a stand-alone lake module and perform a sensitivity analysis, iii) to model global surface temperatures with PCR-GLOBWB, iv) to validate the model PCR-GLOBWB with global data and test the performance to simulate the spatial and temporal variations in fresh water surface temperatures.

First data was collected, analysed and prepared for both models. A study period of several decades was chosen as the purpose of the model is to simulate water temperature for long term periods. Validation with long term records was therefore required. On the other hand larger datasets require more computational capacity and older data is less reliable. Also not only water temperature was needed, but also meteorological data. A modelling period of 29 years (1973-2002) was applied to PCR-GLOBWB and monthly and daily data was collected for the period 1975-2000. The model FLake was validated against temperature measurements of 1960-1990 from the NOAA database for 4 lakes and the model PCR-GLOBWB was validated against discharge and water temperature measurements of 1973-2002 on a monthly timescale for 267 global GEMS stations and against daily water temperature for 15 USGS stations located in Northern America

1.4 Study Area

As the main goal of this research was to develop a global model, the study area covers all major fresh surface waters on the globe. For daily validation of the model the study area was reduced to Northern America. Statistical monthly data of different streams and rivers cover a much wider range of areas all over the world and data for a number of the greatest lakes of the world were searched for in articles and in online databases. The number of lakes that are taken into account depends on the scale of the model. In this case this is 0.5° x 0.5°. This contributes to an amount of about 10,000 lakes. From the GLWD dataset only 3721 lakes were available. The study area is described in more detail in 3.4.

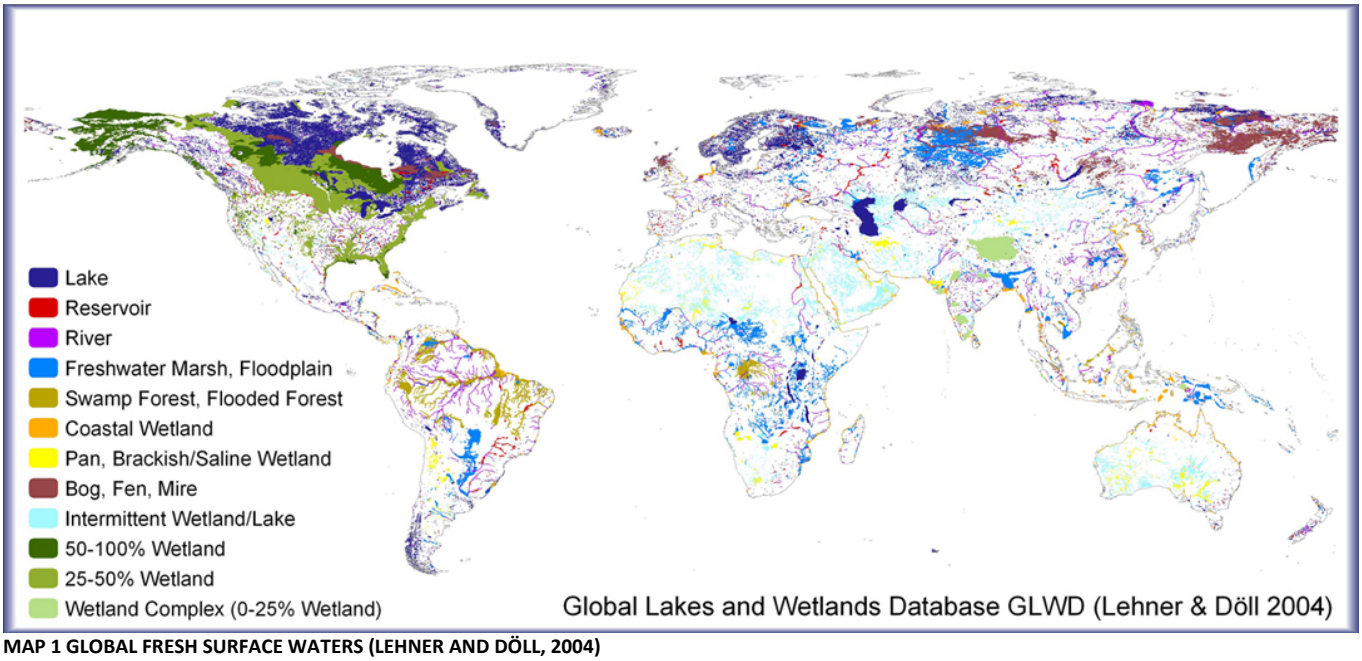

MAP 1 GLOBAL FRESH SURFACE WATERS (LEHNER AND DÖLL, 2004)

1.5 Structure report

The first part of the second chapter describes the background information that forms the basis of this research. The second part of chapter 2 shows the current variety of temperature models and explains the models used to model global fresh surface water temperature. The method, parameterization and data acquisition is described in chapter 3. The model results are shown in chapter 4 where the model is validated. The outcomes are discussed in chapter 5 and in the conclusion the feasibility of a physical model to simulate temperatures is presented. The annexes show more detailed figures and tables with data and results.

2. LITERATURE OVERVIEW

2.1 INTRODUCTION

Fresh surface water temperature is an important environmental variable that is coupled to the main biological and chemical processes in aquatic ecosystems. The thermal regime of rivers is highly influenced by meteorological and river conditions as well as by their geographical setting. There is a growing interest over the last two decennia in the thermal behaviour of fresh surface waters. Recent monitoring, modelling and research have facilitated a collection of information that attributes to the understanding of the fundamental fluxes controlling water temperature behaviour (Webb *et al*., 2008). For state of the art overviews of the thermal behaviour of streams and rivers we refer to Caissie (2006) and Webb *et al.* (2008).
In current research there is a broad consensus that the climate is changing under anthropogenic influences. As a result more and more research show increasing temperature trends in long-term stream and river temperature (Webb, 1996; Webb *et al*., 2008). Also for lakes and reservoirs there is evidence of warming, like for Lake Tahoe over the period 1970-2002 (Coats *et al.*, 2006). Most of the variations in stream water temperatures occur during the summer months due to a combination of a number of variables (depth of water, cloud cover, solar radiation, low flows, etc.). In general discharge is low and solar radiation and air temperature is high. This leads to increased evaporation that works as a buffer as it leads to cooling. The enhanced evaporation causes lower water levels and lower water levels lead to threats. Economically these are transport and fishery. Reduced water transport occurs, because ships can not travel along the water course at very low water levels or ships can not be fully loaded. Fishery is threatened by low water levels and by the disturbance of the ecosystem and thereby the number of micro-organisms that enhances the effect of high nutrient and low oxygen availability. The thermal regime of rivers is such that the water temperatures change on a daily to seasonal basis. Temperature also varies spatially along river reaches. The natural process of heating and cooling of rivers is highly dependent on meteorological conditions and physical characteristics of rivers. High stream temperatures can occur naturally or as a result of human impacts.
Anthropogenic perturbations can be the result of thermal pollution due to water cooling by industries, reductions in river flow, water releases to river from dams/reservoirs upstream, deforestation and climate change. Timber harvesting has significant influence on water temperature due to clear cutting around and close to rivers. The highest increase in water temperature is found due to the removal of vegetation directly from the river banks, which eliminates river protection by shading (Caissie *et al*., 2001). Also there is an inverse effect of micro-organisms on temperature by the modification of light penetration by the biomass and size distribution of plankton. Lakes with similar size, but greater water clarity, will have deeper mixing depths and greater heat content (Mazumber *et al.*, 1990). The warming of water is compensated by evaporation (latent heat) and sensible heat. The former is especially relevant for lakes.
Water temperature is directly or indirectly influenced by human activities in the stream corridor and surrounding watersheds. In particular, urban areas can affect stream temperature in numerous ways, including waste water discharges, urban runoff, reduced baseflows, in-stream impoundments (a body of water, such as a reservoir) and development of riparian areas(Relating to or inhabiting the banks of a natural course of water). Riparian zones are ecologically diverse and contribute to the health of other aquatic ecosystems by filtering out pollutants and preventing erosion areas (Norton and Bradford, 2009). In ecological terms, water temperature is responsible for the health of the ecosystem. It determines growth rate and distribution, because most aquatic organisms have a specific range of temperatures that they can tolerate. Increase in biological activity rates can become problematic where dissolved oxygen is already depleted due to high water temperature. Depending on its severity, increase in water temperature can lead to extinction of some aquatic species or dramatically modify their distribution within river systems. To protect the environment governments have set limits to the maximum temperature of surface waters. For the Netherlands, the Environmental Health Agency (Rijksinstituut voor volksgezondheid en milieu, RIVM) recommends a standard maximum temperature for a Healthy Ecological Status for Dutch rivers of 25 °C (Grinten *et al*., 2007).
Water temperature is inversely related to river discharge, which reflects the reduction in thermal capacity of a water course as the flow volume decreases. Several management strategies to lower water temperature are also based on increasing discharge. There is an expected relation between the travel time and the temperature of the water. Higher stream velocity leads to lower water temperature and a long travel time leads to heating of the water and thus to higher temperatures. Water temperature also depends on the amount of water in the water system that is fed by groundwater. Groundwater in general has a lower temperature compared to surface water.

2.2 FRESH SURFACE WATERS

The fresh surface waters are part of the global hydrological cycle and play an important role in the functioning of the earth. The exchange of water between land en oceans is 40,000 km^3 per year. The other fluxes are shown in figure 1. Streams with over one percent of the total flux are shown in table 1. The greatest river accounts for one sixth of the total flux and the ten greatest rivers together account for one third of the total discharge flux.

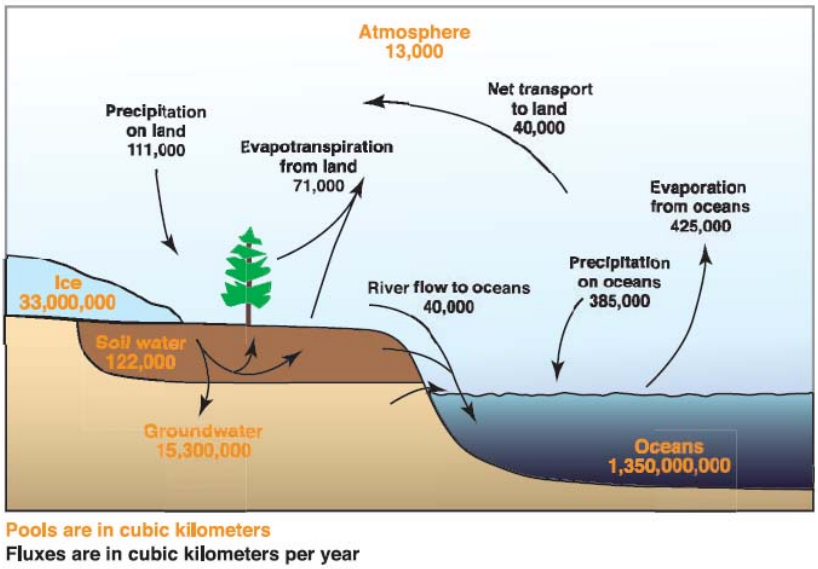

FIGURE 2 GLOBAL POOLS AND FLUXES OF WATER ON EARTH, SHOWING THE MAGNITUDE OF GROUNDWATER STORAGE RELATIVE TO OTHER MAJOR WATER STORAGES AND FLUXES (ALLEY ET AL., 2002).

2.2.1 RIVERS

There are a lot of different types of rivers with specific characteristics. Factors that influence the thermal regime of rivers are topography, atmospheric conditions, stream discharge and the stream bed. The instantaneous balance between inputs, storage and outputs is reflected in the heat content of river water. The energy budgets are dominated by solar, atmospheric and back radiation terms. Heat input includes short wave solar radiation, long-wave radiation and advection of heat from ground water, upstream and tributary inflows. Heat energy is lost by reflection of radiation, evaporation and outflow of the stream. Also energy is lost or gained by convection and by conduction to or from the atmosphere, stream bed and stream banks. Most of the solar radiation is directly absorbed by lake water. Heat transfer along the sediment is small for deep and moderate lakes. Heat loss by thermal conductance is predominantly a surface phenomenon, because of the low thermal conductivity of water. Specific conduction indeed leads to losses to the air and for a smaller amount to the sediments. Also heat is lost due to long wave radiation.

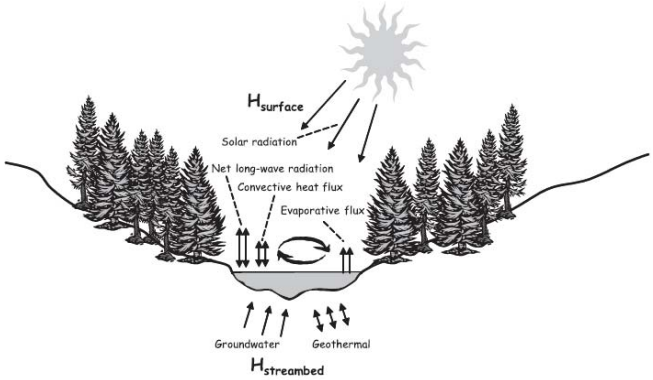

FIGURE 3 RIVER HEAT EXCHANGE PROCESSES (CAISSIE, 2006).

River	Drainage Area (10^3 km^2)	Discharge (m^3/s)
Amazon	7180	190,000
Congo	3822	42,000
Yangtzekiang	1970	35,000
Orinoco	1086	29,000
Brahmaputra	589	20,000
La Plata	2650	19,500
Yenesei	2599	17,800
Mississippi	3224	17,700
Lena	2430	16,300
Mekong	795	15,900
Ganges	1073	15,500
Irrawaddy	431	14,000
Ob	2950	12,500
Sikiang	435	11,500
Amur	1843	11,000
Saint Lawrence	1030	10,400

TABLE 1 WORLD'S LARGEST RIVERS (IN TERMS OF DISCHARGE) (DINGMAN, 1994).

The largest rivers are shown in table 1.

2.2.2 LAKES

The total volume of all lakes on earth is 280,000 km^3 from which 150,000 km^3 is contained in fresh water lakes, 5000 km^3 in Reservoirs and 125,000 km^3 in salty lakes (Dingman, 1994).

Lake	Average depth (m)	Area (km^2)
Caspian sea	190	371,800
Lake superior	***149***	***82,400***
Lake Victoria	42	69,500
Aral sea[a]	14	65,500
Huron	***59***	***59,600***
Michigan	***85***	***58,000***
Tanganyika	1200	32,900
Great Bear	20	31,800
Baikal	1741	30,500
Nyasa	292	29,600
Great slave	16	28,400
Erie	***18***	***25,700***
Winnipeg	12	24,500
Ontario	0.4	19,700
Ladoga	16	17,700
Balkhash	1.9	17,400
Chad[b]	1.4	16,300
Bangweulu	4	9,800
Onego	28	9,600
Titicaca	67	8,300
Athabasca	26	8,100
Nicaragua	13	8,000
Eyre	3	7,700
Turkana	30	6,400

TABLE 2 WORLD'S LARGEST LAKES (DINGMAN, 1994)

[a] The Aral Sea is now much reduced in size

[b] Lake Chad is now much reduced in size

Heat transfer in lakes differs from rivers, because of the great amount of stored water. The main process that influences the temperature of a lake is mixing. Mixing of water with different temperatures depends on the stability of the lake. Stability is the amount of energy that is required to mix the entire volume of water a uniform temperature without addition or subtraction of

heat. Stability is very strongly influenced by lake size and morphometry. The amount of layering of a lake is determined by the energy of the mixing powers like wind and stream flow and the resistance of the water (density) and this is expressed by the Richardson gradient (R_i) (after Spigel and Imberger, 1987):

$$Ri = \frac{g\left(\frac{dp}{dz}\right)}{\rho\left(\frac{du}{dz}\right)^2} = \frac{layerstability}{turbulence}$$

Figure 3 shows physical processes typically observed in lakes. Active turbulence in lakes is confined to the surface mixed layer, to boundary layers on the lake sides and bottom, and to turbulent patches in the interior. The density stratification present is a result of external mechanical energy inputs. There are horizontal processes like river inflow and the wind that induces waves due to shear stress and vertical processes mainly forced by the sun. The river inflow can have a higher or lower temperature compared to the lake but can also have different characteristics based for instance on the amount of nutrients, sediment load and salinity. These characteristics cause the amount and place of intrusion in the lake which leads to layering. During cold nights or in winter the surface is cooling and becomes denser which results in overturning. Based on the typical mixing of a lake during the year a distinction is made between monomictic, dimictic and polymictic lakes. The epilimnion depth is the border between surface water and deep water and plays a crucial role in biological processes.

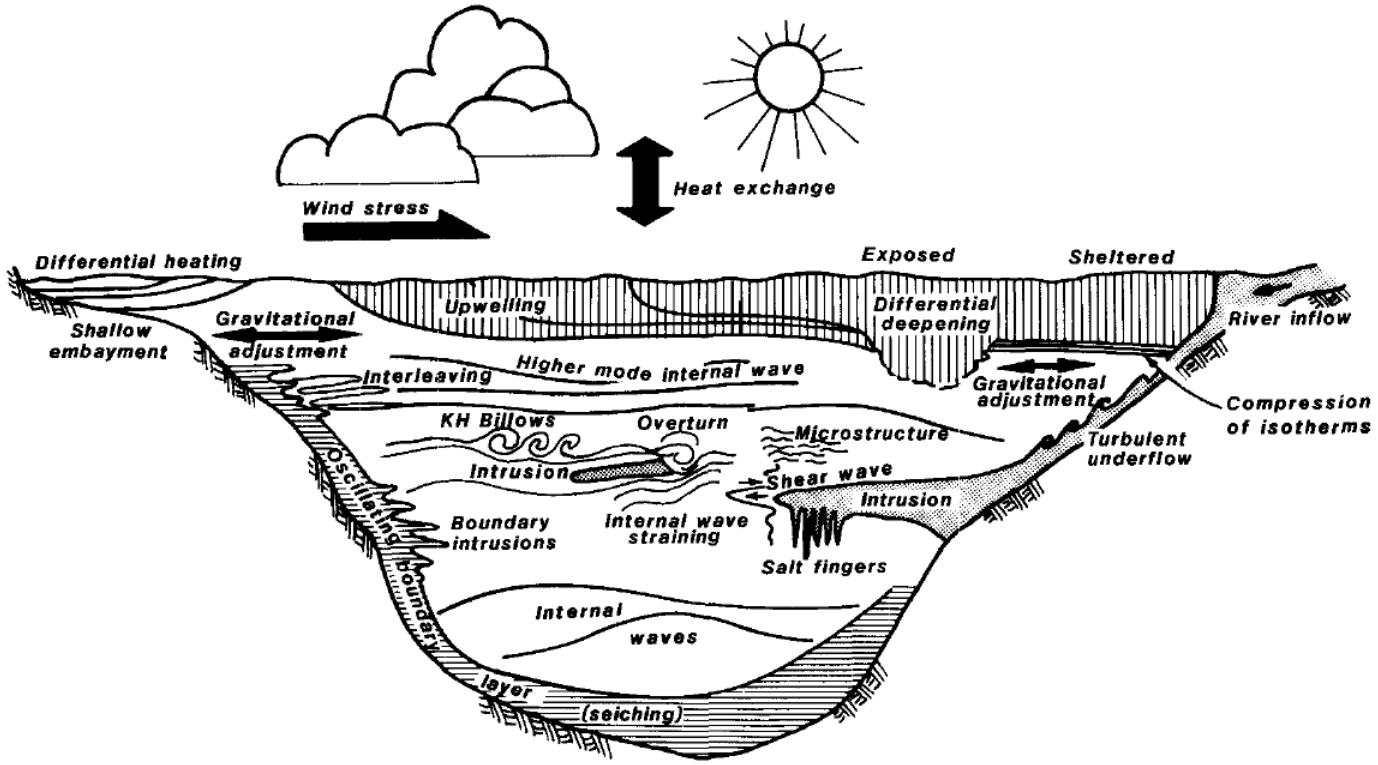

FIGURE 4 SKETCH ILLUSTRATING POSSIBLE MIXING MECHANISMS OPERATING IN A LAKE SUBJECT TO A SUDDEN WIND STRESS (SPIGEL AND IMBERGER, 1987).

2. 3 WATER TEMPERATURE MODELS

2.3.1 INTRODUCTION

There are several types of models. The two main types are physical and empirical models which can both be deterministic or stochastic. A physical model is a model that describes physical relations between compounds of the environment. When concentrating on water temperature, physical models are able to resolve the energy balance and the water balance. Empirical models are based on relations that are found either empirically or based on statistics. Empirical relations are regression models like linear, logistic and multiple linear regressions.

A deterministic model uses cause and effect relations between site conditions and meteorological parameters and their resulting influences on river water temperature. The statistical or stochastic approach can be used to link air to water temperatures since both are responding to similar energy balance components. The regression type models differ from this in that the position of events or timing is not important, while it is in the stochastic models.

Deterministic and statistical approaches each have advantages and disadvantages. Deterministic modelling is better adapted to the analysis of thermal effluent type problems where mixing of waters from different sources and different temperatures occurs and also different scenarios with many different input parameters to research cause and effect responses can be tested. Deterministic modelling can be used at different spatial scale (1D, 2D, etc) as well as for specific sites, but it is most often carried out as a one-dimension model along the river's principal axis, because water temperature in rivers is relatively uniform with depth. Disadvantage is the complexity of deterministic models as it requires a lot of input parameters that are often not available (Caissie *et al*., 2001).

2.3.2 LAKE MODELS

There are two types of one-dimensional lake models. These are eddy-diffusion and turbulence-based models. Eddy-diffusion models simulate the vertical transport of heat in the water with the use of a mixing parameterization based on an eddy-diffusion approach. Turbulence-based models compute the production and available amount of turbulent kinetic energy (TKE), parametrize the vertical transport by eddies, and consider the dissipation of energy (Perroud *et al*., 2009).

Perroud *et al*. (2009) made a simulation of lake water temperature profiles to compare different one-dimensional lake models. According to Perroud *et al*. (2009) only SIMSTRAT and DYRESM reproduce the variability of the water temperature profiles and seasonal thermocline satisfactory. Next to these mechanistic models it is also possible to empirically examine the correlation between a lake's thermal structure and past meteorological conditions. In this case a long-term record of lake temperatures and meteorology has to be available.

Goudsmit *et al*. (2001) used a numerical model for the prediction of the seasonal development of temperature stratification and turbulent diffusivity that describes the vertical fluxes in lakes was applied on two lakes. The transport below the thermocline was described by a model of the seiche energy balance and the production of TKE by the seiche motion was included (see.2.2.2). Peeters *et al*. (2002) had the availability of a 50 year dataset of the thermal profile of Lake Zurich to calibrate and validate the one dimensional numerical k-e lake model 'SIMSTRAT'.

Model	Author	Description	Characteristics	Problems
ELCOM	Hodges *et al*., 2000	Basin-scale internal waves Layer mixing	3D numerical mixed-layer model Correct depth of wind-mixed layer	Numerical diffusion and damping
SIMSTRAT	Goudsmit *et al*., 2002	Diffusive mixing and includes the effect of internal seiches on the production of TKE	1D numerical k-e model	
FLake	Mironov 2008	Bulk heat and kinetic energy budgets Two layer structure: Mixing layer with constant temperature and a thermocline	1D bulk model with self similarity of the temperature-depth curve for the thermocline	No inflow and outflow
DYRESM	Yeats and Imberger, 2003	Lagrangian layer scheme Layers have uniform properties but variable thickness	1D turbulence Process-based vertical mixing model	

TABLE 3 OVERVIEW OF LAKE MODELS

ELCOM (Estuary and Lake Computer Model) is a three dimensional thermodynamic model and was coupled to a regional climate model to test the capability of incorporating lakes in the Canadian Regional climate model (CRCM) model (Hodges *et al*., 2000).

A three dimensional lake model accounts for both vertical and horizontal transport of momentum and heat and provide detailed information about the lake temperature structure, However, a very high computational cost limits their utility to only a few large lakes and to research applications. One-dimensional lake models range from the simplest one-layer models to turbulence closure models based on the transport equations for the second-order turbulence moments. One-layer models characterize the entire water column by a single value of temperature, assuming a complete mixing down to the lake bottom, or to the bottom of a mixed layer of a fixed depth which may vary spatially. This assumption results in a computationally very efficient model, but

it is an oversimplification of the physical processes, because most lakes are stratified over a considerable part of the year and neglecting the lake thermocline results in large errors in the surface temperature.
One-dimensional lake models can be used if vertical gradients are larger than the horizontal ones and if density stratification is present and the influence of wind, in and outflow are not very significant. This is also the case for the model FLake that is based on a two-layer parameterization of the evolving temperature profile and on the integral energy budget for the layers in question (Mironov, 2008).

2.3.3 FLAKE MODEL

FLake is a freshwater lake model capable of predicting the vertical temperature structure and mixing conditions in lakes (as described in 2.2.2) of various depths on time scales from a few hours to many years developed by Mironov (2008). The structure of the stratified layer between the upper mixed layer and the basin bottom, the lake thermocline, is described using the concept of self-similarity (assumed shape) of the temperature-depth curve. It must be emphasised that the empirical constants and parameters of FLake are not application-specific. That is, once they have been estimated using independent empirical and numerical data, they should not be re-evaluated when the model is applied to a particular lake. There are, of course, lake-specific external parameters, such as depth to the bottom and optical characteristics of water, but these are not part of the model physics. In this way FLake does not require calibration. Apart from the depth to the bottom and the optical characteristics of lake water, the only lake-specific parameters are the depth L of the thermally active layer of bottom sediments and the temperature T_L at that depth. These parameters should be estimated only once for each lake, using observational data or empirical recipes. In a similar way, the temperature at the bottom of the thermally active soil layer and the depth of that layer are estimated once and can then used in for instance a numerical weather prediction (NWP) model as two-dimensional external-parameter arrays, but here these output parameters were compared with the outcome of a global hydrological model. If the prediction values of FLake are in better accordance with the observations it would be interesting to use the outcomes of FLake as input variables of the global model in such a way that the models are combined.

MODEL DESCRIPTION

The one-dimensional character of FLake neglects the influence of lateral flow which could be of importance for lake temperature for lakes with high exchange rates. The proposed lake model is intended for use, first of all, in NWP and climate models as a module (parameterization scheme) to predict the lake surface temperature. Apart from NWP and climate modelling, practical applications where simple bulk models are favoured over more accurate but more sophisticated models (e.g. second-order turbulence closures) include modelling aquatic ecosystems. For ecosystem modelling, a sophisticated physical module is most often not required because of insufficient knowledge of chemistry and biology.

THE CONCEPT OF SELF-SIMILARITY OF THE TEMPERATURE PROFILE

The concept of self-similarity of the temperature profile θ (z; t) in the thermocline was put forward by Kitaigorodskii and Miropolsky (1970) to describe the vertical temperature structure of the oceanic seasonal thermocline. The essence of the concept is that the dimensionless temperature profile in the thermocline can be fairly accurately parameterised through a universal function of dimensionless depth:

$$\frac{\theta_s(t) - \theta(z,t)}{\Delta\theta(t)} = \Phi_\theta(\zeta) \quad \text{at} \quad h(t) \le z \le h(t) + \Delta h(t). \qquad (1)$$

Here, t is time, z is depth, $\theta_s(t)$ is the temperature of the upper mixed layer of depth h(t), $\Delta\theta(t) = \theta_s(t) - \theta_b(t)$ is the temperature difference across the thermocline of depth Δh(t), $\theta_b(t)$ is the temperature at the bottom of the thermocline, and ϕ_θ is a dimensionless “universal" function of dimensionless depth that satisfies the boundary conditions $\phi_\theta(0) = 0$ and $\phi_\theta(1) = 1$. In what follows, the arguments of functions dependent on time and depth are not indicated, unless it is indispensable. The temperature profile given by Equation (1) is illustrated in Figure 4.

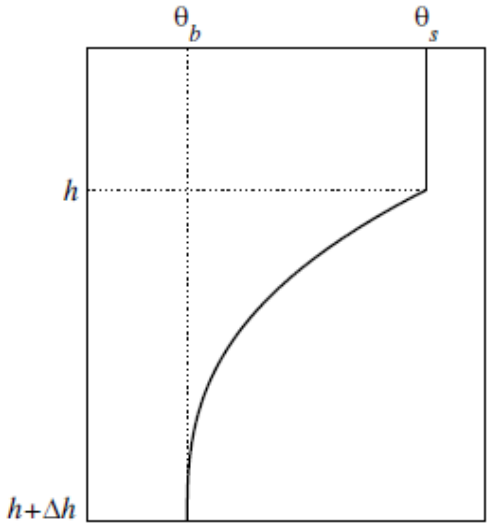

FIGURE 5 SCHEMATIC REPRESENTATION OF THE TEMPERATURE PROFILE IN THE UPPER MIXED LAYER AND IN THE THERMOCLINE (MIRONOV, 2008).

The concept of self-similarity of the temperature profile in the thermocline can be considered as a natural extension of the concept of the temperature uniform mixed layer that has been successfully used in geophysical fluid dynamics over several decades. Indeed, using the mixed-layer temperature θ_s and its depth h as appropriate scales, the mixed-layer concept can be expressed as $\theta(z, t)/\theta_s(t) = \zeta[z/h(t)]$, where a dimensionless function ζ is simply a constant equal to one. The use of $\Delta\theta$ and Δh as appropriate scales of temperature and depth, respectively, in the thermocline leads to Equation (1), where ϕ_θ is not merely a constant but a more sophisticated function of ζ. It should be emphasized that neither the mixed-layer concept nor the concept of self-similarity of the thermocline is well justified theoretically. Both concepts heavily rely on empirical evidence and should therefore be considered phenomenological. However, this phenomenological approach appears to describe the observed temperature structure to a degree of approximation that is sufficient for many applications (Mironov, 2008).

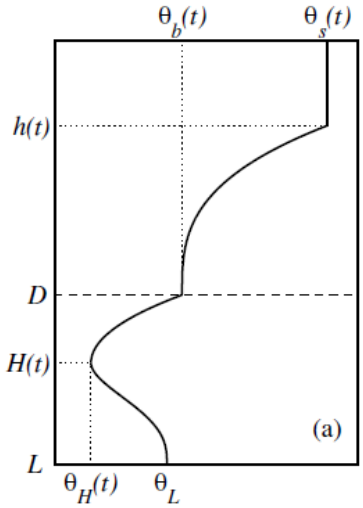

FIGURE 6 SCHEMATIC REPRESENTATION OF THE TEMPERATURE PROFILE IN THE MIXED LAYER, IN THE THERMOCLINE, AND IN THE THERMALLY ACTIVE LAYER OF BOTTOM SEDIMENTS (MIRONOV, 2008).

The evolving temperature profile is specified by several time-dependent quantities. These are the mixed-layer temperature $\theta_s(t)$ and its depth h(t), the temperature θ_b (t) at the water-bottom sediment interface, the shape factor $C_\theta(t)$ with respect to the temperature profile in the thermocline, the temperature $\theta_H(t)$ at the lower boundary of the upper layer of bottom sediments penetrated by the thermal wave, and the depth h(t) of that layer. The temperature θ_L at the outer edge $z = L$ of the thermally active layer of bottom sediments is constant (Mironov, 2008).

MODEL PARAMETERS

The following input data is needed to run FLake:

- Timestep
- Initial temperature of the upper mixed layer
- Initial temperature at the bottom
- Initial mixed layer thickness
- Height of wind measurements
- Height of air temperature measurements
- Lake depth
- Typical wind fetch
- Sediments layer can be switched off
- Latitude (dgr)
  Transparency
- Number of wave-length bands
- Fractions of total radiation flux
- Extinction coefficient

The lake specific parameters are lake depth, wind fetch, latitude and the extinction coefficient. In case a basin-mean temperature structure is a major concern, experience suggests that the best results (first of all, with respect to the lake surface temperature and to the ice cover) are obtained when a mean depth of a lake/reservoir in question is used, not its maximum depth or a depth at a particular location.
This is actually consistent with a single-column nature of the model. FLake is not suitable for deep lakes, where a two-layer representation of the temperature-depth curve with the lake thermocline extending from the outer edge of the upper mixed layer down to the lake bottom becomes inapplicable. Therefore a 'false bottom' is used for lakes with a mean depth of above 50 meters.
Meteorological data needed to run FLake are solar radiation (W/m^2), air temperature (°C), air humidity (mb), wind speed (m/s) and cloudiness (0-1). The model FLake is designed such that it can run only on the input of meteorological data.
The main output variables are surface temperature (Ts), the mixed layer depth (h_ML) and the stratification shape factor (C_T).

SENSITIVITY ANALYSIS

Sensitivity analysis is intended to determine the sensitivity of a model to its parameterisation and identification of the most sensitive parameters and non-linear response (uncertainty and error propagation). There are different methods to perform a sensitivity analysis. The first method is variation of all parameters, one-by-one, which is applied to FLake. A second method is variation within an expected range of parameter variability. Also it is possible to do an evaluation in terms of relative change in the parameter X and the depended model variable Y.
Three long term calculations are presented as test runs for FLake and are tested against observational data on vertical temperature structure.
A sensitivity analysis is applied for Müggelsee to analyse the influence of a range of variables on the surface temperature, the mixed layer depth (m) and the stratification "shape factor" (dimensionless). The lake has a surface of 7.4 km² (max. 4.3 km in length and max. 2.6 km width) and the maximum depth is 8 meter. Lake depth, transparency, wind fetch and the exchange of energy at the water-bottom interface are the input variables that are changed.
Wind fetch is defined as the unobstructed distance that wind can travel over water in a constant direction. Fetch is an important characteristic of open water because longer fetch can result in larger wind-generated waves. The typical wind fetch influences the depth of a stably or neutrally stratified wind-mixed layer. For the Müggelsee the wind fetch is $4.0 \cdot 10^3$ m. A minimum fetch of 0 and a maximum fetch of 4,300 m is possible for this lake. For both situations the influence of a changed fetch is very small.
Lake transparency is expressed as the extinction coefficient of the light that penetrates into the lake. The total sunlight is assumed to reach the lake surface. The light attenuation depends on the water quality of the lake. This is for instance influenced by the load of nutrients, the amount of phytoplankton and suspended material. As expected lowering the extinction coefficient influences the surface temperature negatively (from 9.2 to 5.9 degrees on average for changing the extinction coefficient from 0.7 to 0.1). This indeed is a very low value and not likely to happen.
Changing the lake depth from a minimum of 1.0 meter and to the maximum depth of 8.0 meter influences the mixed layer depth directly from small to bigger depths. The surface temperature is not highly affected.

It is expected that sediment only influences the lake temperature in shallow lakes in cold regions. This is not the case for the Müggelsee which lies in a temperate climate. To analyse the sediment a temperature distinction is made between arctic, boreal and temperate climate. Therefore the temperature is changed by -20, -10 and +10 degrees. Also the sediment is turned on and off and the depth is changed into a shallow lake with a depth of 2 meters.
Just changing the air temperature from low to high influences both the surface temperature and the mixed layer depth from low to higher values.
Switching on and off the sediment layer for the cold region and shallow lake gives no respond for the analysed variables. Increasing the depth for a cold shallow lake of 2 meters to a cold deep lake of 8 meters logically increases the mixed layer depth, but also increases the stratification value slightly.
Both increasing the depth of the thermally active layer of bottom sediments and increasing the temperature at the outer edge of the thermally active layer of the bottom sediments individually lowers the surface temperature with about 1.5 degrees and decreases the mixed layer depth with 0.7 meter.
It seems that transparency (extinction coefficient), lake depth and the meteorological forcing are the dominant parameters in FLake.

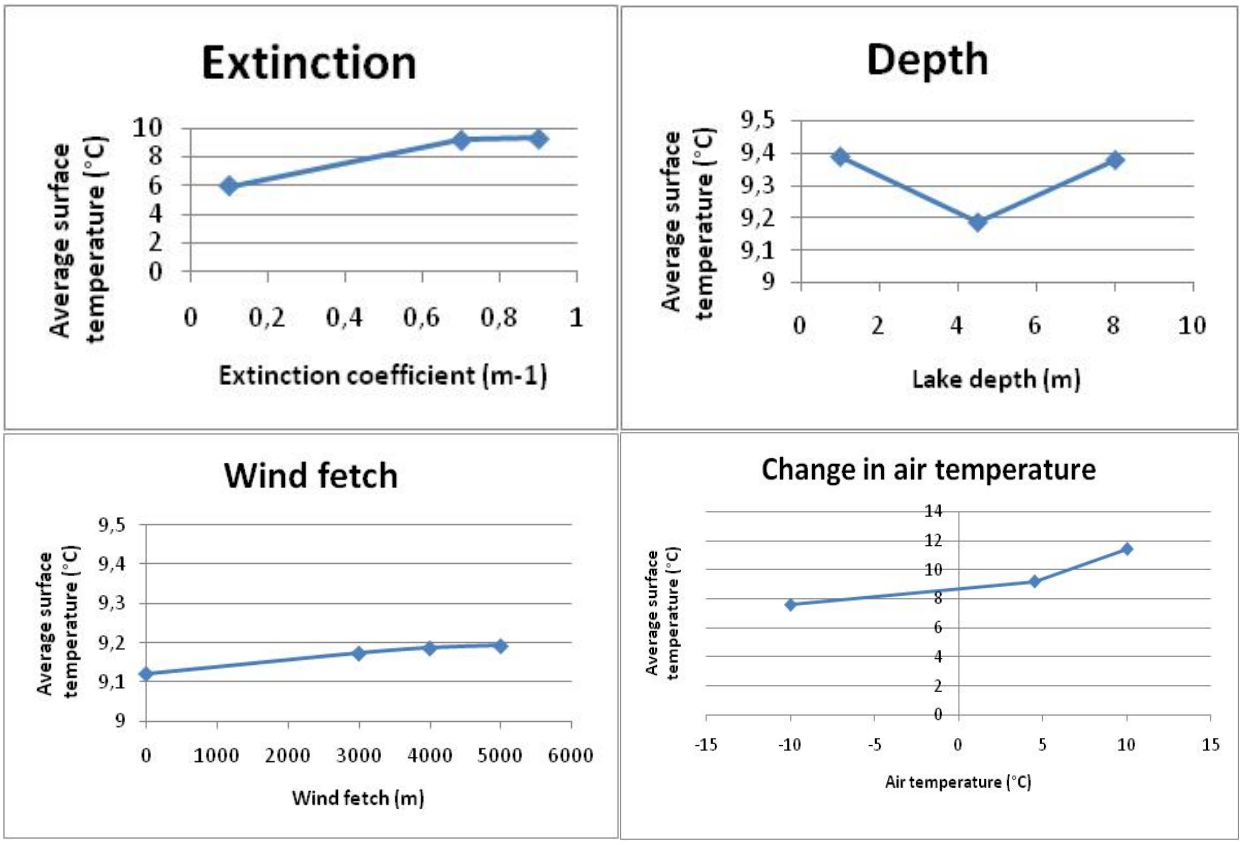

FIGURE 6. DEVELOPMENT OF THE AVERAGE SURFACE TEMPERATURE FOR INCREASING EXTINCTION, LAKE DEPTH, WIND FETCH AND CHANGE IN AIR TEMPERATURE.

2.3.4 RIVER MODELS

Several studies (Caissie *et al*., 2001, Mooij *et al*., 2008) use the relation between air temperature and stream temperature to predict water temperature. Linear regression between stream temperatures and air temperatures is only accurate at moderate air temperatures, e.g. 0 to 208C, and good for interpolation within the record length used in the analysis. Linear regression models do not accurately project stream temperatures at high air temperatures as may be found under a climate-warming scenario. The stream temperature/air temperature relationship resembles an S-shaped function rather than a straight line. Linear extrapolations to high and low air temperatures are therefore not justified. (Mohseni and Stefan, 1999).

A numerical model based on a finite difference solution of the unsteady heat advection-dispersion equation is formulated to predict water temperatures in streams at time increments of 1 hour which includes the energy balance, sun shading and wind sheltering. The model is calibrated with temperature records (Sinokrot and Stefan, 1993).

A two-dimensional model, named CE-QUAL-W2, to simulate discharge, temperature and water quality in the Tualatin River was used by Rounds *et al*., 1999. This model is best applied to water bodies whose quality has distinct variations with length and depth and few differences from side to side. This is often the case for relatively broad rivers and it can only be applied to slow moving rivers, because it is written for lakes or reservoirs. To model the water temperature meteorological parameters together with boundary conditions like air temperature, temperature of water inflows and insolation were either measured of estimated. Shading was calibrated until a good match was reached. The model is a good tool for water management. Norton and Bradford (2009) compared CE-QUAL-W2 with the Stream Network Temperature Model (SNTEM).

Model	Author	Description	Problems
CE-QUAL-W2	Cole and wells, 2003	2D model, 1s	More suitable for narrow rivers
SNTEMP	Theurer *et al*., 1984	1D steady state model of the USGS, requires daily stream flow data	Only a stream temperature model and cannot be used for hydrological modelling
Air-water temperature relation	Sinokrot and Stefan, 1993	1h	The air-water relation is not always valid
PClake	Mooij *et al*., 2007	Ecological model based on air-water temperature relation	The air-water relation is not always valid

TABLE 4 OVERVIEW OF STREAM TEMPERATURE MODELS (MODIFIED FROM: NORTON AND BRADFORD, 2009).

Table 4 gives an overview of different types of models to simulate stream or river temperature. All models are able to reproduce stream temperature but the models differ in the request of input data and temporal resolution. Also the scale and the underlying research goal of applying these models differ from regional management strategies to local ecological effects.

Next to the effects of climate change LeBlanc *et al*. (1997) modelled the effects of changes in land use on water temperature in streams with a stream temperature model that considers the gains and losses of thermal energy resulting from radiation, convection, conduction, evaporation and advection. A sensitivity analysis showed that shade/transmissivity of riparian vegetation, groundwater discharge and stream width had the greatest influence on stream temperature. These three variables are also highly influenced by land use (LeBlanc *et al*., 1997).

The effect of projected global climate change due to a doubling of atmospheric CO_2 on water temperatures in five streams in Minnesota was estimated by Sinokrot and Stefan (1993) using a deterministic heat transport model. The model calculates heat exchange between the atmosphere and the water and is driven by climate parameters and stream hydrologic parameters. The model is most sensitive to air temperature and solar radiation. The model was calibrated against detailed measurements to account for seasonally variable shading and wind sheltering. Simulation with the complete heat budget equations were also used to examine simplified water temperature/air temperature correlations (Sinokrot and Stefan, 1993).

The model of Stefan *et al*. (1998) is a deterministic, one dimensional model to simulate daily water temperature profiles for temperate zone lakes by including the both open water and ice cover periods for lakes. They use the model to conclude that the sediment/water heat exchange is most significant for simulation of ice covered lakes because heat released from the sediment during the winter warms the lake water. Model input consists of daily weather data (air temperature, dew point temperature, wind speed, solar radiation, cloud cover and precipitation) and lake parameters (surface area, maximum depth, Secchi depth). The results of a doubling CO_2 climate scenario are a shortened ice cover period and delayed ice formation, while water temperature maxima at the lake surface are projected to increase 3 to 4 °C, and water temperature stratification in summer will be stronger (Stefan *et al*. 1998). Comparable research is done by Fang and Stefan (1999) where the effects of climate change on water temperature characteristics of small lakes in the contiguous U.S. are investigated and results in confirming conclusions. A more ecological prediction of the effect of climate change on temperate shallow lakes is given by Mooij *et al*. (2007) who use the ecosystem model PCLake. The results show a change in nutrient status and thereby project the shift from clear to a turbid state (Mooij *et al*., 2007).

Some deterministic models used a shading component to study the dynamics of riparian vegetation and solar heating. These models generally calculate solar input based on sun position, stream location, orientation and other relevant parameters. The selection of a particular water temperature model depends on the modelling objective as well as the data requirements (Caissie, 2006).

2.3.5 PCR-GLOBWB

The macro-scale hydrological model PCR-GLOBWB was developed to simulate terrestrial hydrology at macro-scales under various land use and climate conditions with an operational temporal resolution of one to several days. The name PCR-GLOBWB stands for PCRaster Global Water Balance. The main hydrological processes are described physically and by parameterization to deal with limited data availability. The model was developed to simulate terrestrial hydrology at macro-scales. The model was based on the HBV-model (Bergström, 1995).

MODEL DESCRIPTION

PCR-GLOBWB describes the terrestrial part of the hydrological cycle and thus follows the most direct pathways of water that reaches the Earth surface back to the ocean or atmosphere. The basic assumption for the PCR-GLOBWB model is the assumption that the fresh surface water temperature is the net result of all incoming en outgoing fluxes. The global hydrological model PCR-GLOBWB contains a water and heat budget. The heat balance is solved using the following terms: short-wave insolation, long-wave atmospheric radiation, water-surface backscatter, evaporation, air/water conduction and can be simplified into lateral and advective energy. The water budget exists of precipitation, surface and subsurface runoff, ice thickness, evaporation, discharge and groundwater flow. The model is based on a grid of 0.5 by 0.5 °, which corresponds to squares of about 50 to 50 km. The model concept is shown in figure 7.

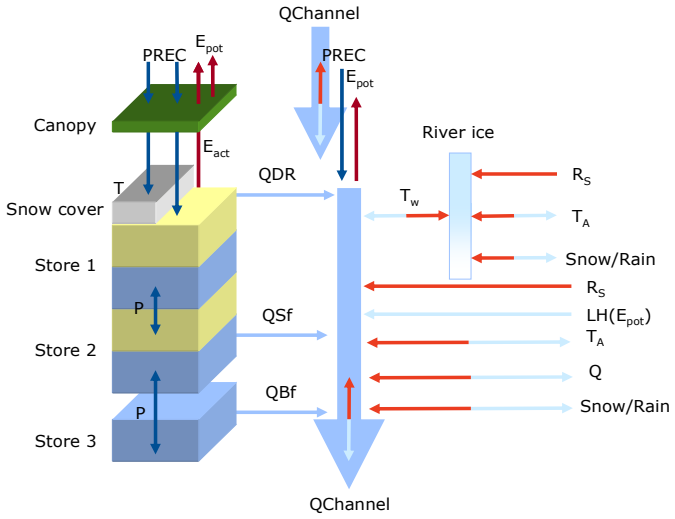

FIGURE 7 MODEL CONCEPT: ON THE LEFT, THE SOIL COMPARTMENT, DIVIDED IN THE TWO UPPER SOIL STORES AND THE THIRD GROUNDWATER STORE AND THEIR CORRESPONDING DRAINAGE COMPONENTS OF DIRECT RUNOFF (QDR), INTERFLOW (QSF) AND BASE FLOW (QBF). IN THE CENTRE, THE RESULTING DISCHARGE ALONG THE CHANNEL (QCHANNEL) WITH LATERAL IN- AND OUTFLOW AND LOCAL GAINS AND LOSSES ARE DEPICTED, ON THE RIGHT THE ENERGY BALANCE FOR THE FRESH WATER SURFACE AND THE POSSIBLE FORMATION OF ICE (VAN BEEK, 2008).

The meteorological model input is total precipitation, temperature and potential evapotranspiration from observations or from GCM results. At the moment the models treats the outflow of lakes and wetlands as purely depended to the storage and turbulence and mixing are not yet incorporated.

To predict water temperature of a river or stream the horizontal and vertical energy fluxes to the stream are calculated and the stream itself is also defined as an energy flux. The vertical fluxes can be defined by the energy balance that includes the exchange of heat from the water-atmosphere is calculated, whereas the exchange of heat from the soil-water boundary is not included. The advective fluxes like inflow by rivers, groundwater and precipitation. First the vertical energy balance is calculated, next the advective heat fluxes are added and then the total new energy flux is routed to the next cell. Evaporation is calculated apart of the model script. The meteorological parameters are on a daily timescale, but the model calculations are in sub daily time steps. The model starts with initial values. The initial water temperature is set as the yearly mean air temperature. For the first time steps this mean air temperature is relatively high for the northern hemisphere and relatively low for the southern hemisphere.

PCR-GLOBWB is sensitive to ice formation and ice melt which is mostly influenced by albedo and the maximum allowed ice thickness. Although albedo is lowered, the ice melt in summer is still unsatisfactory, thereby ice thickness increases over the years and too much ice is accumulated. To prevent this, the maximum ice thickness is set to 7.5 meter for deep lakes and is lowered with decrease in lake or channel depth. The maximum ice thickness is defined such that this value has minimal influence on the automatic process of ice formation and ice melt, but still gives an acceptable result.

The model produces maps with the difference between air temperature and water temperature to the role of heat transport in rivers. Tropical rivers will have higher water temperatures compared to the air temperature more downstream, whereas rivers in more temperate regions transport water that is much colder than the air temperature. The amount of heat transport also depends on the season. The difference between air and water temperature will be very high in regions that are covered with ice. Special interest is given to regions with water and air temperature differences as the model is especially designed to include this.

MODEL PARAMETERS

The model is driven by different parameters. The major group of data is meteorological data like precipitation, radiation and air temperature. Also constants for the energy balance are defined as shown below.

Constants for the energy balance:

tt: threshold temperature for snowmelt
rho_w: density of water [kg/m3]
lv: latent heat of vaporization [J/kg]
lf: latent heat of fusion [J/kg]
cp: specific heat of water [J/kg/degC]
hw: heat transfer coefficient for water [W/m2/degC]
hi: heat transfer coefficient for ice [W/m2/degC]
aw: albedo of water [-]
ai: albedo of snow and ice [-]

The energy balance, all totals in [MJ]:

totStorLoc: 1D storage used for energy scheme [m]
totEW: energy storage in surface water per m^2 surface area

The surface water energy fluxes [W/m^2]:

SHI: surface energy flux (heat transfer phi) of ice (+: melt)
SHW: heat transfer to surface water
SHR: heat transfer due to short and long wave radiation
SHA: advected energy due to rain or snow
SHQ: advected energy due to lateral inflow
SHL: latent heat flux, based on actual open water evaporation

Ice formation:

DSHI: net flux for ice layer [W/m^2]
wi: thickness of ice cover [m]
wh: available water height
dwi: change in thickness per day, melt negative

3. METHOD

3.1 INTRODUCTION

In this research two models were used, namely the PCR-GLOBWB model that models the temperature of all fresh surface waters, and the model FLake that only models lakes. To analyse the performance of the models several modelling steps were taken. First, the stand alone FLake model was used to model lake water temperature. The FLake model calculates surface temperature including lake turbulence. Mixing takes place due to instability of temperature with depth. When the surface is cooling due to low air temperature this water will sink and deep water will travel towards the surface. These simulations are compared with long term daily lake temperature observations. Also the influence of all the different parameters on the modelling result was tested with a sensitivity analysis (as described in 2.3.3).
Next, temperatures are modelled with the current version of the model PCR-GLOBWB without any adaptations. These results are compared with monthly and daily observations. To run PCR-GLOBWB properly first several test runs were made, where the modelled water temperature was compared to the air temperature for a number of time steps. Also the model results were compared with discharge data of the selected rivers to assure the model gives realistic values. The final results were split in daily water temperature records for the 15 stations from the USGS database and in monthly water temperature records for the GEMS stations. Both were compared with the observations (see 3.3).
Also the comparison between monthly air temperature and water temperature was made to analyse the need for a hydrological model in terms of space and time.
For model application data and initial parameters are needed. The model PCR-GLOBWB was applied to all major lakes and rivers in de world. From the ILEC database data is collected to describe lake specific characteristics like depth, surface, transparency, mixing type, timing and length of ice cover period. These data can be used in an additional research to compare the results of PCR-GLOBWB and FLake for these major lakes. The temperature records of National oceanic and atmospheric administration (NOAA) were used to evaluate the simulations made by the FLake model. This data covers a total period from 1960-1990. For some periods data was missing for frozen and dried surfaces.
The Global lakes and wetlands database (GLWD) database contains a list of 3721 lakes and reservoirs with location (long, lat) and lake area (km^2) (Lehner and Döll, 2004). The International Lake Environment Committee (ILEC) also has a world lake database. A quality check was performed for the data in the GLWD database by comparing the values with data from other sources. For instance lake depth can both be found in the GLWD database as in the ILEC database. Next, regionalization was needed to assign values to lakes where no data is available.
Long term daily river data was collected from the USGS database, which only contains data for Northern America. Rivers were selected for the period 1975-2005 with more than 40% coverage of data. The period 1975-2002 contains daily meteorological data and therefore this time period was taken as the modelling period for PCR-GLOBWB. Next, monthly mean data was available from the GEMS stations that are spread over the world for the period 1973-2002 (29 years).
To produce model results a reallocation of the data stations was needed to ensure that the stations correspond with the river where they refer to. This was not the exact same location according to the coordinates given for the stations, because of the inaccuracy of the routing scheme.
A classification was made between different climate zones for both the lake and river stations (as shown in map 2-4). It was expected that the performance of the models is not equally over the different climate zones. The seasonal difference between stations from the same climate zone located on the northern and the southern hemisphere was concerned.
The relative error between water and air temperature was mapped to discover the areas in the world where heat transport by surface waters plays an important role. Extrapolation to simulate climate change in the future can be done by changing the meteorological parameters rather than extrapolating in time.

3.2 MODEL VALIDATION

The performance of the model can be analysed by comparing the outcomes with the total simulation period for different parameter combinations. During the verification the model is set to certain conditions so that it matches the main assumptions based on seasonality. The definition of model validation is testing the model for other datasets to discover how well the model matches the observations.
Errors can be caused by different factors like the position (A) of the station which influences the drainage area, the discharge (Q) due to inaccuracy in the model and the forcing. Also the water temperature (Tw) itself contains errors based on the model and other (meteorological) forcing. To assign the value of the model the amount of errors were checked locally to achieve an absolute confidence and globally to show the relative effects.
The FLake model was validated against temperature measurements of 1960-1990 from the NOAA database for 4 lakes and the PCR-GLOBWB model was validated against discharge and water temperature measurements of 1975-2000 on a monthly timescale for the 267 global distributed GEMS stations and against daily water temperature for 15 USGS stations located in

Northern America. The models were run with the current set of parameters, initial and boundary conditions. A calibration of PCR-GLOBWB was not performed as it is assumed that the model is capable of producing acceptable results in the current state.
The results of both FLake and PCR-GLOBWB were analysed with a linear correlation. A regression line was fit through the data and the origin. For this regression the R^2 and the slope (α) without intercept were conducted. The coefficient of determination (R^2) gives the proportion of variability that is accounted for by the model. In this case R^2 is the square of the correlation coefficient between observed and simulated data values and gives information about the goodness-of-fit (how well the regression line approximates the data points).

The relation for the Pearson-correlation coefficient (r) is the linear dependence between two datasets and is as follows:

$$r = \frac{\sum (x - \bar{x})(y - \bar{y})}{\sqrt{\sum (x - \bar{x})^2 \sum (y - \bar{y})^2}}$$

Where x and y are the means.
The factor of determination (r^2) is the squared root of the correlation coefficient. It gives the part of the variety in the observations that is caused by the variety in the simulations.
Also, the Spearman's rank correlation (ρ) was performed as this correlates the data one to one, whereas R^2 compares the data with the fitted regression line. The Spearman's rank correlation coefficient is a measure to which extent the simulations follow the observations. If one value increases, the other should also increases.
Next, the performance was determined by defining the standard error (SE) of the simulations compared to the observations. The standard error (SE) gives information about the size of the error in the simulation for each observation.
The relation for the standard error of the predicted y-value is as follows:

$$\sqrt{\frac{1}{(n-2)}\left[\sum (y - \bar{y})^2 - \frac{\left[\sum (x - \bar{x})(y - \bar{y})\right]^2}{\sum (x - \bar{x})^2}\right]}$$

Where x and y are the means and n the number of values.
To filter out the difference between climates and temperatures the standard error has to be compared with the observational mean. Therefore the relative standard error (RSE) was calculated. The RSE is simply the standard error divided by the mean and expressed as a percentage. If the SE is small compared to the mean, the RSE is <1. The RSE was used for assessing the reliability of the model. In general, if the RSE is less than 25%, results have reasonable accuracy.

Additional information about the performance of the model is given by the Root mean squared error (RMSE) and the Nash-Sutcliffe coefficient (NSC). The Nash-Sutcliffe coefficient (NSC) which can be considered the proportion of variation explained:

$$NSC = 1 - \frac{\sum_{i=1}^{n} (T_{sim_i} - T_{obs_i})^2}{\sum_{i=1}^{n} (\bar{T}_{obs} - T_{obs_i})^2},$$

Where NSC is the Nash-Sutcliffe coefficient, $Tsim$ is the simulated water temperature, $Tobs$ is the observed water temperature, and $Tobs$ is the mean observed water temperature.

Root mean squared error ($RMSE$) expresses the standard error of prediction and was also evaluated:

$$RMSE = \sqrt{\frac{\sum_{i=1}^{n} (T_{sim_i} - T_{obs_i})^2}{n - 4}}$$

However, the $RMSE$ statistic was used cautiously because outliers can have a large effect on the value.
A perfect correlation between observed and simulated data would have a NSC of 1 and a $RMSE$ of zero.
The Standard Error gives the discrepancy between the observation and the model result and is calculated by division of the standard deviation with the square root of the number of observations as shown in the equations below.

3.3 DATA

Interest in water quality developed further in time compared to the interest in water quantity. Temperature is a parameter that is more coupled to water quality and detailed records of temperature data are thus relatively recent. Measuring water temperature is relatively easy, although it can be measured in diverse ways depending on the location, number of observations in the water course, time and frequency of measuring, the measuring device and its accuracy. Therefore, data that are comparable, detailed and long term are rare. Some world-wide information on river water temperatures is available from the Global Environmental Monitoring System water quality monitoring project (GEMS/Water) where data is based on infrequent monitoring (Webb, 1996). GEMStat is a global water quality database of the UN and contains water temperature data.
Another option is to look in literature for data used by other studies, but few long-term data sets were available to enable the implication of climate change for the thermal conditions of rivers to be studied effectively. Webb and Nobilis (2007) carried out a long-term study that analysed 90 years of water temperature data from north-central Austria.
Rivers that pass several climatic boundaries compared to long rivers within one specific climate zone are interesting to compare. Also locations with observations that are spread over the world or when focussing on Northern America that are spread over the continent will improve the simulation.
Generation of data for models can be done either by measurements or by calculation from other parameters by using specific relations. GCMs can also supply data for hydrological models if data for future predictions is needed.
For measurements different methods can be used and in extracting data from all over the world the differences in these methods have to be considered and included as an additional uncertainty within the data. Meteorological data are point observations and have to be regionalized to large scale values.
The Global Runoff Data Center (GRDC) was used to collect data of river discharge. GEMS stations were selected located at or near GRDC stations.
The Global Lakes and Wetlands Database (GLWD) has been developed in partnership with the Center for Environmental Systems Research, University of Kassel, Germany and contains a list of 3721 lakes and reservoirs (Lehner and Döll, 2004).
In 1988 the International Lake Environment Committee (ILEC) started a data collection project entitled "Survey of the State of World Lakes" in cooperation with the United Nations Environment Programme (UNEP). The aim of this project is to gather basic and important environmental information on natural and artificial lakes and its dissemination for their best use especially in developing countries and countries with economies in transition. The data is sorted on lake name in the World Lakes Database. This database contains not only general information, but also on physiographic, biological and socio-economic data. The ILEC database was used to gain data about lake depth and transparency (list of data is given in Appendix IX).
Next, there is the global lake database of LakeNet to bring together people and solutions to protect and restore the health of the world's lakes. LakeNet was a global network of people and organizations in more than 100 countries dedicated to the conservation and sustainable development of lake ecosystems. The network was guided by an international steering committee with regional representatives in Africa, Asia, Europe and the Americas. From 1998-2008, the network was supported by the LakeNet Secretariat (formerly Monitor International), a U.S.-based non-profit organization governed by a 15-member Board of Trustees and supported by a team of professional staff. LakeNet was used to compare the depth with the other sources.

Data overview:

- GEMS monthly river temperature (1975-2004) (number of stations=267)
- GRDC monthly river discharge (1975-2004) (number of stations=267)
- USGS daily river temperature and discharge (1975-2004) (number of stations=15)
- GLWD lakes stations (number of stations=3721)
- ILEC lake depth and transparency (number of stations=211)
- NOAA lake temperature (1960-1990) (number of stations=4)
- Meteorological data (1973-2000)

The time period of the observations and the simulations have the same length but the time period of the simulation was shifted two years earlier due to the meteorological input data that was only available until 31-12-2002. It was assumed that this small difference will not have a significant influence.
For the USGS stations, data from the period 1975-2004 was searched for coverage of 40% in this period. The lack of data causes for most stations a delay in the start of the timeseries. In total 15 suitable locations were found in the USGS database from these there are only two locations that match to the locations with GEMStat data. For each station the daily simulation was compared with the daily observation from the first available observation date toward 31-12-2002. The last two years of observations were not used. Each station covers the longest period of available data. On the other hand, monthly data was compared for the total time period.

The long-term river water temperature data was downloaded from the USGS online database. This database contains quantitative and qualitative parameters for a lot of streams in the US. First, the most important locations that have both a GRDC station and GEMStat data are searched in the database for water temperature data for the period 1975-01-01 to 2004-12-31. Two search criteria (period 1975-2004 and at least 4380 observations, 40% coverage) were used to find all stations in the database that contain sufficient water temperature data for the period 1975-2004. The long term data is shown in the graphs of Appendix IA.
The period 1960-1990 was used for FLake and all lakes are compared for this same total period. The temperature data from the NOAA database is shown in the graphs of Appendix IB.
The GEMS dataset was used to evaluate the seasonal performance of the simulations on a global scale and the USGS was used to analyze the local performance and if the simulation is capable of showing daily and in between years variability, which was the same for FLake.

3.3.1 DATA QUALITY

Data is shared with research done by M. v. Vliet at Wageningen University on the Impact of climate change and its induced changes in river flow on surface water temperatures, and associated consequences for freshwater ecosystems and public utilities. This PhD study is part of the FP6 Water and Global Change (WATCH) EU project. Global data is provided by GEMStat, the global water quality database of the UN. This dataset contains monthly statistics (mean, median, min, max, n, stdev). GEMS stations that are located at GRDC stations (discharge stations) and that contain temperature statistics are selected. For some of the stations there is no data for all months and also some statistics are only based on two or three observations per month.
The period of data acquisition from the GEMS database was set on 1980-1999. The first quality control was to check if the measurement stations contain as many as possible water temperature data for the total period. A minimum period of 5 following years in the period 1980-1999 was set as the minimum requirement to analyse data.
In addition, sufficient discharge measurements from the GRDC database at the same station or from a nearby station are needed for the total period. Also information about the location in the river, the depth of the measurements and other characteristics like located near a dam or at the inflow of a tributary were searched for. The data is checked on gaps in the data and minimum cover of 50% of the period is set. General statistics were computed for the daily data (mean, min, max, standard deviation, covariance (st dev/mean).
The results of the quality check are shown in the table below. The error (GEMS measurements- USGS measurements) varies between 0 °C and a maximum error in May of 6.2 °C. The GEMStat data is compared with the matched locations in the USGS dataset. These are the Delaware River and the Potomac River.

Monthly mean	GEMSTAT	Average USGS	Error	GEMSTAT	Average USGS	Error
January	2.5	1.7	0.8	3.8	2.7	1.1
February	-	2.5	-	-	-	-
March	5.3	5.7	-0.4	6.6	7.8	-1.2
April	9.3	11.0	-1.7	12.1	13.8	-1.7
May	23.6	17.4	6.2	18.7	19.8	-1.1
June	22.2	22.5	-0.3	24	24.6	-0.6
July	-	25.6	-	26.9	27	-0.1
August	25.1	25.1	0.0	27.8	27.2	0.6
September	-	20.9	-	24.4	23.2	1.2
October	12.8	14.4	-1.6	16.5	16.5	0
November	8.7	8.3	0.4	11.1	9.8	1.3
December	5	3.6	1.4	8	4.7	3.3

TABLE 5 DATACHECK OF GEMS STATISTICS

3.4 DESCRIPTION STUDY AREA

3.4.1 DESCRIPTION LAKES

From the ILEC database input information for the FLake model of all major lakes was collected. Unfortunately, at the moment there are no long term observational water temperature records for these lakes. Only information is found at the NOAA database for the Great Lakes in Northern America. For these four lakes the period 1940-1990 was used, because this is the maximum time length with available daily water temperature. The four lakes, Lake Huron, Erie, Superior and Michigan (figure 8) located in the Great Lakes Basin can serve well as a representative of major global lakes, because of the great amount of water that is stored in these lakes. Also a lot of research is concentrated on this region. All maps are classified to climate zones according to the world map of holdridge life zones (Leemans, 1989) as it was expected that the model performance was not equal for all different climates.

FIGURE 8 MAP OF THE GREAT LAKES BASIN (NATURAL RESOURCES CANADA, 2003).

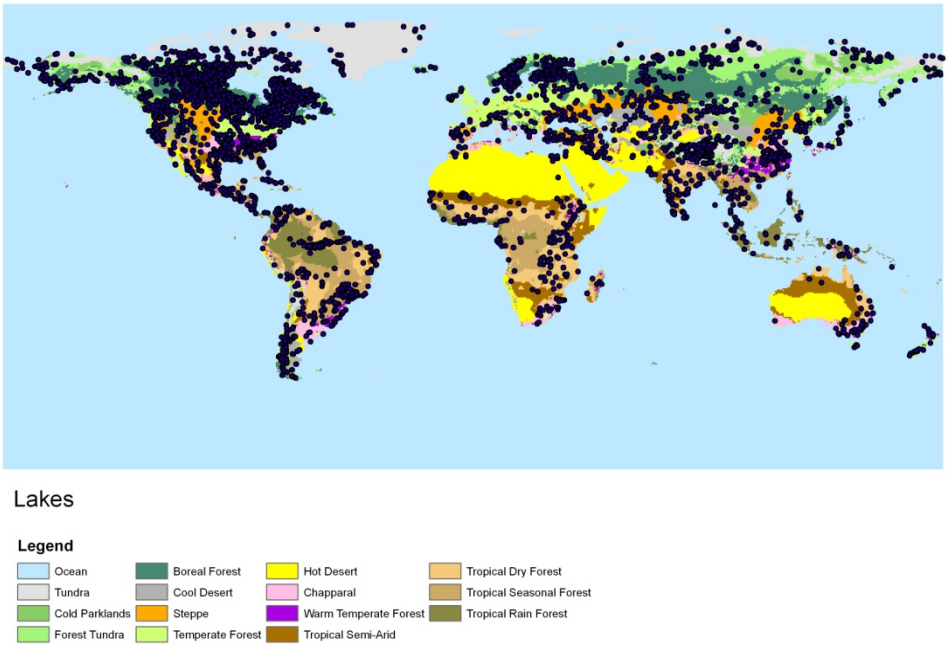

MAP 2 LAKES OF THE ILEC DATABASE.

3.5.2 DESCRIPTION RIVERS

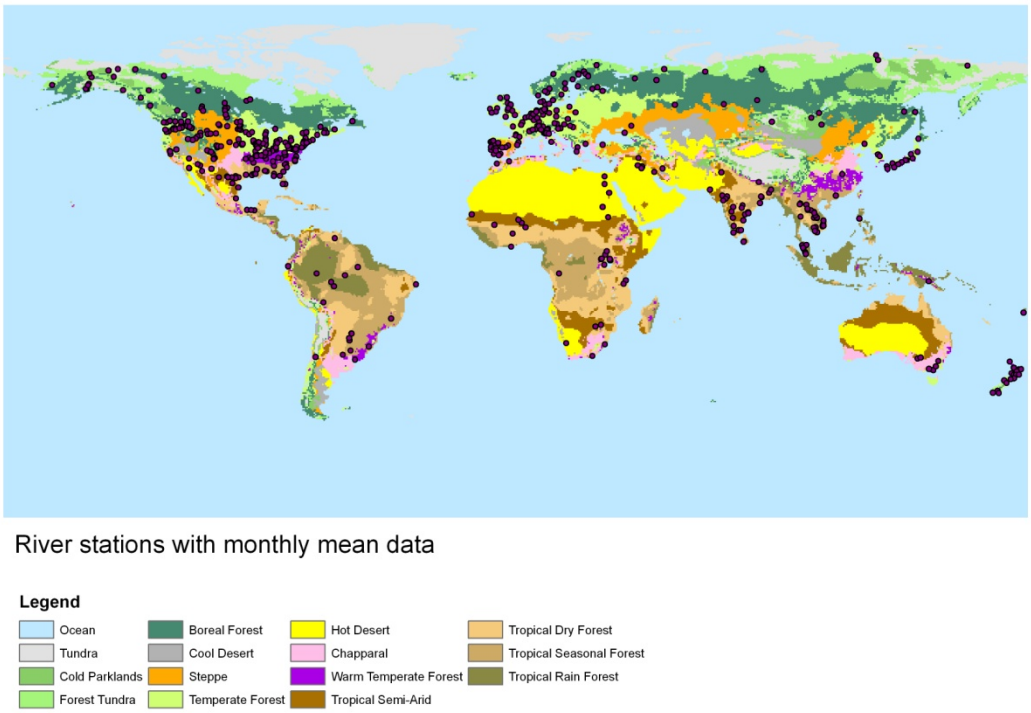

MAP 3 GEMS STATIONS

The long-term river data selected from the USGS covers several rivers in Northern America that differ in size of drainage area (as shown in map 4). For some rivers there is more than one station located on the river (see table 6).

ID	Location	Data coverage (%)	Latitude (degrees)	Longitude (degrees)	Drainage area (km^2)	Discharge data (USGS station)
1	Arkansas_abovePueblo	56	38.27	-104.00	12142	yes
2	Arkansas_JohnMartinr	56	38.07	-102.02	49179	yes
3	Arkansas_Lasanimas	55	38.08	-103.00	37484	yes
4	Colorado_Cameo	67	39.24	-108.02	20930	yes
5	Colorado_LeesFerry	48	36.86	-111.00	290680	yes
6	Colorado_Silver	66	32.05	-100.01	38766	yes
7	Colorado_Utahstateli	43	39.09	-109.00	46540	yes
8	Delaware_Trenton	87	40.22	-74.01	17628	yes
9	Greenriver_Campbellsville	50	37.24	-85.01	1773	yes
10	Jacksonriver	78	37.95	-79.02	897	yes
11	Potomac_nearWash	50	38.95	-77.01	30056	yes
12	SanJoaquin_Vernalis	93	37.68	-121.02	35194	yes
13	Mckenzie_SouthFork	67	44.14	-122.01	541	yes
14	StCroix_Milltown	62	45.17	-67.01	3783	no
15	Whiteriver_Centerton	82	39.50	-86.00	6354	yes

TABLE 6 LONG TERM RIVER DATA FOR THE PERIOD 1975-2004

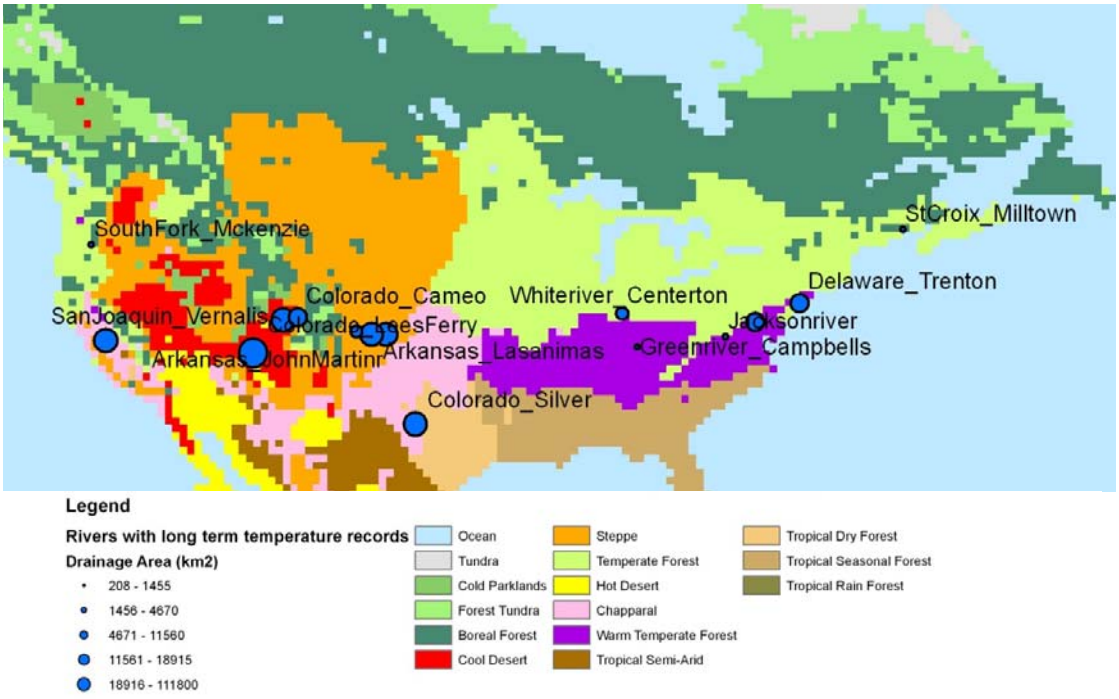

MAP 4 LOCATIONS WITH LONG-TERM RIVER DATA IN NORTHERN AMERICA.

The Arkansas River is a major tributary of the Mississippi River. The Arkansas generally flows to the east and southeast. At 2,364 km it is the sixth longest river in the United States, the second-longest tributary in the Mississippi-Missouri system. The Arkansas River drainage basin covers nearly 505,000 km².

The White River is a 1,162 km long river that flows through the U.S. states of Arkansas and Missouri. Despite being much shorter than the Arkansas River, it carries nearly as much water.

The Colorado River (or the Red River), is a river in the south-western United States and north-western Mexico that crosses several climate boundaries. Total flows of the river range from 113 m^3/s in droughts to 28,000 m^3/s in severe floods. With the construction of massive power dams on the lower course of the river, flows of over 2,000 m^3/s are unusual.

The Delaware River is a major river on the Atlantic coast of the United States.

The Jackson River is a major tributary of the James River, which is formed by the confluence of the Jackson River and the Cowpasture River.

The Potomac River flows into the Chesapeake Bay, located along the mid-Atlantic coast of the United States. The river is approximately 616 km long, with a drainage area of about 38,000 km².

The San Joaquin River is 530 km long.. The San Joaquin and its eight major tributaries drain about 83,000 km^2 of California's San Joaquin Valley. It originates high in the Sierra Nevada and drains south.

The McKenzie River is an 138 km long and drains mainly towards the west.

The St. Croix River (Maine – New Brunswick) is a river in north-eastern North America, 102 km in length. In the 20th century, the river was heavily developed for hydroelectric power. The river had previously hosted a large population of Atlantic salmon, however, the salmon population was reduced after building hydroelectric dams upriver from Calais-St. Stephen. The river is an estuary between Calais-St. Stephen and the river's mouth at Robbinston and St. Andrews. This tidal area extends for approximately 25 kilometres along this section and exhibits a tidal bore.

3.5 PARAMETERS

The parameters for lakes were conducted from two main datasets. The GLWD and the FLake dataset contain several similar parameters, but they do not cover the same lakes. The GLWD dataset was taken as the basic database for the locations taken into account and was extended with data from FLake. The quality of FLake mean depth reflects lake mean depth much better compared to the depth given in the GLWD dataset. This was randomly tested with the depth given by the ILEC database. The ILEC database gives ecological, biological, historical and economical information about lakes.

3.5.1 DEPTH

To assign the mean depth to the lakes from the GLWD dataset first the FLake depth was selected. If the depth was not available in both Flake and GLWD, the mean depth (Z) was calculated from the total volume (V) and the lake surface (Ao) as given in the GLWD dataset.

$Z=V/A_0$

The log-linear relation between area and volume was also used to estimate the volume for lakes that do not contain volume in the used datasets.

Storage-depth relation for volumes and lakes was assumed as follow (Liebe *et al*., 2005):

$V_{lake}=1/3A \cdot h$

Where A is the lake surface (l^2)

Assumed is an equal ratio between length and depth:

$H=l/c$

This is substituted in the volume relation:

$V_{lake}=1/3A \cdot l/c$

3.5.2 WIND FETCH

Fetch is the longest axis of a lake exposed to wind. Wind fetch can be estimated as the square root of the surface area, although it is possible that it then will overestimate the actual wind fetch due to the presence of islands and complex basin structures (Mazumber et Taylor, 1994). For the FLake model it is sufficient that the wind fetch is very large. Thus the wind fetch is assumed the square root of the surface area.

3.5.3 TRANSPARENCY

The thermal structure of lakes is determined by extrinsic features of the lake, such as inflows and meteorological factors (as described in 2.2.2). Next it is determined by intrinsic factors like basin morphometry and water clarity. Water clarity is highly determined by the number of planktonic organisms. The influence of water clarity on the thermal structure among a large number of lakes varying in surface area is examined by Mazumber and Taylor (1994). The results show that increasing Secchi depth is associated with deeper epilimnion within lakes and lake groups of comparable size. In larger lakes the epilimnion depth is deeper. Also with increasing water clarity the epilimnion depth is deepening at constant lake depth. Lake size and water clarity are both important in influencing epilimnion depth in small and large lakes.

The simplest form to represent the vertical decline of incoming light is the percentage intensity.

$I_z/I_o.100$

I_o = Radiation intensity at the surface

I_z = Radiation intensity at z meters depth

The extinction coefficient (ε) gives the amount of penetrated light at a specific depth.

$I_z = I_o.e^{(-\varepsilon z)}$

$\varepsilon = 1/z \ln(I_o/ I_z)$

The extinction coefficient is determined by the decline of light in water itself, by solved organic material and by anorganic or organic particles. Possible values are < 1 m^{-1} to < 0,1 m^{-1} in clear water and >20 m^{-1} for very turbid water.

The specific depth used to determine the extinction coefficient is based on the Secchi-depth. The Secchi-depth is originally measured with a so called Secchi disc which is about 25 cm and the depth at which the disc cannot be recognized reflects the point where the photosynthetic active radiation is about 10-20% of the radiation measured at the surface.

The relation between Secchi-depth (z_{SD}) and the Light-extinction coefficient (ε) is based on a 18% light intensity.

$\varepsilon = 1,7/z_{SD}$

The influence of the extinction coefficient on the mean surface temperature was analysed in FLake. Therefore only the extinction coefficient was changed over the possible range and all other conditions were kept the same. The lower range of extinction coefficients caused a great difference in surface temperature compared to the mean extinction coefficient. An extreme high extinction coefficient indeed increases the surface temperature only slightly, meaning that a higher extinction coefficient has little additional effect. So, a change in extinction in the lower range has more influence on the surface temperature compared to a change in the higher range (asymptotic effect).
Transparency data is collected from the ILEC database (Appendix IX). The data is highly variable for the amount of observations and the timing of the observation. Lake Chilwa located in South-Africa is an extreme non transparent lake with a mean transparency of a few centimetres. The lake has a maximum depth of 2.7 m and is dry for a major part of the year and lies in a swamp area. The transparency data from the ILEC database was used to complete the total lists of lakes from the GLWD database. Matches between ILEC and GLWD were made, but the ILEC database did not include all lakes of the GLWD database. To assign a transparency value to the missing lakes a relation between transparency and another lake characteristic was needed. First, the extinction was sorted to lake mixing type as it was expected that more frequently mixing would decrease the extinction coefficient. There seems to be a decreasing extinction coefficient with frequently mixing (shown in figure 9), but this trend is not very accurate and is not valid for polymictic lakes. It was therefore not used to estimate the extinction coefficient.

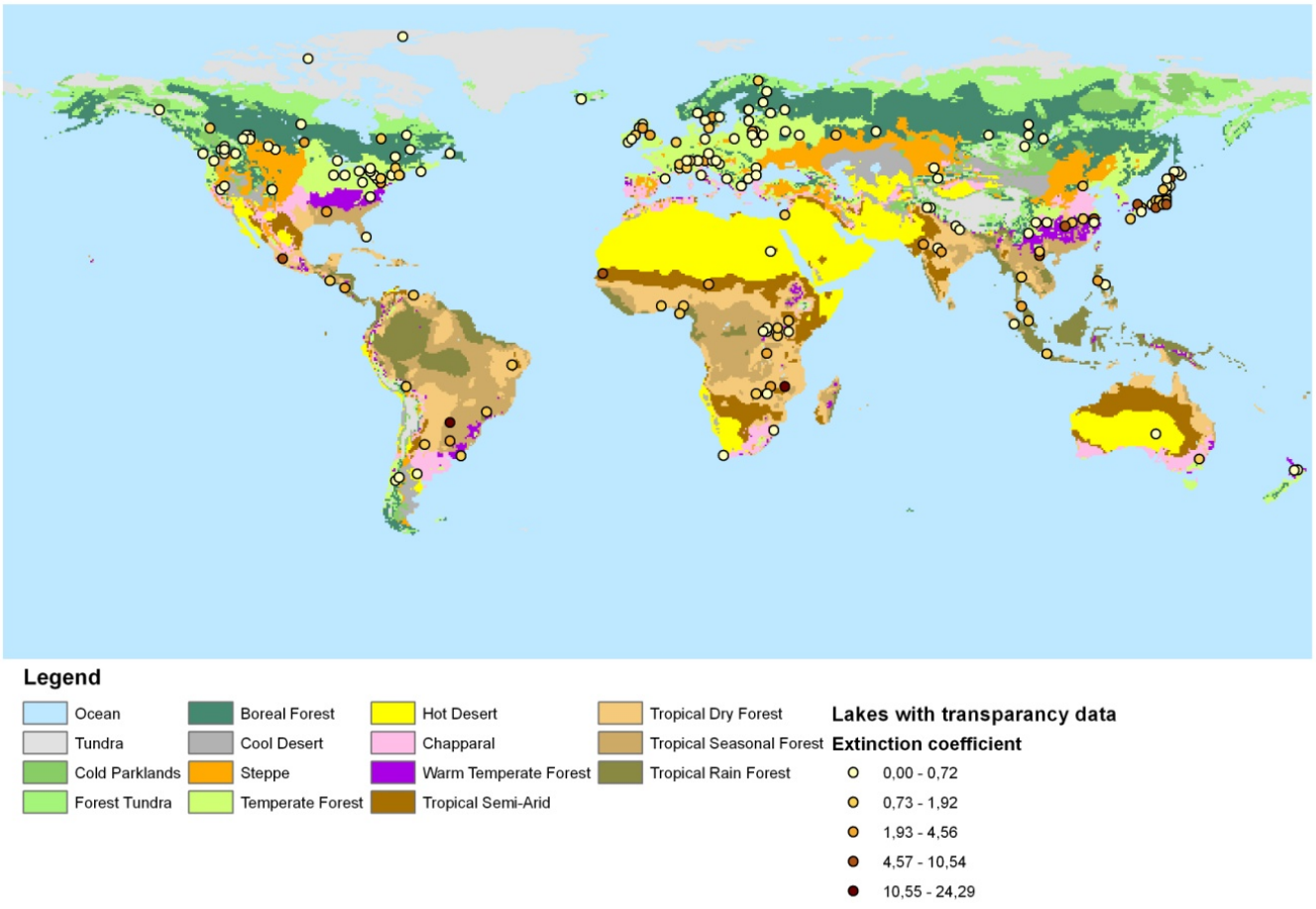

MAP 5 TRANSPARENCY

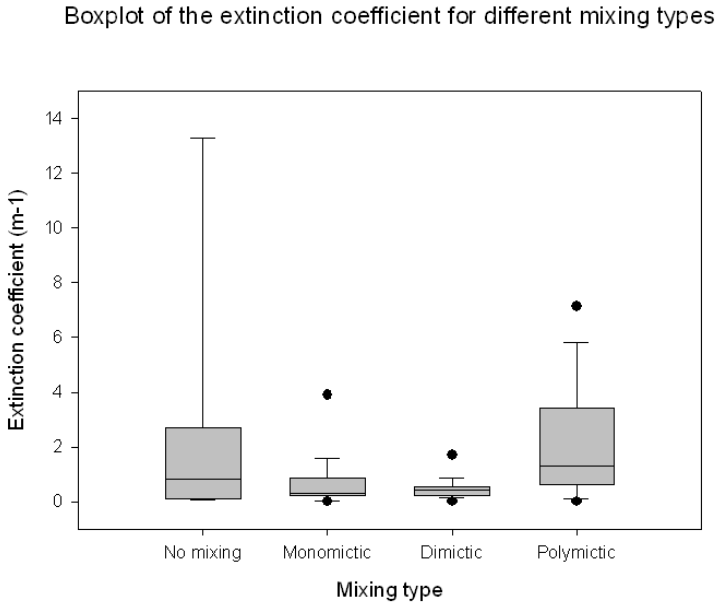

FIGURE 9 BOXPLOT OF THE EXTINCTION COEFFICIENT FOR DIFFERENT MIXING TYPES

Next, the mean extinction coefficients sorted by climate zones was compared to analyse if there was a distinguished mean extinction for each climate zone. However, the graph shows that the values are widespread over the different climate zones and there is also a lot of missing data for particular climates.

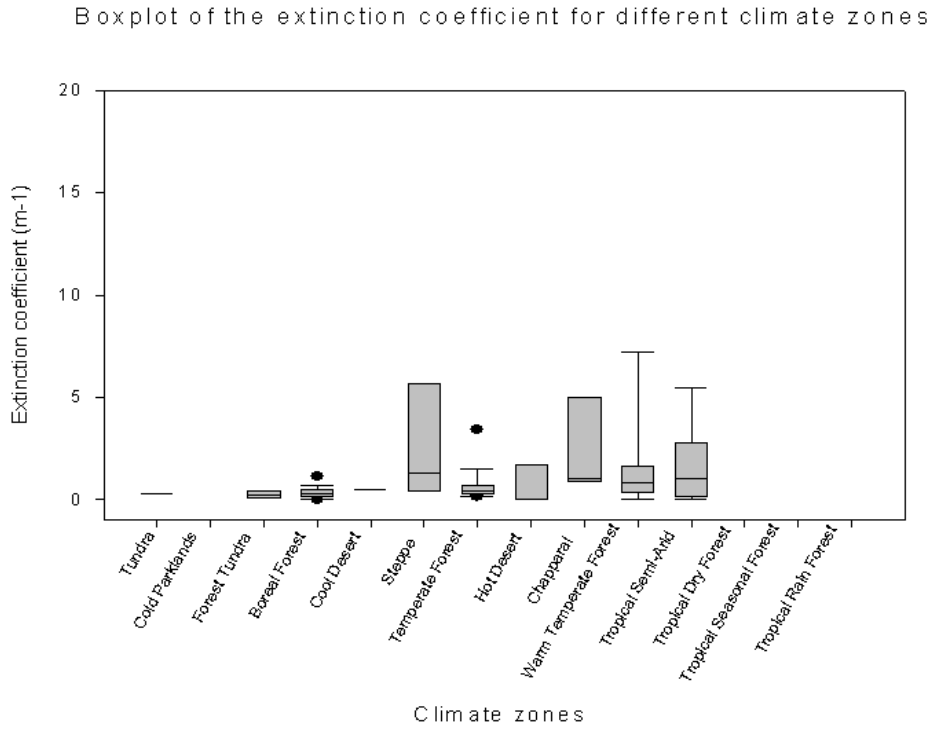

FIGURE 10 BOXPLOT OF THE EXTINCTION COEFFICIENT FOR DIFFERENT CLIMATE ZONES

Both mixing type and climate zone could not be used to estimate the extinction coefficient of lakes, but this parameter is needed for the FLake model. Therefore the extinction coefficient was related to the mean depth of the 211 lakes from the ILEC database on a logarithmic scale. This is a direct relation, because the depth of the penetrating light is directly influenced by the depth of the lake. The log-linear relationship shown in figure 11 was used to assign the extinction values to the lakes.

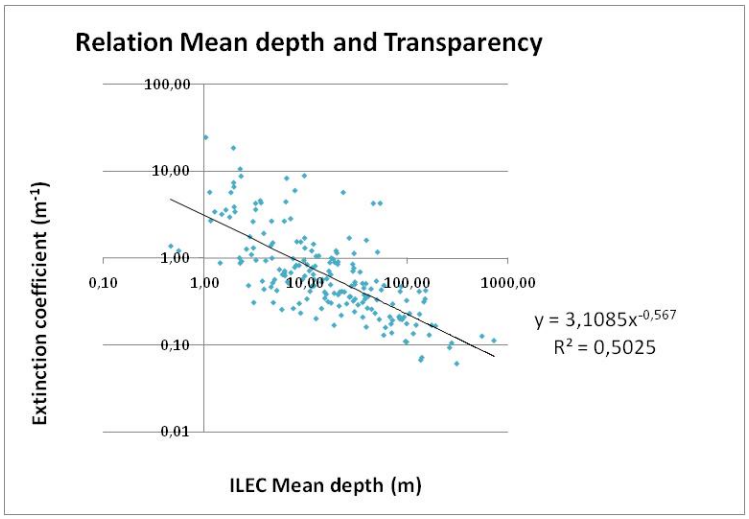

FIGURE 11 RELATION MEAN LAKE DEPTH AND EXTINCTION COEFFICIENT ON A LOGARITHMIC SCALE (N=211)

Lake Issyk-kul was not used to construct the relation mean depth and transparency and was used to test the performance of the relation. The extinction coefficient of Issyk-kul is 0.085 and was estimated as 0.13 by the model.

3.5.4 METEOROLOGICAL DATA

Both FLake and PCR-GLOBWB require meteorological data. FLake was forced with daily air temperature data which is available for the period 1960-1990. The Climate Research Unit (CRU) provides global climate data for macro-scale hydrological models as PCR-GLOBWB that requires precipitation, evapotranspiration and temperature. The advantage of the CRU products is that they are based on observations, covering the global land mass, and processed in a consistent manner. The period covered extends back over the past century, spanning the years 1901-2002 inclusive, for which sufficient meteorological data are available. The reference potential evapotranspiration and the crop factors derived from the CRU TS 2.1 dataset necessitate an update to the processing of the evapotranspiration in PCR-GLOBWBWB. In the model, a distinction is made between bare soil evaporation, which is drawn from the upper soil layer after deduction of any evaporation of liquid water stored in the snow cover, and transpiration by vegetation, which is drawn from both soil layers in proportion to the relative root volume present after deduction of any evaporation of intercepted rainfall. So far, mainly actual evapotranspiration, *e.g.*, from the ECMWF ERA-40 reanalysis, was imposed. This actual evapotranspiration was fractioned on the basis of vegetation cover only and merely limited by the availability of soil moisture in the pertinent layers. Evapotranspiration requires the formulation of crop factors and the calculation of reference potential evapotranspiration according to the FAO guidelines (Allen et al., 1998). Following the land surface division in PCR-GLOBWB, crop factors have to be defined for three surfaces (i.e., short and tall vegetation and open freshwater) and over time. The basic assumption that natural vegetation and planted crops strive to maximize the available resources underlie the definition of the crop factors. Temperature and moisture availability limit the available growing season and is relative only. The influence of the actual vegetation, as it arises from local conditions as nutrient availability etc., is taken into account through the parameterization of the LAI and vegetation heights as associated with the GLCC dataset.
ERA-40 is a ECMWF re-analysis of the global atmosphere and surface conditions for 45-years, over the period from 1957 through 2002 by ECMWF and contains daily air temperature data. This data was used to refine the timescale.

4. RESULTS

4.1 INTRODUCTION

The results are divided over the model performance on discharge, and the model performance for lakes. Then, first the performance for global monthly stations for different months and for different climates is analysed. Thereafter, a selection of these monthly stations is made for the largest rivers. Next, the daily data of Northern America is given for each station. To conclude, the importance of using a physical based model is provided by the difference between water and air temperature for different climates and for summer and winter.

4.2 DISCHARGE

First, the modelled discharge was evaluated and since the model was designed to simulate discharge the results of r^2 were very good. Though, for most months the discharge is slightly overestimated ($\alpha>1$). The RSE is also too high as a result of the high SE compared to the average observation for each month. The GEMS stations on the other hand contain a lot of stations with high difference in contributing drainage area and this could explain the variety between the discharges of the rivers.

Month	RSE	$\bar{O}$	SE	R^2	α
January	1.54	1838.59	2829.96	0.91	1.13
February	1.32	1982.92	2615.38	0.91	0.95
March	1.32	2170.10	2859.22	0.94	0.94
April	1.42	2397.51	3408.00	0.94	1.06
May	1.42	2997.22	4268.61	0.93	1.24
June	1.05	3881.20	4084.50	0.95	1.39
July	1.06	3359.36	3576.51	0.94	1.34
August	1.00	3881.20	3874.51	0.91	1.27
September	1.02	3359.36	3440.42	0.89	1.25
October	0.83	3127.70	2591.02	0.90	1.25
November	0.80	2711.41	2180.42	0.91	1.28
December	1.16	2088.85	2429.25	0.91	1.31

TABLE 7 STATISTICS OF GEMS MEAN AVERAGE DISCHARGE

The statistics of the discharge for all GEMS stations are shown in Appendix V. The results show that 154 of the 253 stations (61%) have a $R^2>0.7$. Further results for discharge can be found for the largest rivers and for the USGS stations.

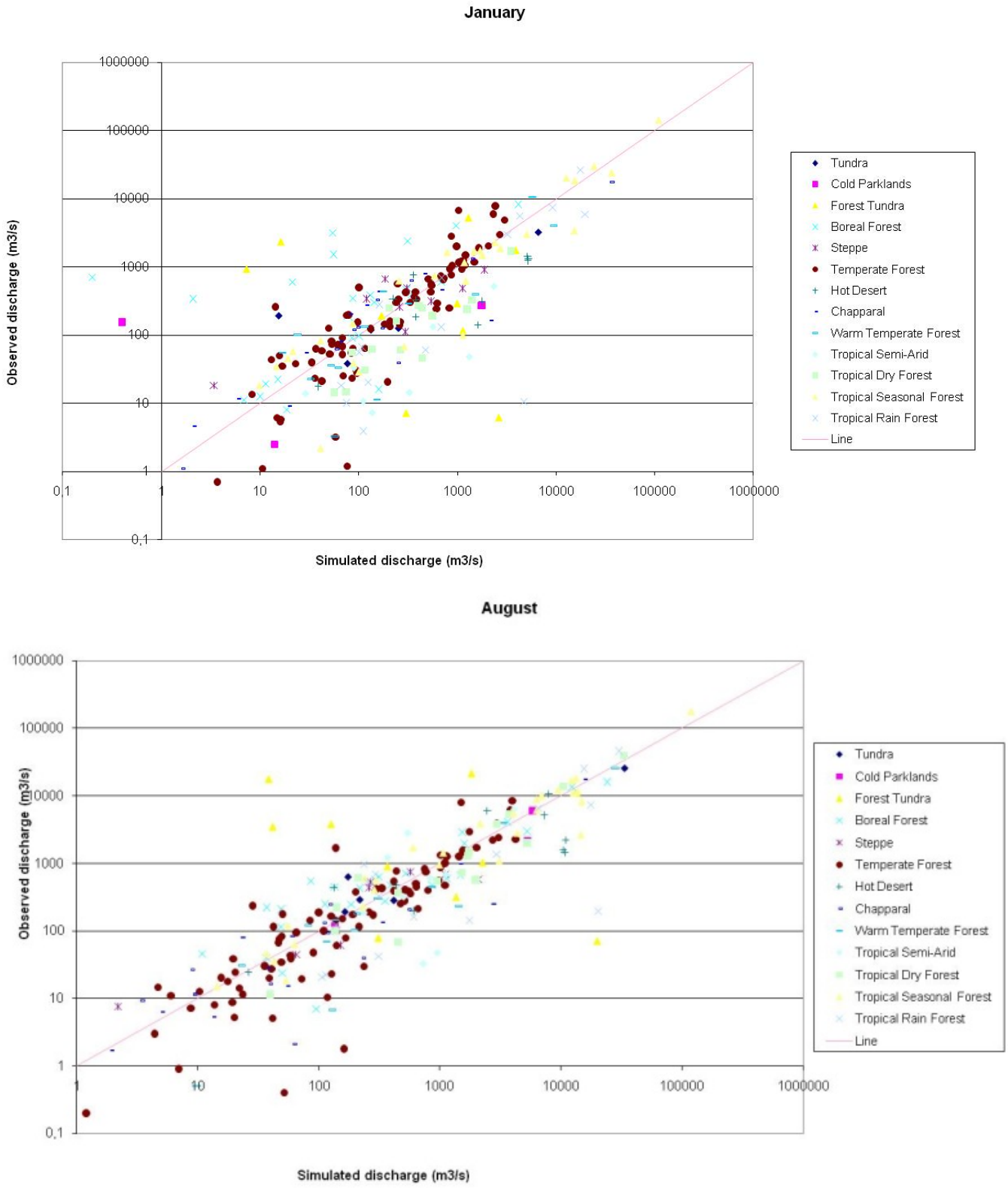

FIGURE 7 SIMULATED AND OBSERVED DISCHARGE FOR JANUARY AND AUGUST. EACH SYMBOL REFLECTS A DIFFERENT CLIMATE

4.3 COMPARISON OF RESULTS PCR-GLOBWB AND FLAKE FOR THE GREAT LAKES

The observations were compared with the model results of FLake for the period 1960-1990 with a linear correlation. For Lake Michigan data for the months in autumn were missing and this influences the results.

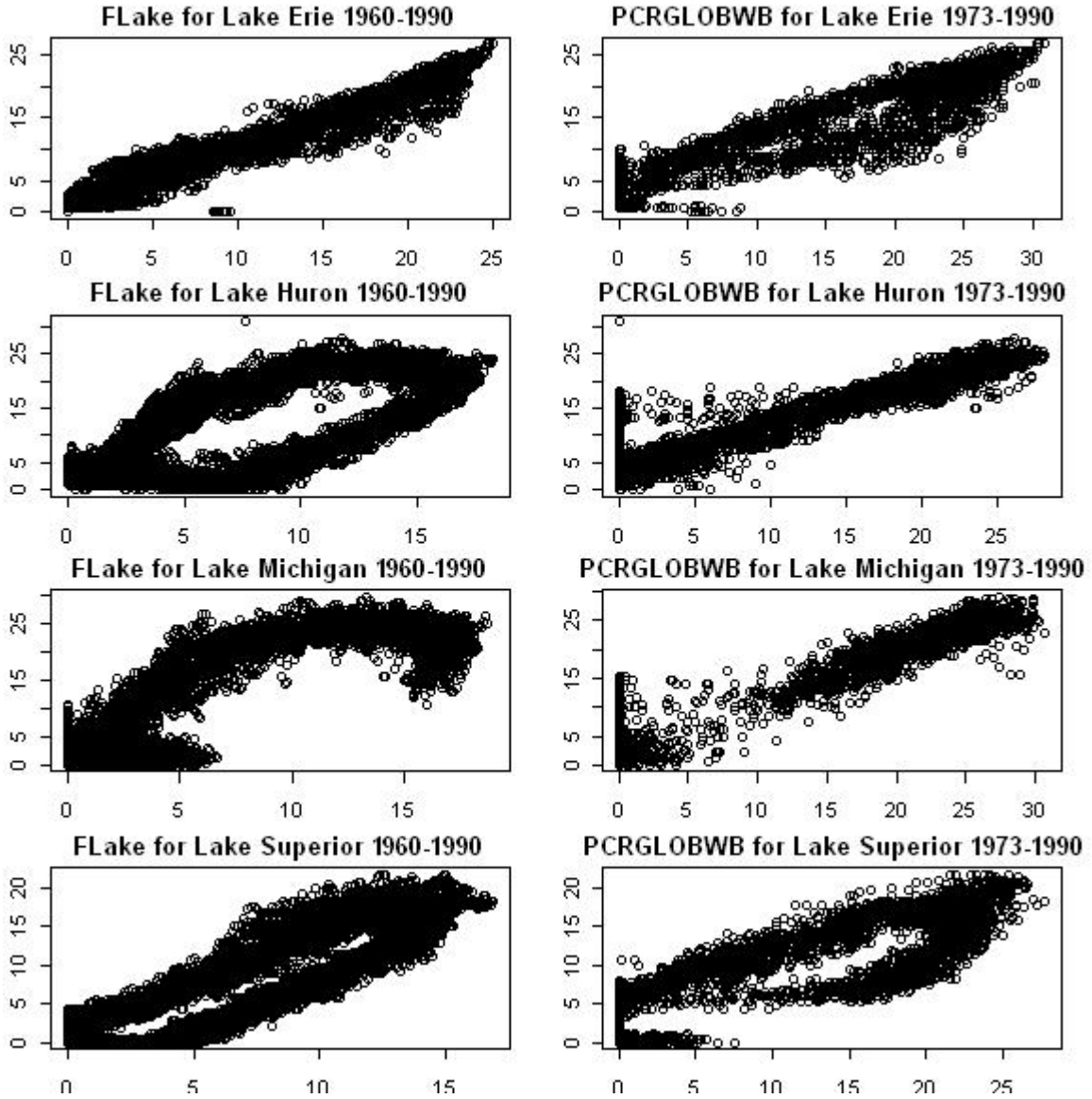

FIGURE 13 RELATION SIMULATED AND OBSERVED TEMPERATURE FOR THE GREAT LAKES OVER 1960-1990 WITH FLAKE (LEFT) AND WITH PCR-GLOBWB (RIGHT) (X=SIMULATED TEMPERATURE IN DEGREES CELCIUS AND Y=OBSERVED TEMPERATURE IN DEGREES CELCIUS)

	Spearman Correlation FLake	***Spearman Correlation PCR-GLOBWB***	***FLake***			**PCR-GLOBWB**		
Lake			R^2	*α*	*Standard error*	R^2	*α*	*Standard error*
Erie	0.98	0.93	0.97	0.98	1.43	0.88	1.11	3.58
Huron	0.99	0.88	0.5	1.3	3.8	0.86	0.98	3.65
Michigan	0.79	0.92	0.66	0.5	3.37	0.92	0.99	3.13
Superior	0.89	0.87	0.8	0.8	2.1	0.8	1.2	3.7

TABLE 8 STATISTICS OF THE GREAT LAKES FOR FLAKE AND PCR-GLOBWB

The models both show acceptable results (table 8), although it can be seen that for Lake Erie the results of FLake are very good. Yearly graphs of the observations and simulations can be found in Appendix IIA and IIB. The FLake model does not reflect an overall improvement compared to PCR-GLOBWB. The advective energy fluxes alone produce the observed lake temperatures very well. Inclusion of mixing and the use of a few input parameters like in the FLake model gives on the other hand also good results and takes less computational modelling time.

Lake	Average Tobserved (°C)	Average Tsimulated (°C)	RMSE	NSC
Erie	11.00	10.25	1.13	0.99
Huron	11.28	7.91	7.89	0.33
Michigan	13.16	7.32	10.65	0.24
Superior	6.33	5.76	3.99	0.59

TABLE 9 RESULTS FLAKE SIMULATION AND OBSERVATION OF FOUR LAKES

Additional information about the performance of the model is given by the Root mean squared error (RMSE) and the Nash-Sutcliffe coefficient (NSC). The NSC reflects the signal and thus the peaks of the simulation. This causes a better result for lake Huron compared to lake Michigan, where data is missing for autumn. A combination of the *RMSE* and the *NSC* is a good addition in the interpretation of the data, while the NSC is highly influenced by outliers. The results in table 8 show that the simulations of FLake are best for lake Erie and lake Superior. For lake Huron the match is much smaller.

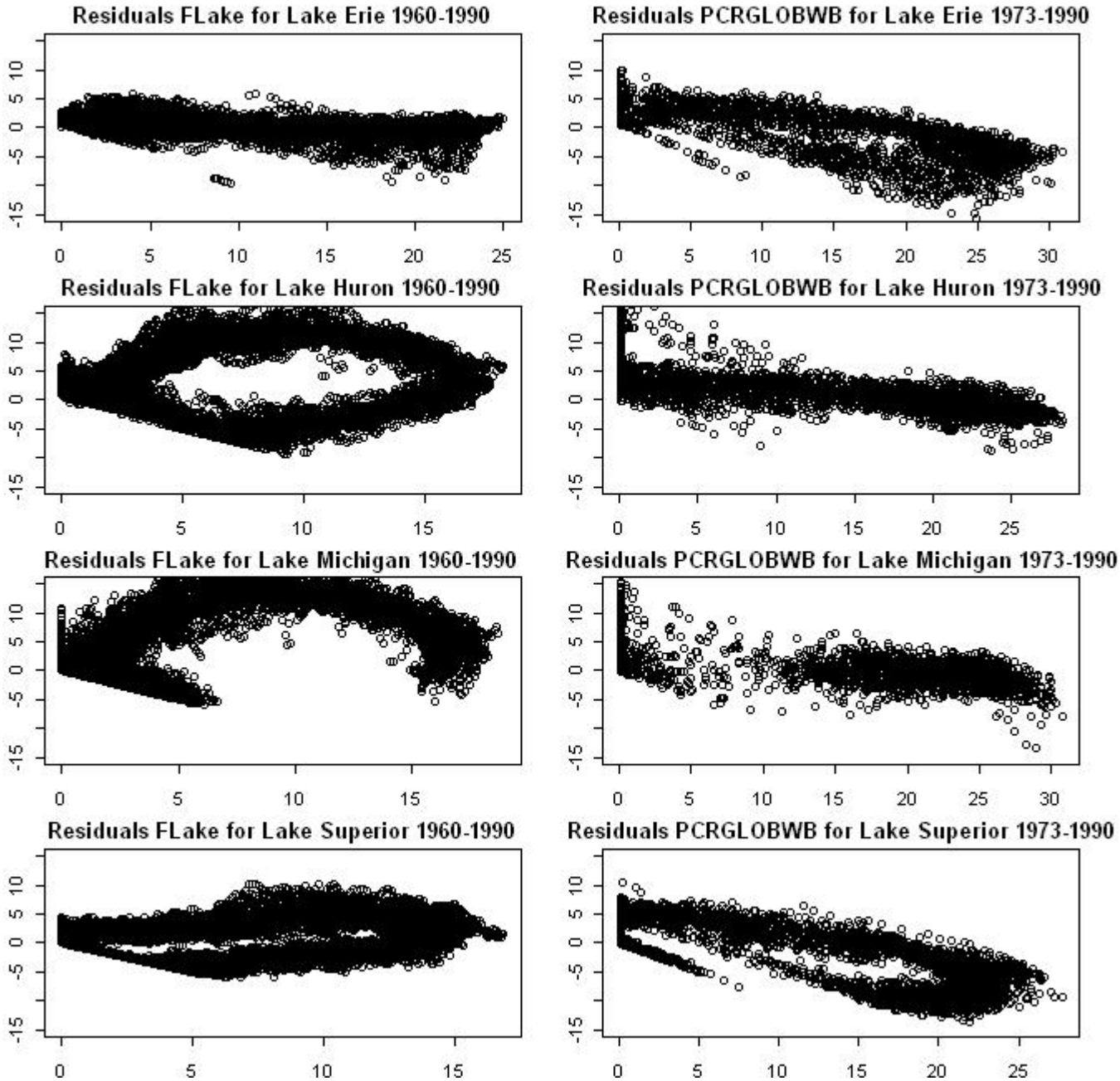

FIGURE 14 RESIDUALS OF FLAKE (LEFT) AND PCR-GLOBWB (RIGHT) (X=SIMULATED TEMPERATURE IN DEGREES CELCIUS, Y=OBSERVED-SIMULATED TEMPERATURE).

Residual plots were made in order to visualize the difference between observed and simulated temperature for each lake. The period for PCR-GLOBWB is reduced until 1990, because there were only observation from 1960-1990 for the Great Lakes. For

PCR-GLOBWB a slightly negative slope can be observed, which means a small underestimation in winter and overestimation in summer.

4.3 CLIMATOLOGY GEMS STATIONS FOR DIFFERENT MONTHS

The global results are covered in the GEMS stations. The seasonal performance is given in the statistics where for all stations for the total period each month of the year was analysed (table 10). An error can be based on a displacement, r^2, or by a different error, reflected in α, like positioning which can lead to a different upstream area. A comparison for all GEMS stations, which were assumed to represent all global rivers, was made of the modelled temperature with the observations. The relative drainage error varies from -0.9 to 160, but 43% has a error less then 10%. The highest relative standard error is 1.66 for the Lena river. The results for all 267 stations are shown Appendix IV sorted by the relative standard error. Based on the RSE (≤0.25) about 80% of the stations show reasonable accuracy.
Table 10 shows the statistics for each month to analyse the performance over the year.

Month	*RSE*	*$\bar{O}$*	*SE*	*R^2*	*α*
January	0.22	11.83	2.64	0.92	0.93
February	0.20	12.32	2.49	0.94	0.98
March	0.20	13.35	2.62	0.93	1.00
April	0.18	14.59	2.68	0.92	1.01
May	0.28	18.82	5.33	0.49	1.12
June	0.17	19.12	3.30	0.79	1.07
July	0.17	20.45	3.41	0.73	0.85
August	0.14	20.80	2.85	0.81	0.88
September	0.13	18.75	2.47	0.88	1.02
October	0.14	16.28	2.35	0.92	1.01
November	0.19	13.87	2.58	0.91	0.97
December	0.19	12.45	2.36	0.94	1.08
Min	0.13	11.83	2.35	0.49	0.85
Max	0.28	20.80	5.33	0.94	1.12

TABLE 10 STATISTICS OF GEMS MEAN AVERAGE TEMPERATURE.

The standard deviation was also modelled. The average standard deviation is between 1.88 and 2.3 degrees Celsius. This is relatively small compared to the average temperature that lies between about 12 en 21 degrees Celsius. The R^2 for the average temperature is lowest for the month May and this is also the only month with a low R^2, for all other months the R^2 is very high and also the slope varies around 1. Melting water plays an important role in May, but also a random error could cause the discrepancy. The overall result over the year is equal and consistent.

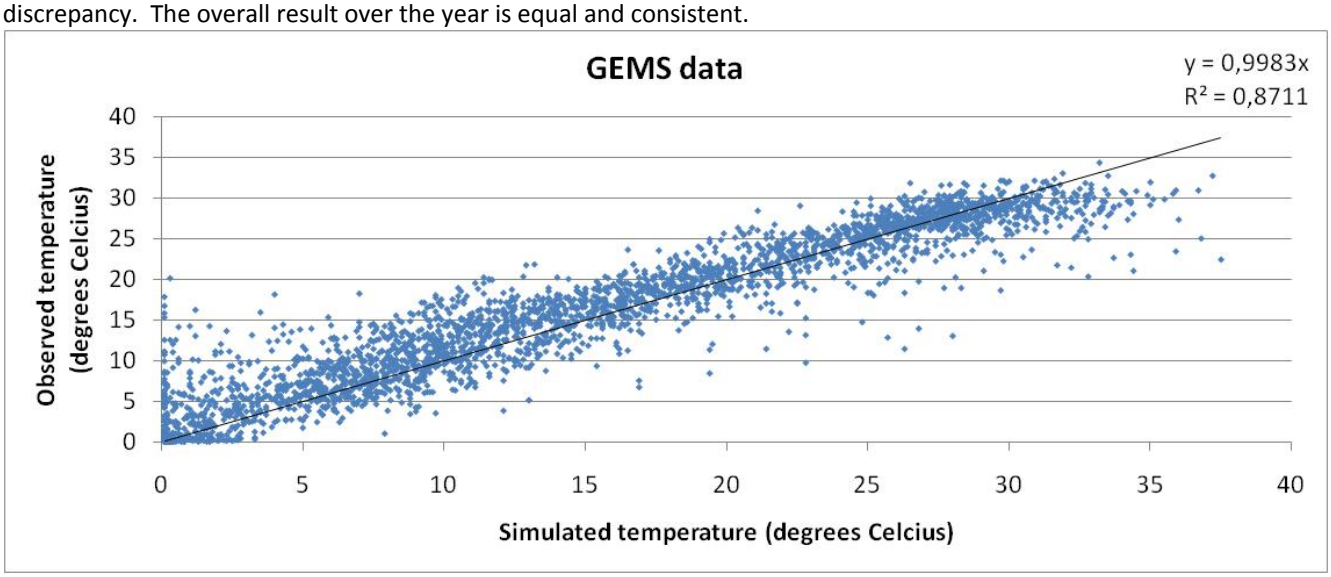

FIGURE 15 RELATION BETWEEN SIMULATED AND OBSERVED TEMPERATURE FOR ALL GEMS STATIONS FOR THE PERIOD 1975-2004.

In figure 15 the relation between observed and simulated temperatures for all GEMS stations were plotted through the origin and the result shows a slope close to 1 and more than 87% of the simulations are predicted correctly by the model.

4.4 CLIMATOLOGY OF GEMS STATIONS FOR DIFFERENT CLIMATES

It was expected that the model had difficulties for certain specific climates as could be observed from the RSE in Appendix IV. Plotted as a boxplot in figure 16, it becomes clear that the RSE decreases with warmer climates. High RSE strictly occurs for colder climates (Tundra, Forest Tundra, Boreal Forest, Cold Parklands and Temperature Forest). Warmer climates on the other hand have very small RSE. To analyse this, the data of the GEMS stations was divided over different climates for the total period of 1975-2004. The responses for typical climate zones are shown for both a summer and a winter month to discover the ability of the model to simulate different climates and to analyse spreading of the results around the linear 1:1 line. The match between simulated and observed temperature and discharge for the all months can be analysed from the figures in Annex VI en VII. As shown in figure 17 for both winter and summer all climates perform well. It can only be observed that there is an increase in temperature from winter to summer for the temperate climates. The R^2 is low for Tundra and Tropical Rain Forest. The relative standard error is high for climates with low observational mean temperature and low for climates with high mean temperature. This means the error made for colder climates is relatively large. An overview of the results is shown in table 11.

Climate	n	RSE	$\bar{O}$	SE	R^2	α
Tundra	58	0.84	6.44	5.43	0.42	1.11
Cold Parklands	36	0.68	4.37	2.98	0.75	0.85
Forest Tundra	125	0.60	5.09	3.04	0.64	1.15
Boreal Forest	288	0.57	6.33	3.58	0.65	1.10
Cool Desert	0	-	-	-	-	-
Steppe	80	0.19	11.70	2.28	0.91	0.87
Temperate Forest	1040	0.22	11.30	2.47	0.82	0.99
Hot Desert	115	0.21	22.41	4.69	0.73	1.13
Chapparal	254	0.18	15.67	2.77	0.82	1.00
Warm Temperate Forest	154	0.17	15.24	2.56	0.84	0.91
Tropical Semi-Arid	106	0.07	25.78	1.82	0.83	0.98
Tropical Dry Forest	235	0.09	27.65	2.52	0.63	0.97
Tropical Seasonal Forest	327	0.07	24.70	1.81	0.84	1.01
Tropical Rain Forest	145	0.07	27.45	1.85	0.26	0.98

TABLE 71 STATISTICS OF GEMS AVERAGE TEMPERATURE FOR DIFFERENT CLIMATES

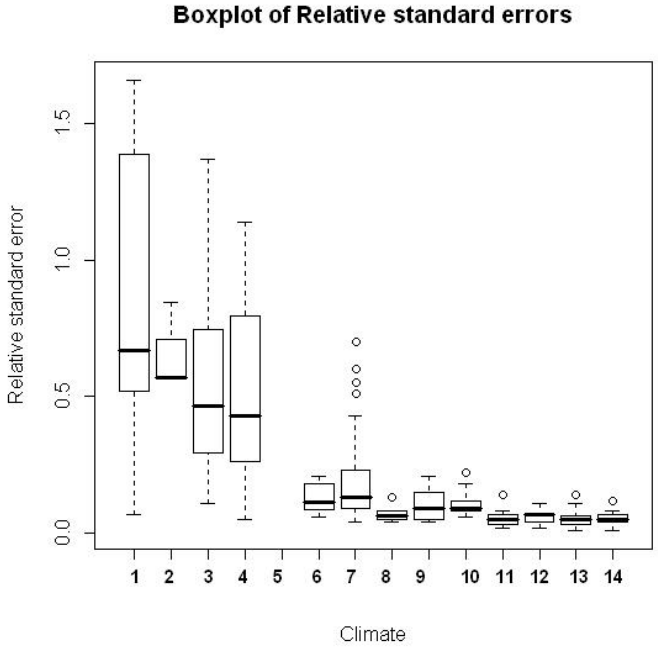

Nr	Climate name
0	Oceans
1	Tundra
2	Cold Parklands
3	Forest Tundra
4	Boreal Forest
5	Cool Desert
6	Steppe
7	Temperate Forest
8	Hot Desert
9	Chapparal
10	Warm Temperate Forest
11	Tropical Semi-Arid
12	Tropical Dry Forest
13	Tropical Seasonal Forest
14	Tropical Rain Forest

FIGURE 16. BOXPLOT OF THE RELATIVE STANDARD ERRORS FOR DIFFERENT CLIMATES.

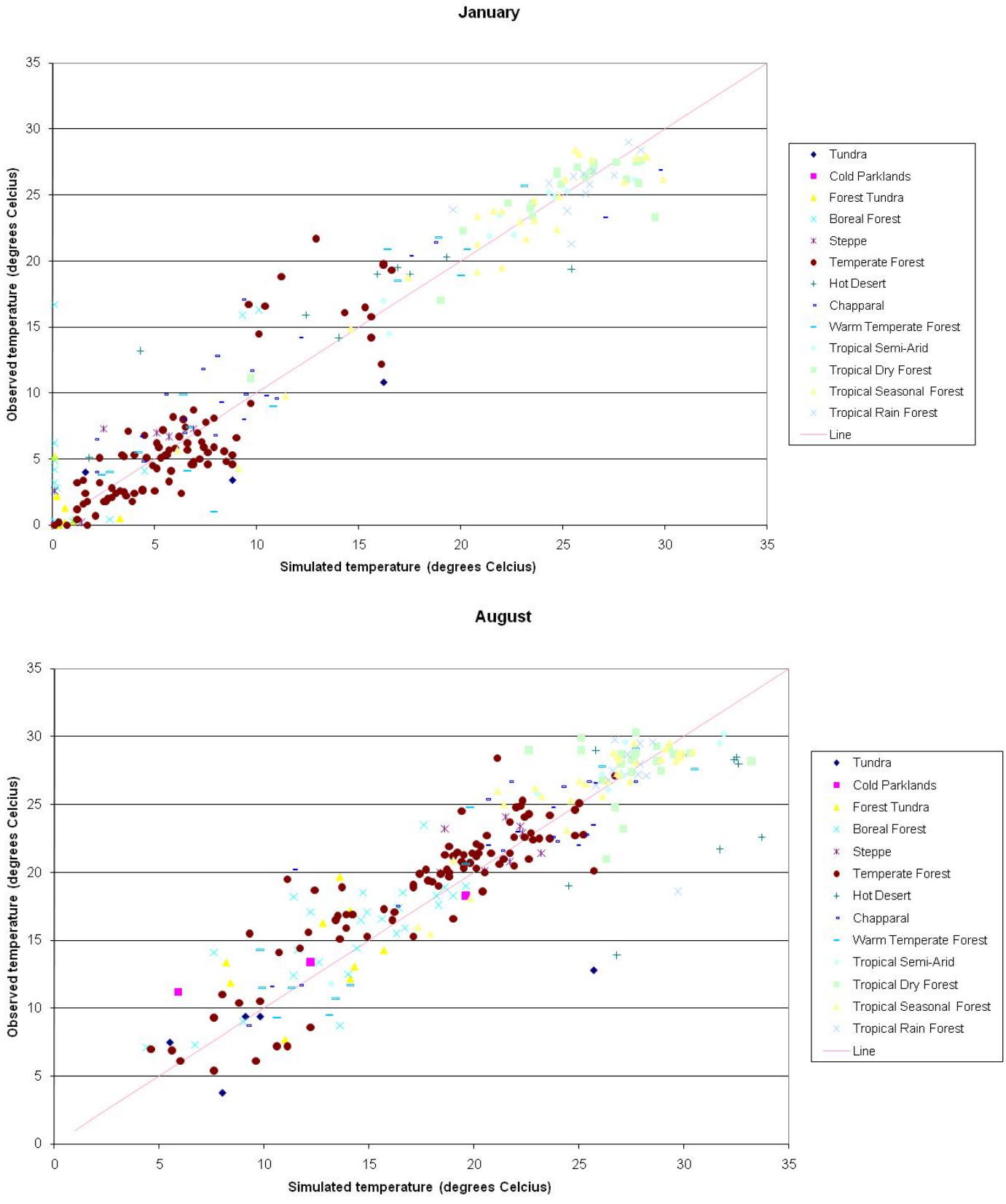

FIGURE 87 SIMULATED AND OBSERVED WATER TEMPERATURE FOR JANUARY AND AUGUST. EACH SYMBOL REFLECTS A DIFFERENT CLIMATE

4.5 STATISTICS FOR LARGEST RIVERS

From the list of GEMS stations the available largest rivers (given in section 2.2.1) were selected to analyse them in more detail.

GEMS ID	*River name*	*Drainage area error*	*Average Temperature*					*Average Discharge*				
			RSE	**Ō**	**SE**	**R^2**	**α**	**RSE**	**Ō**	**SE**	**R^2**	**α**
5001	Yangtze River (Chang Jiang)	0.45	0.10	17.90	1.85	0.94	0.88	0.14	13588.75	1874.86	0.97	0.84
26009	Amur River	0.04	**0.83**	9.97	8.28	0.21	1.26	0.23	9522.53	2225.35	0.91	1.00
26011	Ob River	-0.16	**0.66**	4.93	3.27	0.78	1.28	0.44	13083.76	5761.20	0.73	1.12
26018	Lena River – Kusur	-0.003	**1.37**	2.86	3.93	0.46	1.05	0.48	17096.35	8255.77	0.87	1.17
26701	Mississippi River - Vicksburg MS	0	0.09	17.66	1.60	0.98	1.00	0.20	18581.27	3802.26	0.69	1.08
28021	St. Lawrence River - Massena NY	-0.8	0.19	11.29	2.20	0.94	1.10	0.04	7800.63	300.47	0.60	4.38
54009	Mekong River - Chiang Saen	0.03	0.09	23.26	2.01	0.48	1.10	0.13	2522.58	337.47	0.96	1.35
54010	Mekong River - Nakhon Phanom	0.01	0.04	26.77	1.15	0.76	0.95	0.27	6403.53	1707.49	0.92	1.29
54011	Mekong River - Khong Chiam	0.01	0.07	26.43	1.73	0.31	0.92	0.25	9281.12	2282.70	0.94	1.50
136002	Lower Ganges River - at Padha	-	0.08	26.48	2.12	0.41	0.93	0.12	11024.33	1333.21	0.99	1.10
136003	Brahmaputra River	-	0.05	27.74	1.29	0.80	1.04	0.14	22547.41	3221.35	0.97	1.66
303012	Amazonas River – Obidos	-	0.06	28.11	1.73	0.39	0.93	0.15	170712.52	24975.15	0.74	1.29

TABLE 8 THE RELATIVE DRAINAGE AREA ERROR AND STATISTICS FOR LARGEST RIVERS FOR THE AVERAGE TEMPERATURE AND AVERAGE DISCHARGE.

The bias in average temperature cannot be explained by the modelled discharge as shown in table 12. It is more likely that the model faces problems for colder regions. The temperature of colder rivers like the Amur, Ob and the Lena are underestimated, whereas the RSE for the other rivers is relatively good.

4.6 DAILY DATA OF USGS STATIONS

Next to the monthly signal it is also interesting to validate the model with daily data to examine the ability to simulate the daily pattern with its peaks. The results are shown in table 13. The modelled temperatures over the year are shown in Annex III. Contrary to the GEMS stations the correlation for the discharge simulated for the USGS stations is very low, whereas for most of the USGS rivers the model performs well for the temperature as shown by the RSE. The temperature result for Colorado LeesFerry is the poorest. The results for Colorado Silver in the Colorado River although is of good quality. The temperature peak in summer (Appendix III) for St. Croix, Colorado Cameo and Colorado Utahstateline River are underestimated in the simulations. This is also shown by α that is small for these stations. For five stations α indicates underestimation. For the USGS stations, the low Spearman correlations (ρ) for Colorado_LeesFerry and McKenzie_SouthFork correspond with the lowest R^2. McKenzie_SouthFork also has a large drainage area error of 307%. Remarkable is also the relative good result of Jackson river with a drainage area error of 171%.

ID	River name	Coverage	Drainage error	ρ	Average Temperature					Average Discharge				
					RSE	Ō	R^2	α	SE	RSE	Ō	R^2	α	SE
1	Arkansas_abovePueblo	56	-0.6	0.8	0.4	11.0	0.6	1.0	5.3	1.4	5.56	0.0	0.1	7.83
2	Arkansas_JohnMartinr	56	0.09	0.8	0.3	12.5	0.8	0.1	3.7	1.8	30.41	0.1	1.3	56.97
3	Arkansas_Lasanimas	55	0.36	0.9	0.2	13.2	0.8	0.1	3.8	2.4	23.88	0.0	2.0	57.37
4	Colorado_Cameo	67	-0.09	0.8	0.2	10.1	0.7	0.0	2.9	3.6	44.80	0.0	1.6	163.3
5	Colorado_LeesFerry	48	-0.02	**0.3**	0.9	9.18	0.0	2.7	8.8	1.6	280.0	0.2	2.9	452.2
6	Colorado_Silver	66	0.01	0.9	0.1	18.3	0.9	0.8	2.3	0.2	235.4	0.0	0.1	58.33
7	Colorado_Utahstateline	43	0.19	0.9	0.3	11.5	0.7	0.1	3.5	1.3	192.7	0.2	0.8	256.5
8	Delaware_Trenton	87	0.06	0.9	0.1	13.3	0.9	1.0	1.9	0.4	302.3	0.4	0.6	145.7
9	Greenriver_Campbellsvill	50	0.39	0.7	0.3	12.7	0.2	0.8	4.7	0.7	27.02	0.0	0.3	19.54
10	Jacksonriver	78	1.71	0.7	0.1	15.0	0.9	0.9	2.7	0.8	16.47	0.0	0.6	14.08
11	Potomac_nearWash	50	0.04	0.9	0.2	11.7	0.4	0.9	3.2	0.3	262.8	0.2	0.2	98.95
12	SanJoaquin_Vernalis	93	0.05	0.9	0.1	16.7	0.8	0.7	2.6	2.6	218.8	0.0	1.3	579.7
13	Mckenzie_SouthFork	67	3.07	**0.5**	0.2	7.72	0.1	1.0	1.9	1.0	44.11	0.0	1.7	48.05
14	StCroix_Milltown	62	-0.42	0.8	0.1	11.8	0.7	0.5	1.6	0.4	54.81	0.1	0.4	22.98
15	Whiteriver_Centerton	82	-0.25	0.8	0.1	14.7	0.8	0.8	2.7	0.8	63.08	0.1	0.4	55.06

TABLE 9 COVERAGE, DRAINAGE ERROR, SPEARMAN CORRELATION (P) AND STATISTICS OF USGS STATIONS

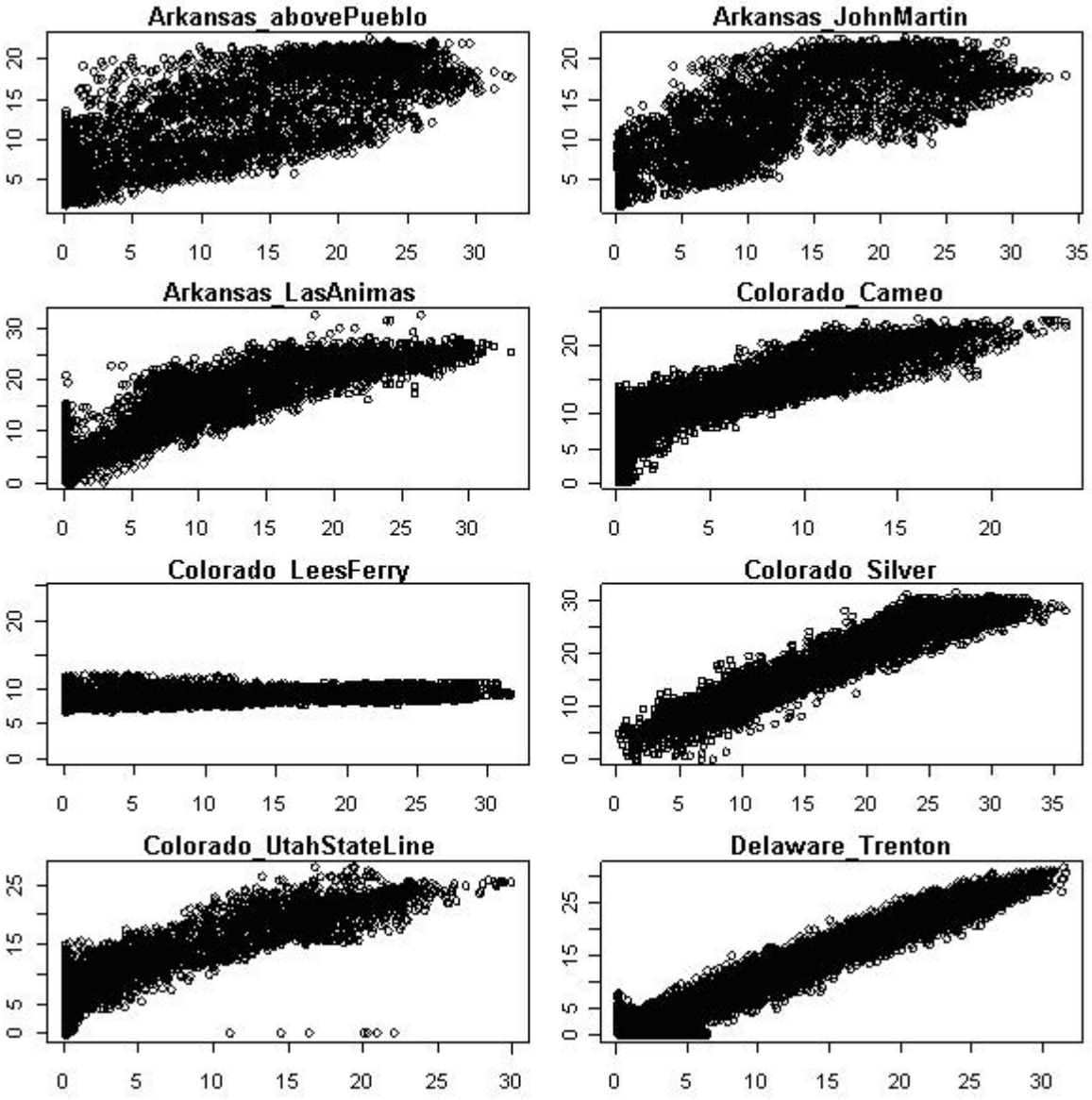
Arkansas_abovePueblo
Arkansas_JohnMartin
Arkansas_LasAnimas
Colorado_Cameo
Colorado_LeesFerry
Colorado_Silver
Colorado_UtahStateLine
Delaware_Trenton

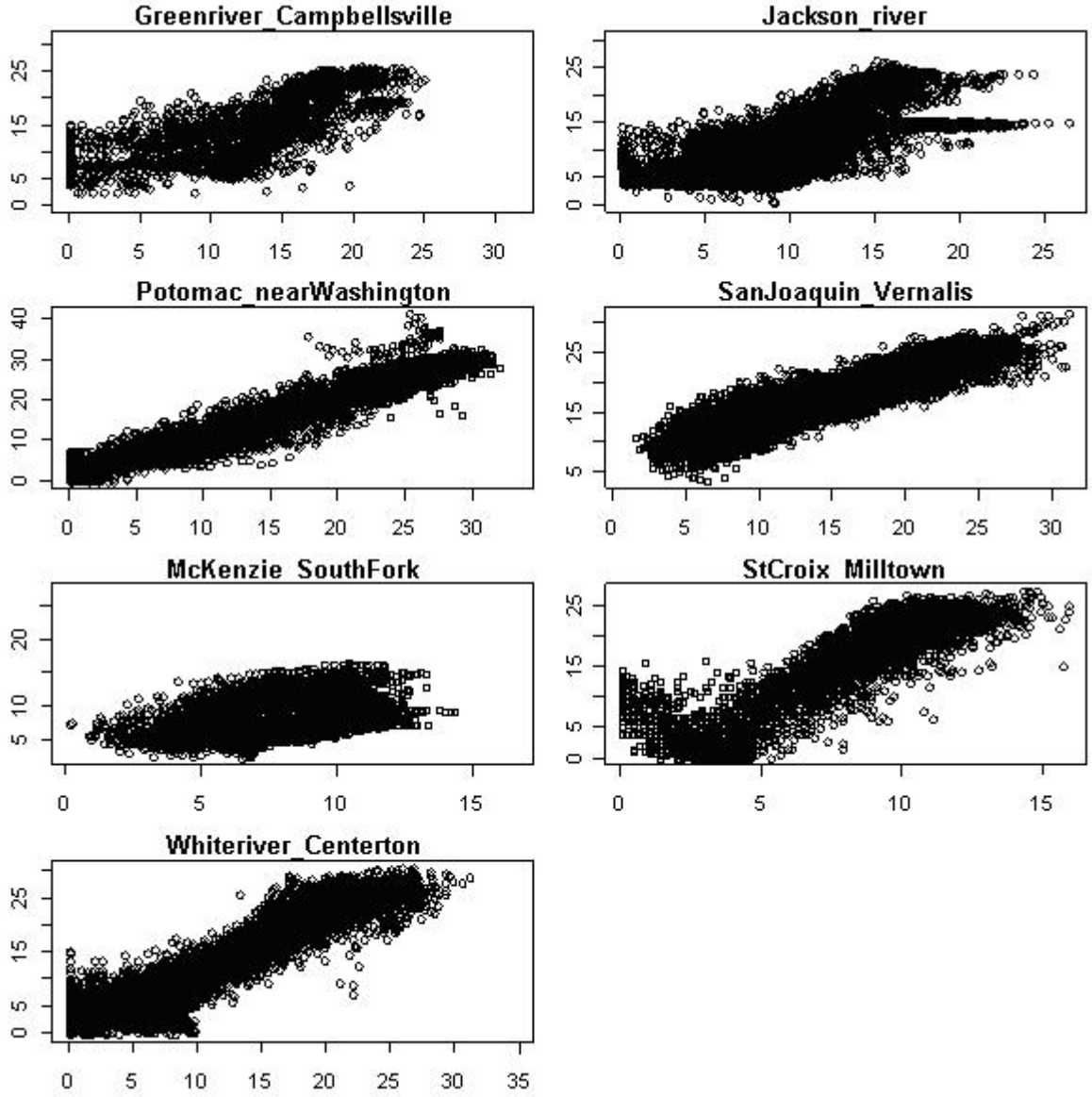

FIGURE 18 RELATION SIMULATED AND OBSERVED TEMPERATURE FOR THE USGS STATIONS FOR 1975-2002 (X=SIMULATED TEMPREATURE (DEGREES CELCIUS, Y=OBSERVED TEMPERATURE (DEGREES CELCIUS))

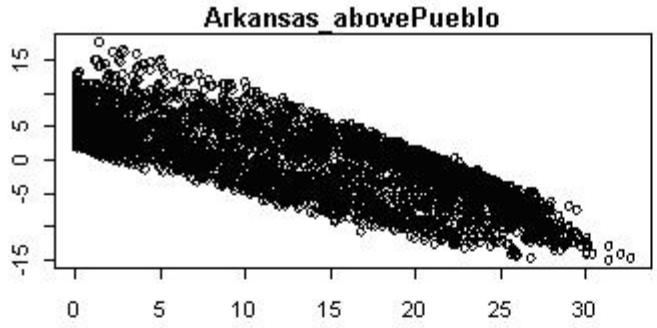
Arkansas_abovePueblo

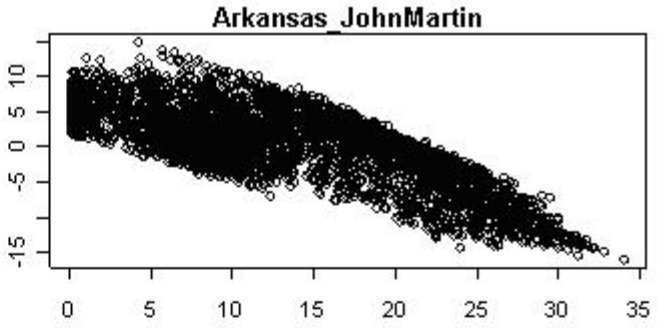
Arkansas_JohnMartin

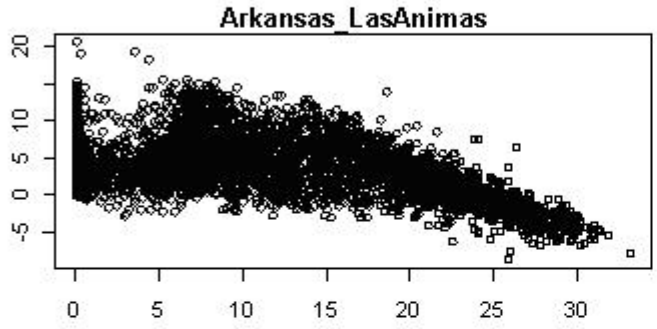
Arkansas_LasAnimas

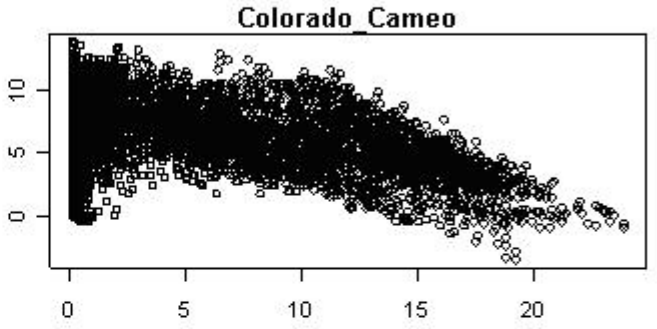
Colorado_Cameo

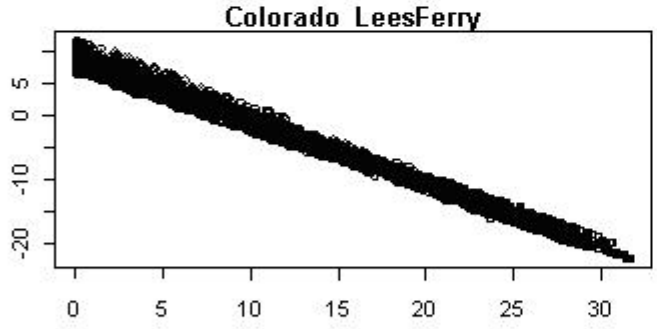
Colorado_LeesFerry

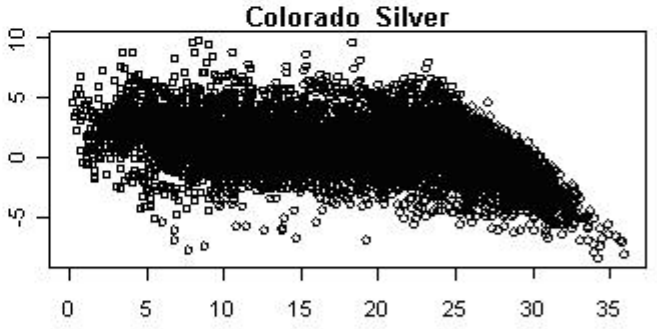
Colorado_Silver

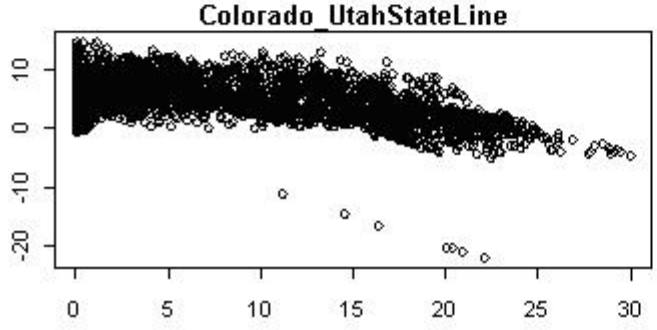
Colorado_UtahStateLine

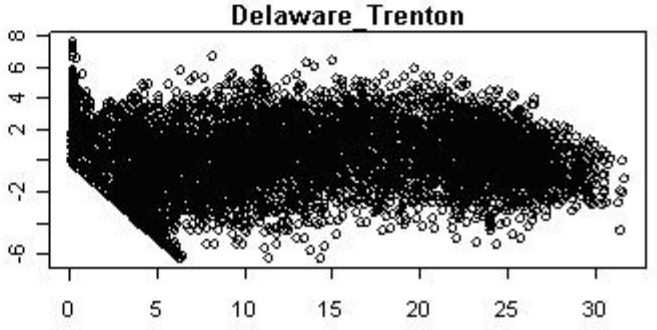
Delaware_Trenton

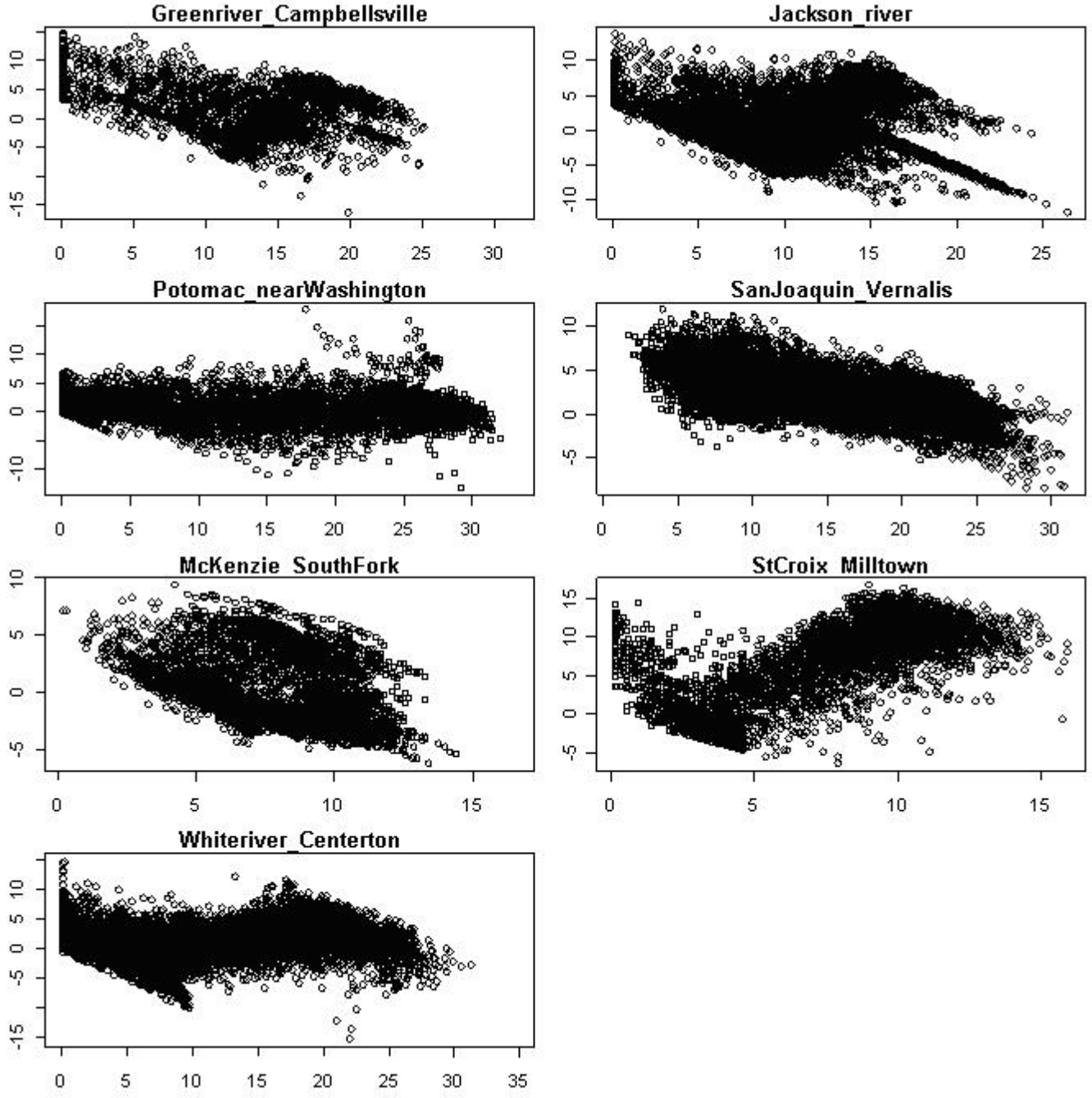

FIGURE 19 RESIDUALS FOR THE USGS RIVERS (X=SIMULATED TEMPERATURE IN DEGREES CELCIUS, Y=OBSERVED-SIMULATED TEMPERATURE)

4.7 Difference between water and air temperature

With the use of the difference between air temperature and surface water temperature it is possible to analyse the areas and timing where inclusion of water temperature is mostly needed. The difference is expressed as:
$\Delta T = \sum |(T_{air}-T_{water})/n|$
This comparison was made for all 267 stations from the GEMS database.

Figure 20 shows the development of the difference between water and air temperature over the year for the GEMS stations, split up for the 14 different climates. The number of stations were not equally divided over the climates, which causes a bias in the results. The monthly average for the stations on the southern hemisphere were shifted six months and included in the figure. The difference is highest for the colder regions like the cold parklands, (forest) tundra and boreal forest. For the warmer climates the difference is much smaller and also equal over the year as shown for the tropical forest.

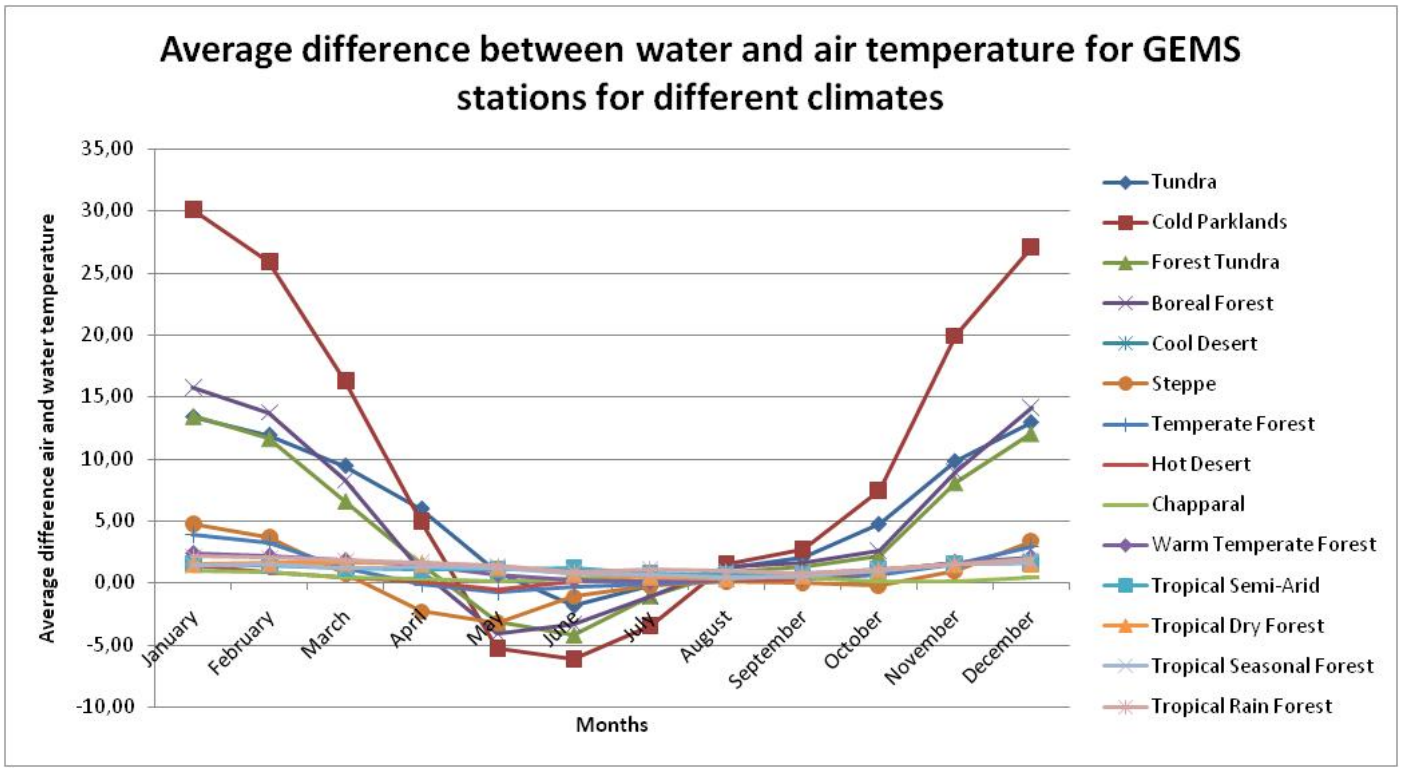

FIGURE 20 DIFFERENCE BETWEEN WATER AND AIR TEMPERATURE FOR EACH MONTH FOR ALL GEMS STATIONS SPLIT UP OVER THE DIFFERENT CLIMATES

Maps 6 shows the surface temperature difference between water and air for winter and summer at the start of the modelling period (1975) and for the year 2000. They show that the over result is the same during the modelling period.
A close up is given in map 7 and 8 where the difference of the river temperature compared to its surrounding can be observed.

Δavg for January 1975

Δavg for January 2000

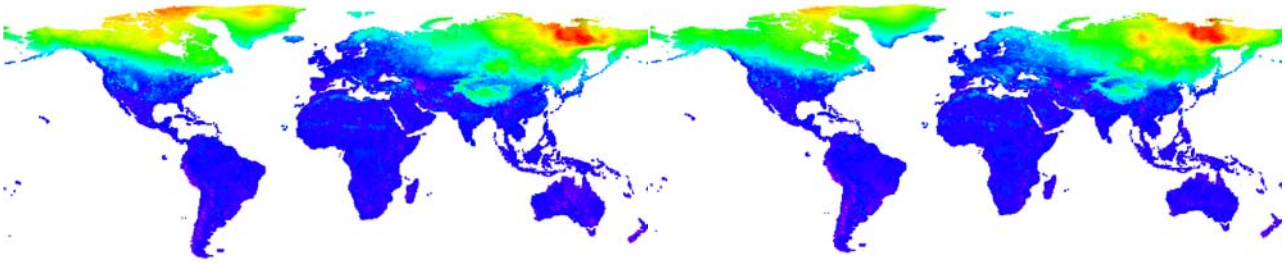

Δavg for August 1975

Δavg for August 2000

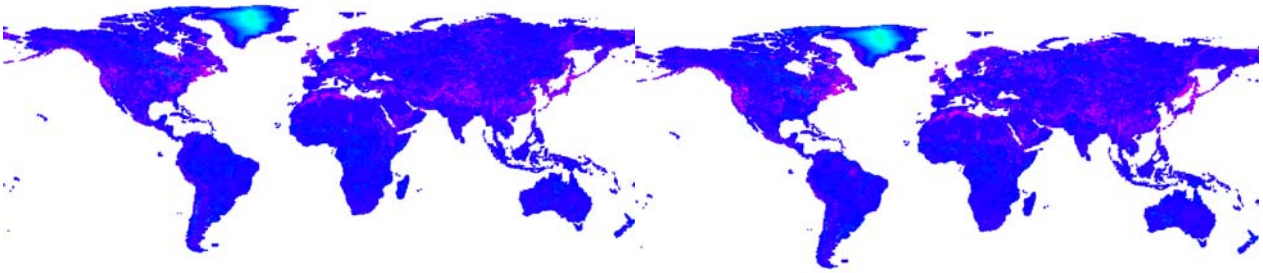

Tavg for January 1975 in kelvin

Tavg for January 2000 in kelvin

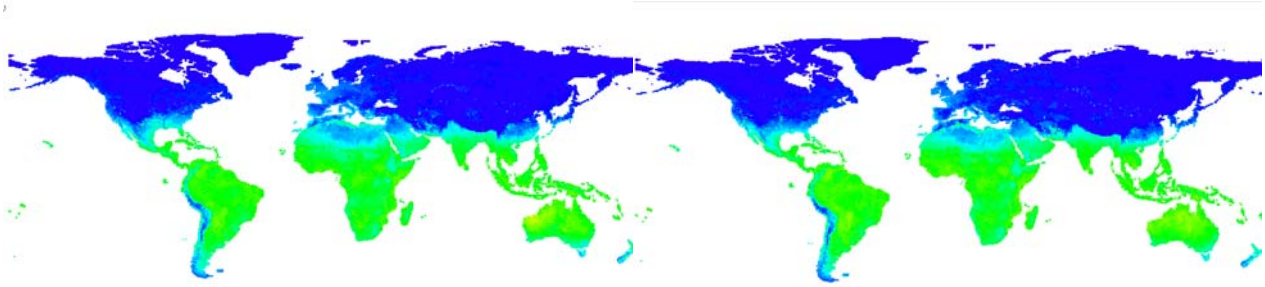

Tavg for August 1975 in kelvin

Tavg for August 2000 in Kelvin

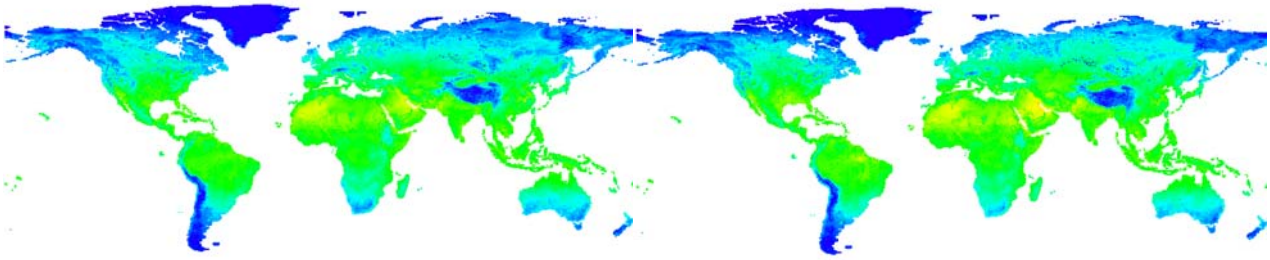

MAP 6. ΔAVG (DEGREES CELCIUS) AND TAVG (KELVIN) FOR WINTER AND SUMMER 1975 AND 2000

The difference between water and air temperature is highest in winter in the upper northern regions and the Himalaya. In the red area differences are over 50 degrees Celsius. This can be explained by the very low freezing air temperatures, whereas the water temperature is limited to a minimum of 0 degrees Celsius.
In summer a negative difference (purple spots) was found for a lot of smaller spots. This indicates places where the water temperature is lower compared to the air temperature. This becomes more clearly in map 7 where water that is cold compared to the air temperature is red.

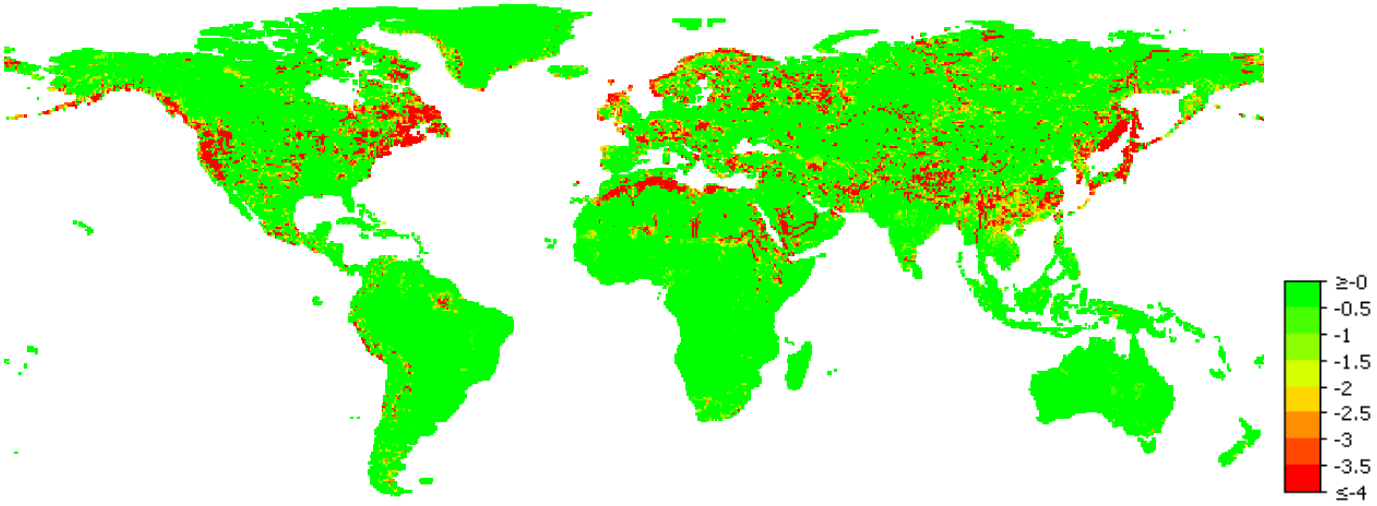

MAP 7 NEGATIVE DIFFERENCE BETWEEN WATER AND AIR TEMPERATURE IN AUGUST

Locations where the water temperature is above the air temperature (without freezing) have a Δavg>0 and these rivers transport heat. In map 8 they are shown from yellow to red. Greenland shows Δavg of around 15 degrees Celsius which can be explained by the year-round snow cover (also present in the Alps, Andes and Himalaya). Places that contain very few water also show Δavg>0, but this is more likely a model error due to low water availability.

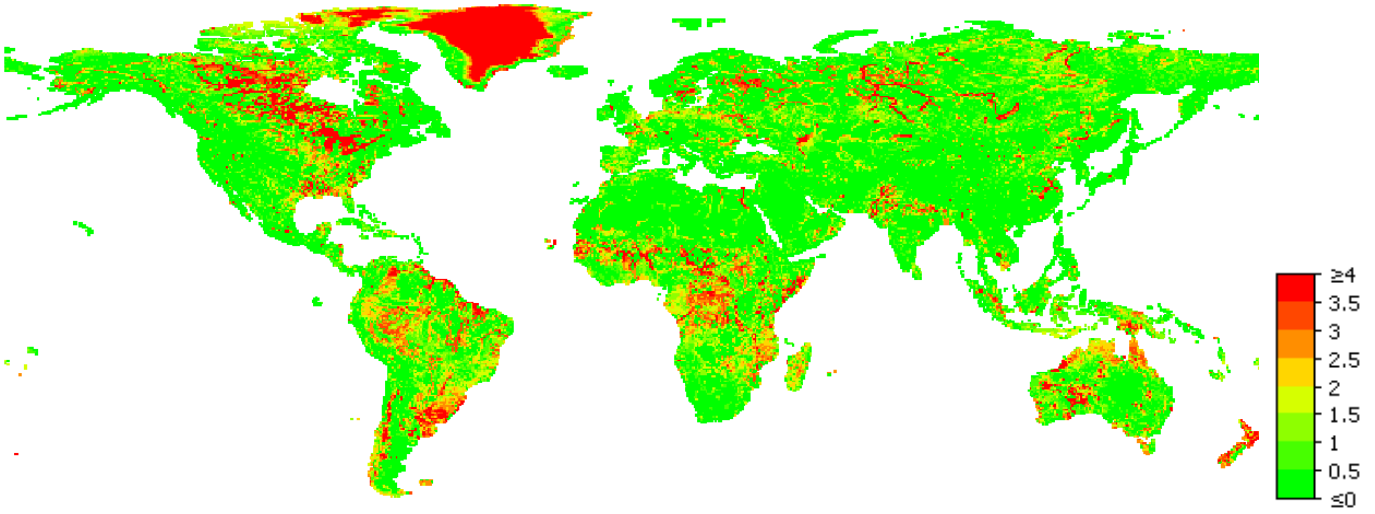

MAP 8 POSTIVE DIFFERENCE BETWEEN WATER AND AIR TEMPERATURE IN AUGUST

Map 9 and 10 give the average water temperature and were used to compare river temperature with the temperature of the surrounding. In summer the rivers are colder in the northern region and in winter the Nile is warmer compared to its surrounding.

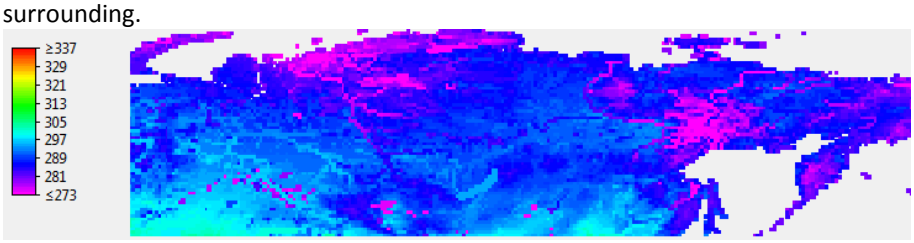

MAP 9 RIVER TEMPERATURE ANOMALIES RELATIVE TO THEIR SURROUNDING IN AUGUST IN KELVIN

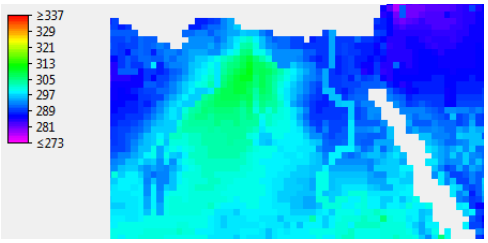

MAP 10 HEAT TRANSPORT IN THE RIVER NILE IN JANUARY IN KELVIN

5. DISCUSSION

Data collection is a major part of research and data on long term studies is extremely rare. Therefore it is not always possible to collect the most optimal locations for calibration. To construct a global fresh surface water model it seems relevant to calibrate the model with temperature data from different climate zones. During data collection it was seen that temperature data is frequently available in North America, but extremely rare in other parts of the world, especially for fresh surface waters on the southern hemisphere. Although there are several studies that use long-term records, the data is not always accessible. Especially, more lake data is needed for further evaluation of the contribution of FLake to the model results. The GLWD database is a good starting point for lake research, but should be extended with long-term time series of several parameters.
On the other hand, GEMS has global cover and the daily data from the USGS has good quality. Also for this research a selection of the USGS available data was made based on a minimum coverage for the period 1975-2004, but also data is available for other decades or shorter periods.
Comparable to the modelling with FLake is the research of Peeters *et al.* (2002) that uses SIMSTRAT to model a long term record of a large central European lake. In the study however the model is only applied to one specific lake, namely Lake Zurich, and the performance of the model for other lakes is not evaluated. Furthermore there are no other studies that use a physical model to simulate fresh surface water temperature on a global scale.
Due to the growing interest of the effects of climate change there has been a lot of research on surface water temperature on local scales. Indeed there has not been made attempt to model fresh surface water temperatures globally. This research shows how a physical model can be used to model the complex relations between water and atmosphere. The model can be used for a wide range analysis and the results influence a broad range of disciplines, such as fishery, shipping, industries using cooling water and governmental decision making against climate change.
The monthly data shows less reliable results for colder climates when concentrating on climates and to the largest rivers. This suggests that the model can be improved with a calibration that especially focuses on the colder regions. The water height and ice thickness can be further analysed as these are important endpoints of the model. Also the model has a relatively coarse grid size which leads to errors in the localization of measurement stations and thus errors in the drainage area. To evaluate the effects of small rivers and lakes the grid size should be reduced, although the reduction of grid size depends on the computation capacity needed to run the model. Also, more detailed data like meteorology is needed to facilitate a smaller grid. In particular data accessibility plays an important role in further modelling together with data quality, because a lot of data ranges contain a lot of missing values or have a limited time range. On the other hand the increasing number of field investigations has revealed the complexity of the heat fluxes fundamentally controlling water temperature behaviour. The model results give the possibility to apply a climate scenario to predict future temperatures globally or for a specific region like the inflowing rivers of the Arctic Ocean. Next, the allocation of the stations has led to inaccuracy as reported in the relative drainage area error. On the other hand, a higher drainage area error is mostly not directly reflected in the results.
A lot of research is concentrated on the Great Lakes because of the great amount of water that is stored in these lakes. Especially Lake Erie has been subject to different types of research, because it has an area of about 80 km in width and 200 km long, but with only a mean depth only 18 m and it is therefore the shallowest lake of the Great Lakes Basin. For instance a one-dimensional model for the vertical mixing in Lake Erie in summer was developed (Ivey and Patterson, 1984). Also the thermal stratification of the South Bay (Lake Huron) is analysed with the use of an extensive empirical data set. Research to the data of Lake Superior has shown the increase in water temperature over the last decades (Austin and Colman, 2008). Lake Michigan has been used for ecological research such as fish population and substances in the food chain. Modelling these specific lakes with FLake was therefore very relevant and useful.
The FLake model produces daily temperature for all major global lakes and this data can be inserted in PCR-GLOBWB on the next day (t+1) to update the lake temperature that was modelled by PCR-GLOBWB. In order to do this the two models have to be converted to the same computer language.
For further exploration of the difference between the performance of Flake and PCR-GLOBWB, the lake data from PCR-GLOBWB that was applied to all global fresh surface waters including all major lakes can be used. The results for these lakes can be compared with result that produced with FLake because the needed input data is already provided for the lakes from the ILEC database as shown in Appendix IX and this list can be expanded with the GLWD lakes if the assumed relation between depth and transparency is applied. A further validation for lakes can be performed if more observations of lake temperature become available.

6. CONCLUSION

The understanding of the physics behind the water and energy fluxes is crucial in modelling fresh surface water temperatures. Also the temporal and spatial variability of fresh surface waters highly influences the temperature. Temperature studies are useful for a broad range of disciplines including hydrology, engineering, ecology, climatology and geography. The findings of this research can be used for river management, decision making in politics and for further research on the topic.

The results of temperature simulation for fresh surface lakes suggest that both the FLake model and the model PCR-GLOBWB perform well. When comparing the two models, PCR-GLOBWB in general over- and underestimates the peaks in summer and in winter, whereas FLake underestimates the maximum summer temperatures. The advantages of FLake are that it needs just few parameters that can be derived relatively easy and it also requires very few calculation time to run the model. The FLake model suggests a high performance for medium sized lakes and. Coupling of the two models combines the advective energy fluxes and mixing processes and is therefore theoretically preferred.

Based on the monthly data, the results for the yearly pattern are statistically very reliable and suggest a high predictability of the model. When concentrating on climates, it is more difficult to simulate the colder regions. The model performs poorest for these regions, but on the other hand performs very well for warmer climates like the tropical forests. The same result applies to the largest rivers, where the temperature and discharge of colder rivers like the Amur, Ob and the Lena are underestimated.

Next to the monthly pattern, also a comparison to daily data reveals reliable results. The stations with daily observed temperatures that are located in North America were very different in size and this was also reflected in the results. Several stations along the same river show different results, but the overall result shows that the daily pattern of the observations were reflected in the simulations.

The differences between water and air temperature over the year and for different climates show where and when transport of heat by rivers is important. The mapped locations confirm the need for a hydrological model for water temperature as it is not sufficient to assume that the fresh surface waters have the same temperature as the air temperature.

LITERATURE

Alley W.M., R.W. Healy, J. W. LaBaugh, T.E. Reilly, 2002, Flow and Storage in Groundwater Systems, SCIENCE VOL 296 14 JUNE 2002

Beek van R., 2008, Forcing PCR-GLOBWB with CRU data, Utrecht University

Caissie D., 2006, The thermal regime of rivers: a review, Freshwater Biology (2006) 51, p. 1389-1406

Caissie D., N. El-Jabi, M.G. Satish, 2001, Modelling of maximum daily water temperatures in a small stream using air temperatures, Journal of Hydrology 251 (2001), 14-28.

Coats R., J. Perez-losada, G. Schladow, R. Richards and C. Goldman, 2006, The warming of lake Tahoe, Climatic Change (2006) 76: 121–148

Fang X. and H. G. Stefan , 1999, Projections of climate change effects on water temperature characteristics of small lakes in the Contiguous U.S., Climatic Change 42: 377–412, 1999.

Global Environment Monitoring System, GEMStat, http://www.GEMStat.org/default.aspx

Global Runoff Data Center, GRDC, http://grdc.bafg.de

Goudsmit G.H., H. Burchard, F. Peeters, A. Wüest, 2002, Application of the K-e turbulence models to enclosed basins: the role of internal seiches, Journal of Geophysical Research, Vol. 107, No. C12, 3230.

Grinten, E., F.C.J. van Herpen, H.J. van Wijnen, C.H.M. Evers, S. Wuijts , W. Verweij, 2007, afleiding maximumtemperatuurnorm goede ecologische toestand (GET) voor Nederlandse grote rivieren, RIVM 2007.

Håkanson L., 1996, A new, simple, general technique to predict seasonal variability of river discharge and lake temperature for lake ecosystem models, Ecological Modelling 88 (1996) 157-181.

Hodges B.R., J. Imberger, A. Saggio, K.B. Winters, 2000, Modelling basin-scale internal waves in a stratified lake, Limnol. Oceanogr., 45(7), 1603-1620.

International Lake Environment Committee (ILEC), world lake database, last update 2001, http://www.ilec.or.jp/database/database_old.html

Ivey G.N., Patterson J.C., 1984, A model of vertical mixing in Lake Erie in summer, Limnol. Oceanogr. 29(3), 553-563.

LeBlanc R.T., R.D. Brown, J.E. FitzGibbon, 1997, Modelling the effects of land use change on water temperature in unregulated urban streams, Journal of Environmental Management (1997) 49, 445-469.

Leemans R., 1989, World Map of Holdridge Life Zones

Lehner, B. and Döll, P. (2004): Development and validation of a global database of lakes, reservoirs and wetlands. Journal of Hydrology 296/1-4: 1-22.

Llebe J. N. van de Giesen, M. Andreini, 2005, Estimation of small reservoir storage capacities in a semi-arid environment: A case study in the Upper East Region of Ghana, Physics and Chemistry of the Earth, Parts A/B/C Vol 30: 6-7, 448-454.

Mazumder A. and W. D. Taylor, 1994, Thermal Structure of Lakes Varying in Size and Water Clarity, Limnology and Oceanography, Vol. 39, No. 4 (Jun., 1994), pp. 968-976, American Society of Limnology and Oceanography.

Mazumder A., W. D. Taylor, D. J. McQueen and D. R. S. Lean, 1990, Effects of Fish and Plankton on Lake Temperature and Mixing Depth, Science, New Series, Vol. 247, No. 4940 (Jan. 19, 1990).

Mironov, D., 2008, Parameterization of lakes in numerical weather prediction. Description of a lake model, Deutscher Wetterdienst, COSMO Tech. Rep. 11.

Mohseni O., H.G. Stefan, 1999, Steam temperature/air temperature relationship: a physical interpretation, Journal of Hydrology 218 (1999) 128-141.

Mooij W.M., J.H. Janse, L.N. De Senerpont Domis, S. Hülsmann, B.W. Ibelings, 2007, Predicting the effect of climate change on temperate shallow lakes with the ecosystem model PCLake, Hydrobiologia (2007) 584: 443-454.

Mooij W.M., L.N. De Senerpont Domis, S. Hülsmann, 2008, The impact of climate warming on water temperature, timing of hatching and young-of-the-year growth of fish in shallow lakes in the Netherlands, Journal of Sea Research 60 (2008) 32–43.

National oceanic and atmospheric administration (NOAA), www.glerl.noaa.gov/metdata/wtemp.html

Norton G.E. and A. Bradford, 2009, Comparison of two stream temperature models and evaluation of potential management alternatives for the Speed River, Southern Ontario, Journal of Environmental management 90, p. 866-878.

Perroud M., S. Goyette, A. Martynov, M. Beniston, O. Anneville, 2009, Simulation of multiannual thermal profiles in deep Lake Geneva: A comparison of one-dimensional lake models, 54(5), 1574-1594.

Rounds S.A., T.M. Wood and D.D. Lynch, 1999, modelling discharge, temperature and water quality in the Tualatin River, Oregon, United states geological survey water-supply paper 2465-B, Reston Virginia.

Sinokrot B.A., H.G. Stefan, 1993, Stream temperature dynamics: Measurements and Modelling, Water Resources Research, vol.29, no. 7, p. 2299-2312, July 1993.

Spigel R.H., J. Imberger, 1987, Mixing processes relevant to phytoplankton dynamics in lakes, New Zealand Journal of Marine and Freshwater Research, 1987, Vol. 21: 361-377.

Stefan H.G., X. Fang and M. Hondzo, 1998, Simulated climate change effects on year-groundwater temperatures in temperate zone lakes, Climatic Change 40: 547–576, 1998.

Uppala S.M., P. W. KÅllberg, A. J. Simmons, U. Andrae, V. Da Costa Bechtold, M. Fiorino, J. K. Gibson, J. Haseler, A. Hernandez, G. A. Kelly, X. Li, K. Onogi, S. Saarinen, N. Sokka, R. P. Allan, E. Andersson, K. Arpe, M. A. Balmaseda, A. C. M. Beljaars, L. Van De Berg, J. Bidlot, N. Bormann, S. Caires, F. Chevallier, A. Dethof, M. Dragosavac, M. Fisher, M. Fuentes, S. Hagemann, E. Hólm, B. J. Hoskins, L. Isaksen, P. A. E. M. Janssen, R. Jenne, A. P. Mcnally, J.-F. Mahfouf, J.-J. Morcrette, N. A. Rayner, R. W. Saunders, P. Simon, A. Sterl, K. E. Trenberth, A. Untch, D. Vasiljevic, P. Viterbo, J. Woollen, 2005, The ERA-40 re-analysis, Quarterly Journal of the Royal Meteorological Society, Volume 131, Issue 612 , p. 2961 – 3012.

Webb B.W. and F. Nobilis, 2007, Long-term changes in river temperature and the influence of climatic and hydrological factors, hydrological sciences 52(1),p.74-85, IAHS Press.

Webb B.W., 1996, Trends in stream and river temperature, Hydrological Processes (1996) Vol. 10, p. 205-226.

Webb B.W., D.M. Hannah, R.D. Moore, L.E. Brown, F. Nobilis, 2008, Recent advantages in stream and river temperature research, hydrological processes 22, p. 902-918.

APPENDIX IA

Observed (left) and simulated (right) long term water temperature data USGS rivers (1975-2004)

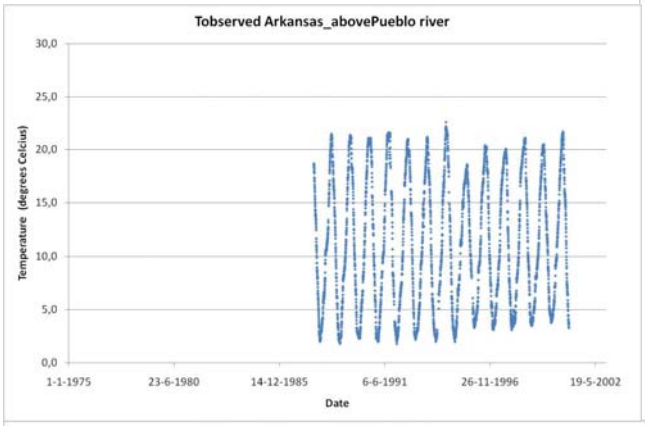

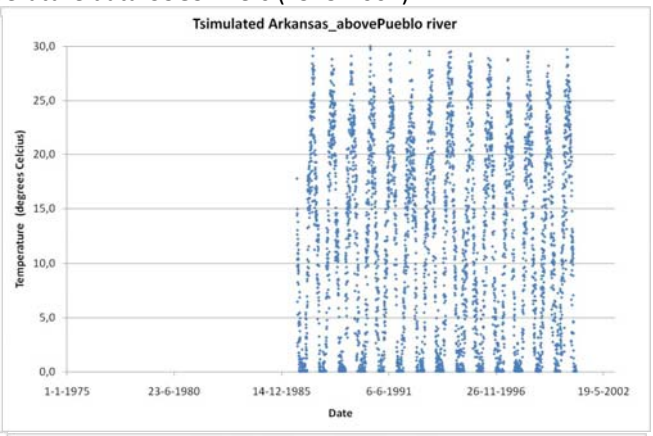

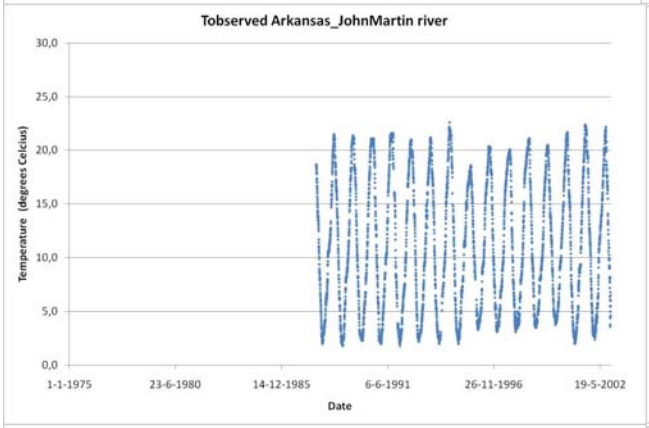

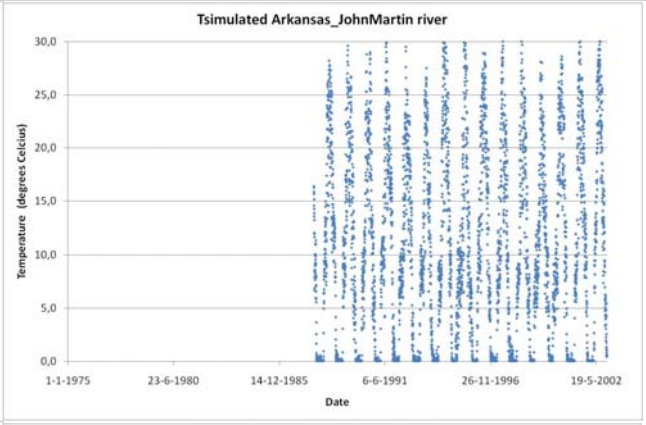

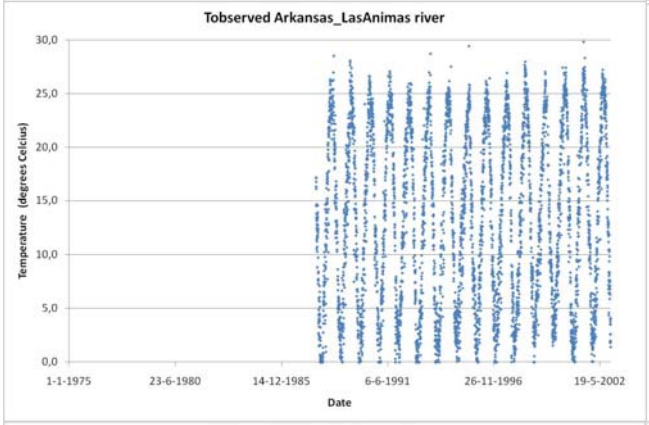

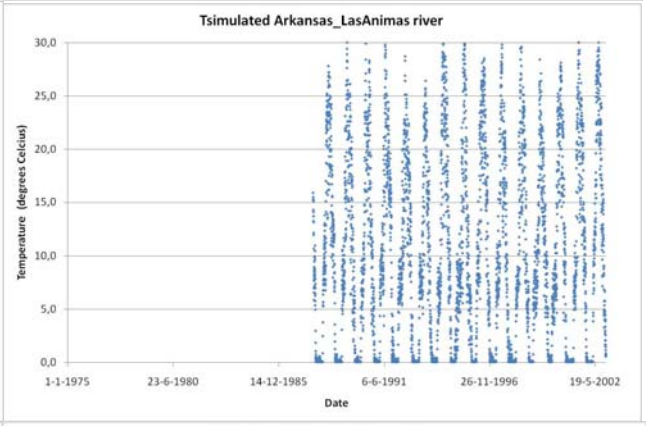

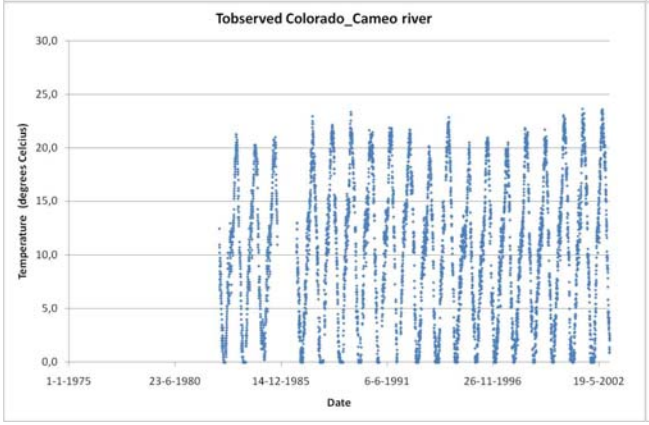

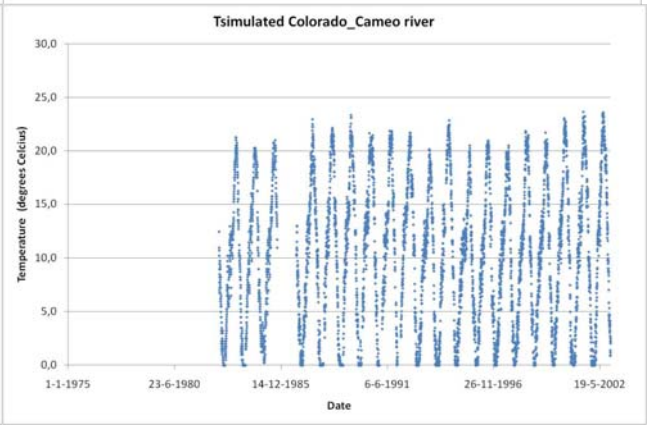

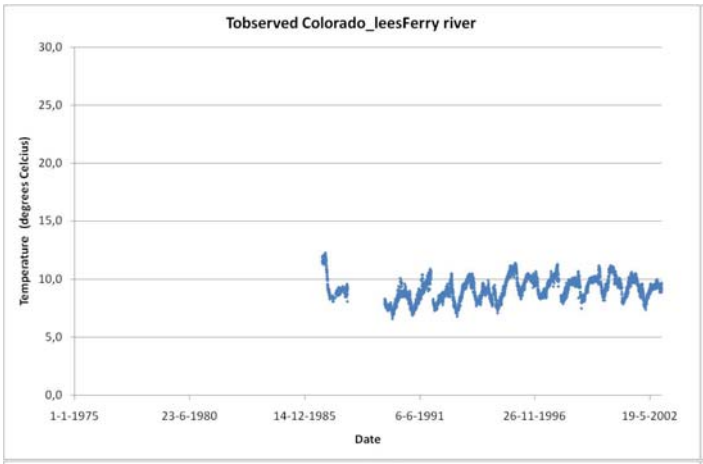
Tobserved Colorado_leesFerry river
Temperature (degrees Celcius)
30,0
25,0
20,0
15,0
10,0
5,0
0,0
1-1-1975
23-6-1980
14-12-1985
6-6-1991
26-11-1996
19-5-2002
Date

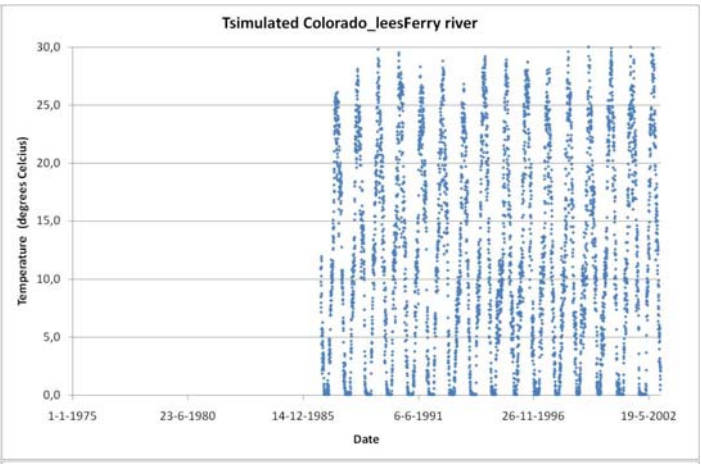
Tsimulated Colorado_leesFerry river
Temperature (degrees Celcius)
30,0
25,0
20,0
15,0
10,0
5,0
0,0
1-1-1975
23-6-1980
14-12-1985
6-6-1991
26-11-1996
19-5-2002
Date

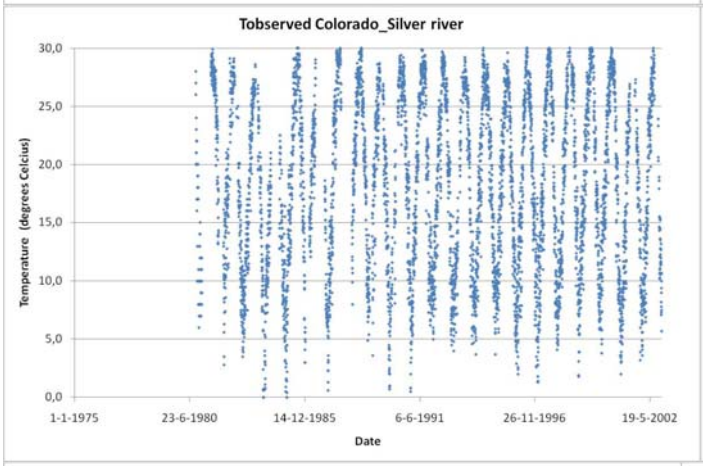
Tobserved Colorado_Silver river
Temperature (degrees Celcius)
30,0
25,0
20,0
15,0
10,0
5,0
0,0
1-1-1975
23-6-1980
14-12-1985
6-6-1991
26-11-1996
19-5-2002
Date

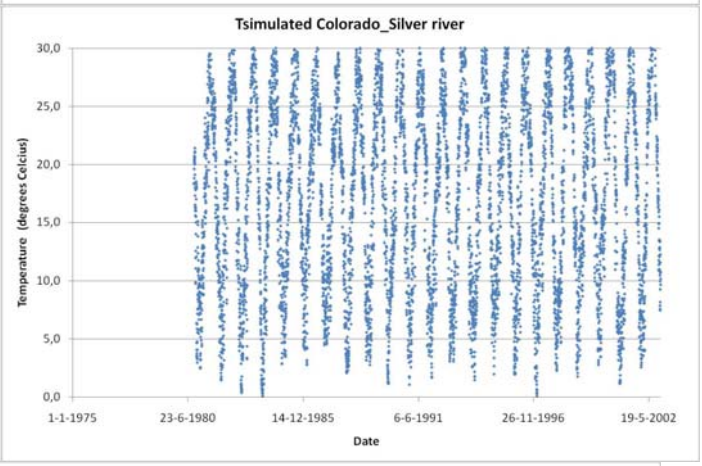
Tsimulated Colorado_Silver river
Temperature (degrees Celcius)
30,0
25,0
20,0
15,0
10,0
5,0
0,0
1-1-1975
23-6-1980
14-12-1985
6-6-1991
26-11-1996
19-5-2002
Date

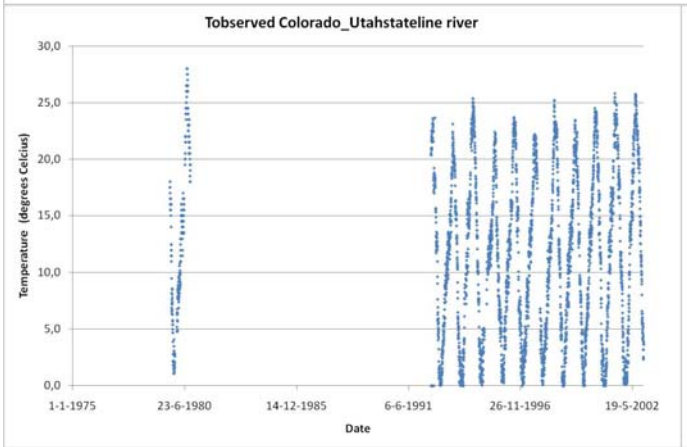
Tobserved Colorado_Utahstateline river
Temperature (degrees Celcius)
30,0
25,0
20,0
15,0
10,0
5,0
0,0
1-1-1975
23-6-1980
14-12-1985
6-6-1991
26-11-1996
19-5-2002
Date

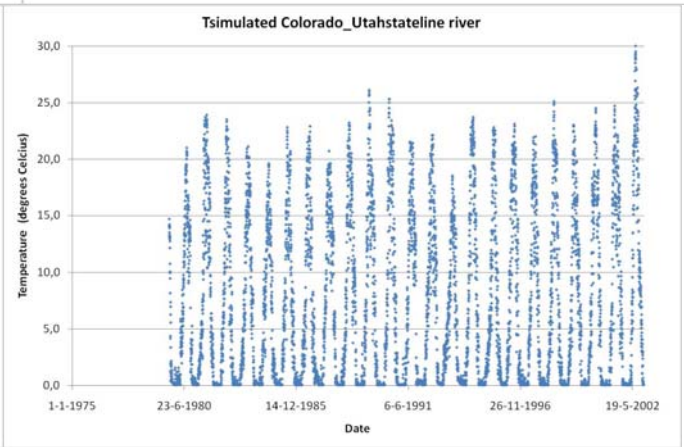
Tsimulated Colorado_Utahstateline river
Temperature (degrees Celcius)
30,0
25,0
20,0
15,0
10,0
5,0
0,0
1-1-1975
23-6-1980
14-12-1985
6-6-1991
26-11-1996
19-5-2002
Date

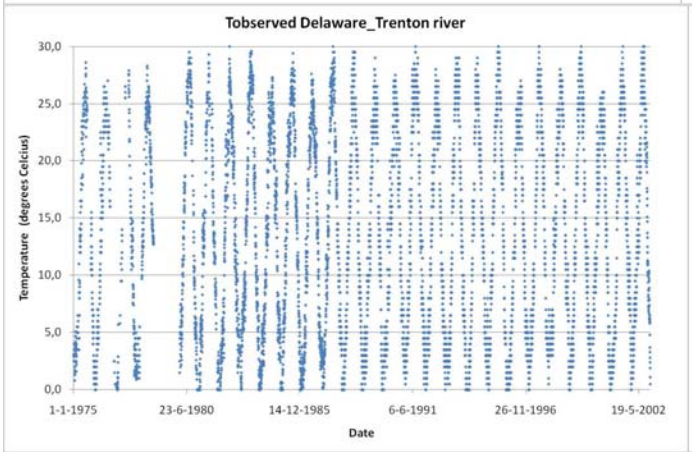
Tobserved Delaware_Trenton river
Temperature (degrees Celcius)
30,0
25,0
20,0
15,0
10,0
5,0
0,0
1-1-1975
23-6-1980
14-12-1985
6-6-1991
26-11-1996
19-5-2002
Date

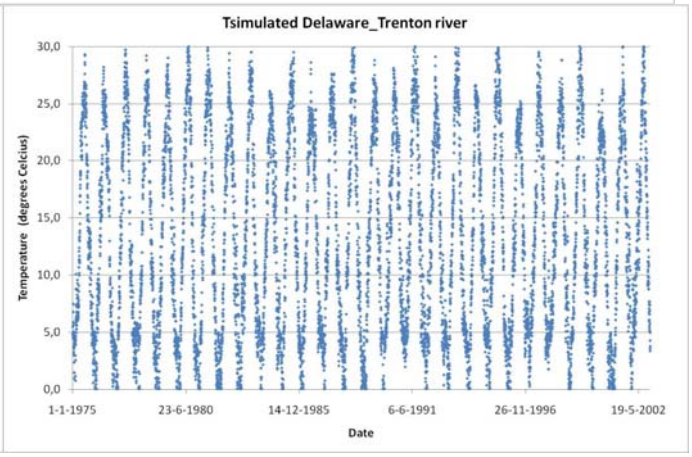
Tsimulated Delaware_Trenton river
Temperature (degrees Celcius)
30,0
25,0
20,0
15,0
10,0
5,0
0,0
1-1-1975
23-6-1980
14-12-1985
6-6-1991
26-11-1996
19-5-2002
Date

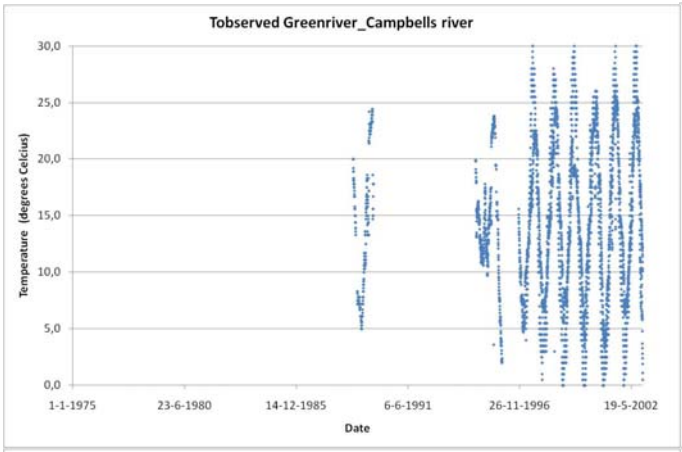
Tobserved Greenriver_Campbells river
Temperature (degrees Celcius)
30,0
25,0
20,0
15,0
10,0
5,0
0,0
1-1-1975
23-6-1980
14-12-1985
6-6-1991
26-11-1996
19-5-2002
Date

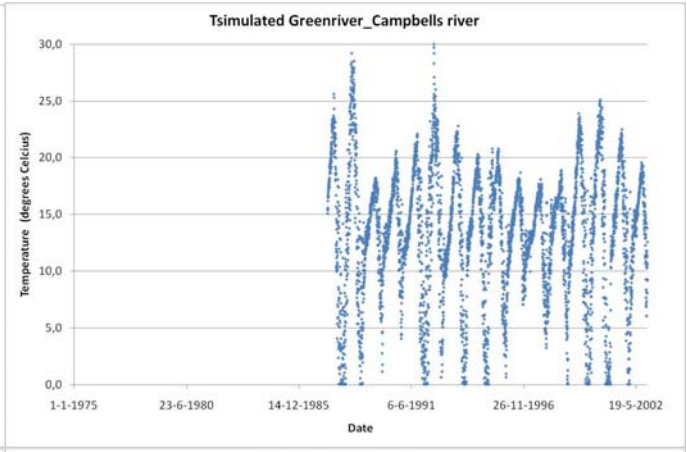
Tsimulated Greenriver_Campbells river
Temperature (degrees Celcius)
30,0
25,0
20,0
15,0
10,0
5,0
0,0
1-1-1975
23-6-1980
14-12-1985
6-6-1991
26-11-1996
19-5-2002
Date

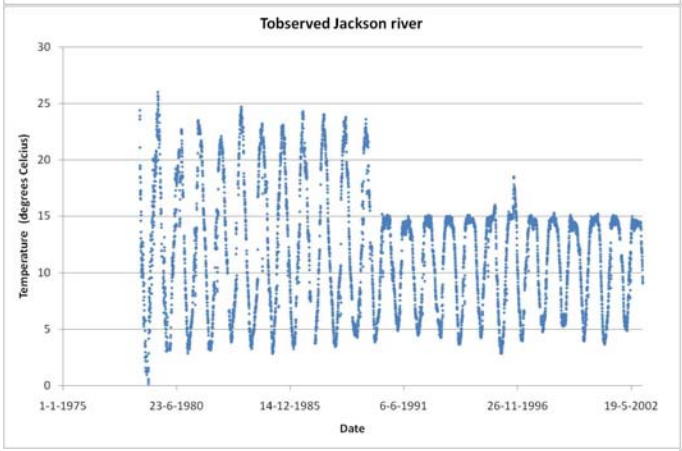
Tobserved Jackson river
Temperature (degrees Celcius)
30
25
20
15
10
5
0
1-1-1975
23-6-1980
14-12-1985
6-6-1991
26-11-1996
19-5-2002
Date

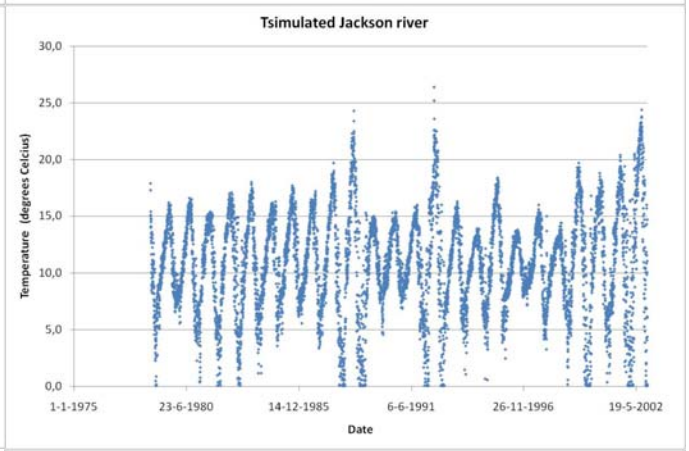
Tsimulated Jackson river
Temperature (degrees Celcius)
30,0
25,0
20,0
15,0
10,0
5,0
0,0
1-1-1975
23-6-1980
14-12-1985
6-6-1991
26-11-1996
19-5-2002
Date

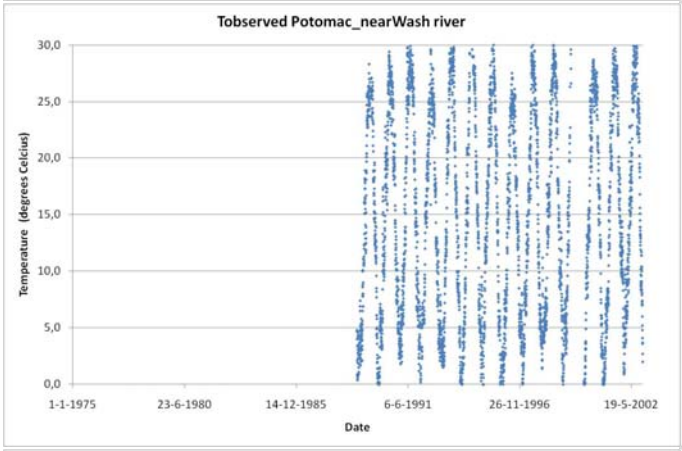
Tobserved Potomac_nearWash river
Temperature (degrees Celcius)
30,0
25,0
20,0
15,0
10,0
5,0
0,0
1-1-1975
23-6-1980
14-12-1985
6-6-1991
26-11-1996
19-5-2002
Date

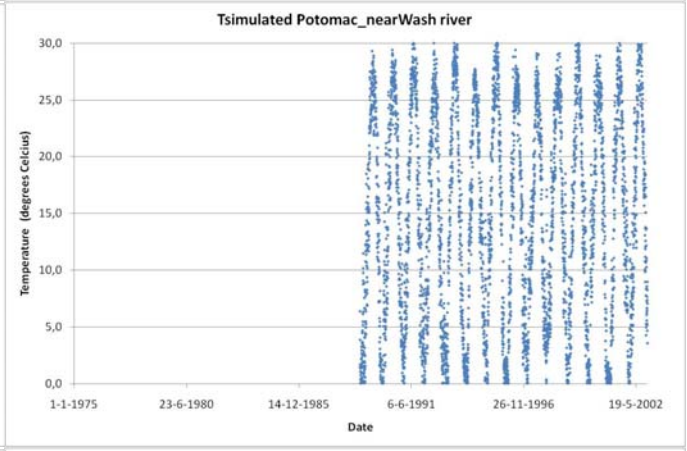
Tsimulated Potomac_nearWash river
Temperature (degrees Celcius)
30,0
25,0
20,0
15,0
10,0
5,0
0,0
1-1-1975
23-6-1980
14-12-1985
6-6-1991
26-11-1996
19-5-2002
Date

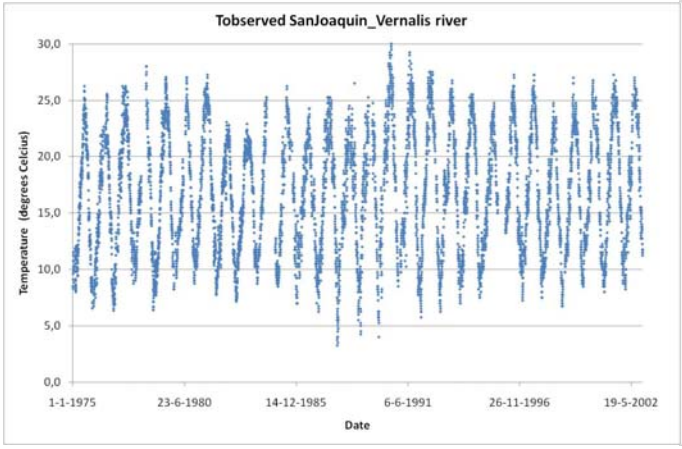
Tobserved SanJoaquin_Vernalis river
Temperature (degrees Celcius)
30,0
25,0
20,0
15,0
10,0
5,0
0,0
1-1-1975
23-6-1980
14-12-1985
6-6-1991
26-11-1996
19-5-2002
Date

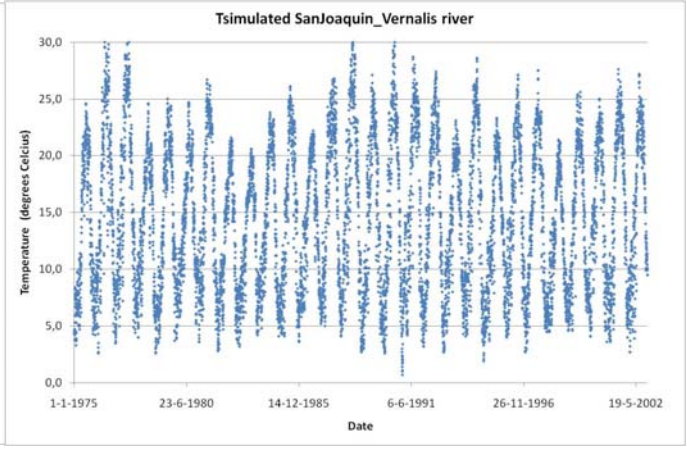
Tsimulated SanJoaquin_Vernalis river
Temperature (degrees Celcius)
30,0
25,0
20,0
15,0
10,0
5,0
0,0
1-1-1975
23-6-1980
14-12-1985
6-6-1991
26-11-1996
19-5-2002
Date

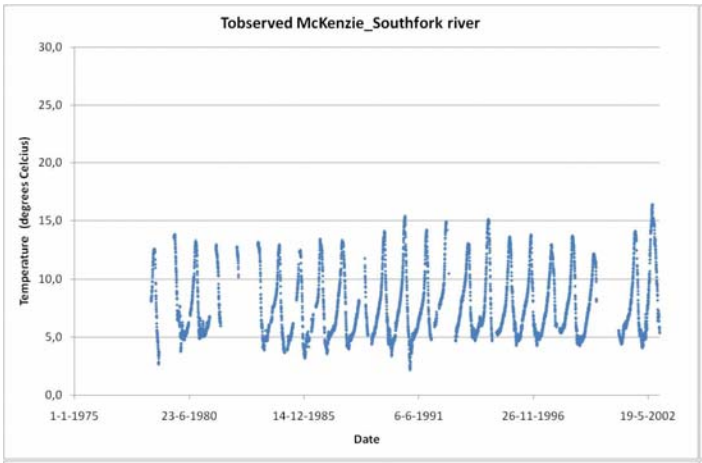
Tobserved McKenzie_Southfork river
Temperature (degrees Celcius)
30,0
25,0
20,0
15,0
10,0
5,0
0,0
1-1-1975
23-6-1980
14-12-1985
6-6-1991
26-11-1996
19-5-2002
Date

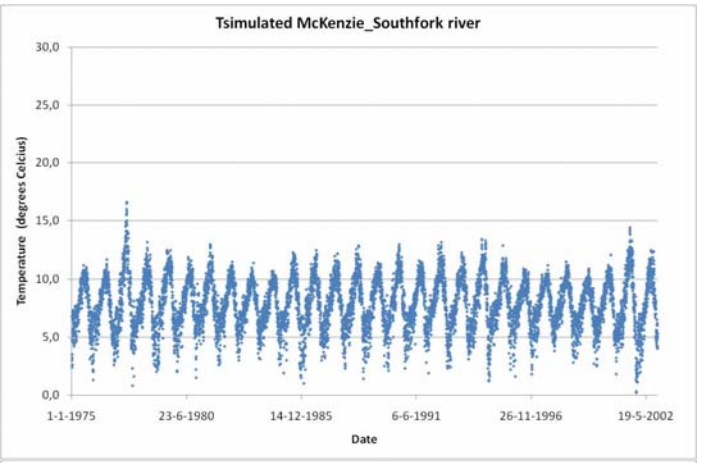
Tsimulated McKenzie_Southfork river
Temperature (degrees Celcius)
30,0
25,0
20,0
15,0
10,0
5,0
0,0
1-1-1975
23-6-1980
14-12-1985
6-6-1991
26-11-1996
19-5-2002
Date

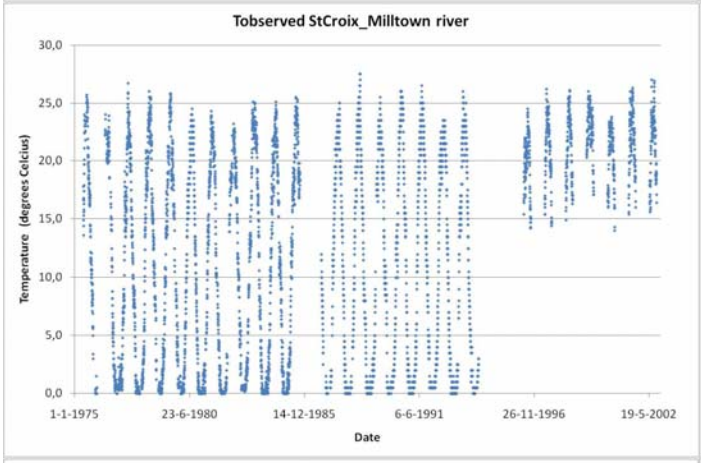
Tobserved StCroix_Milltown river
Temperature (degrees Celcius)
30,0
25,0
20,0
15,0
10,0
5,0
0,0
1-1-1975
23-6-1980
14-12-1985
6-6-1991
26-11-1996
19-5-2002
Date

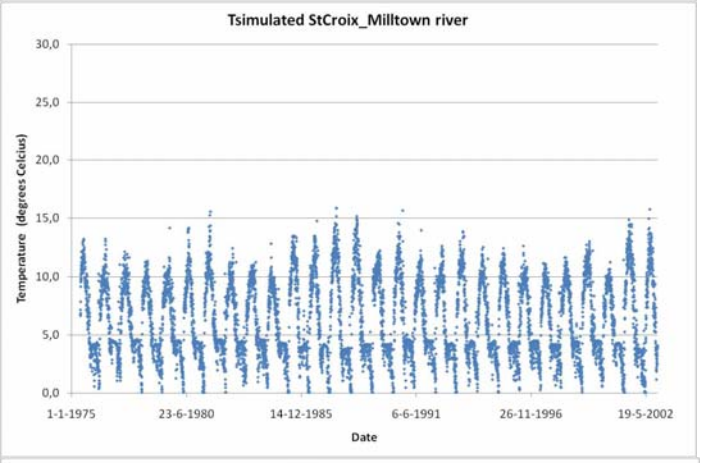
Tsimulated StCroix_Milltown river
Temperature (degrees Celcius)
30,0
25,0
20,0
15,0
10,0
5,0
0,0
1-1-1975
23-6-1980
14-12-1985
6-6-1991
26-11-1996
19-5-2002
Date

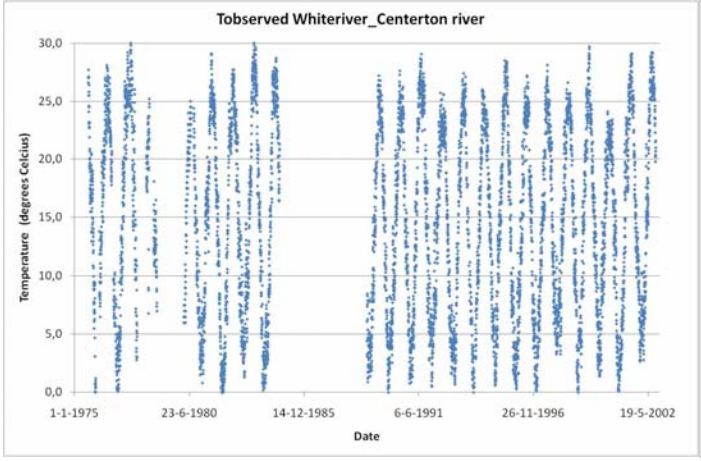
Tobserved Whiteriver_Centerton river
Temperature (degrees Celcius)
30,0
25,0
20,0
15,0
10,0
5,0
0,0
1-1-1975
23-6-1980
14-12-1985
6-6-1991
26-11-1996
19-5-2002
Date

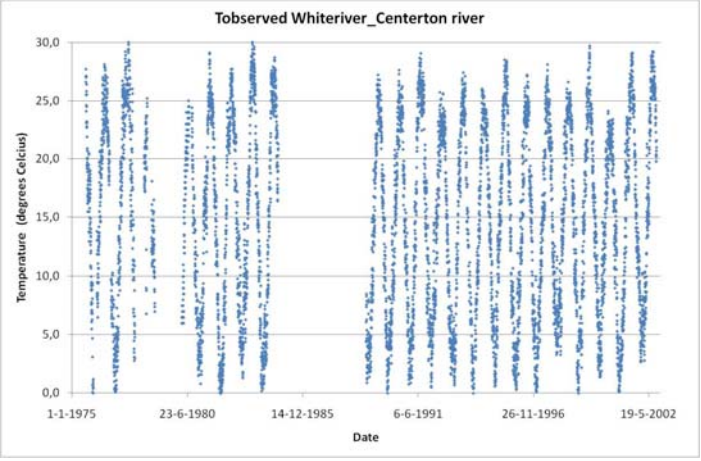
Tobserved Whiteriver_Centerton river
Temperature (degrees Celcius)
30,0
25,0
20,0
15,0
10,0
5,0
0,0
1-1-1975
23-6-1980
14-12-1985
6-6-1991
26-11-1996
19-5-2002
Date

APPENDIX IB

Observed (left) and simulated (right) with FLake long term water temperature of lakes (1960-1990)

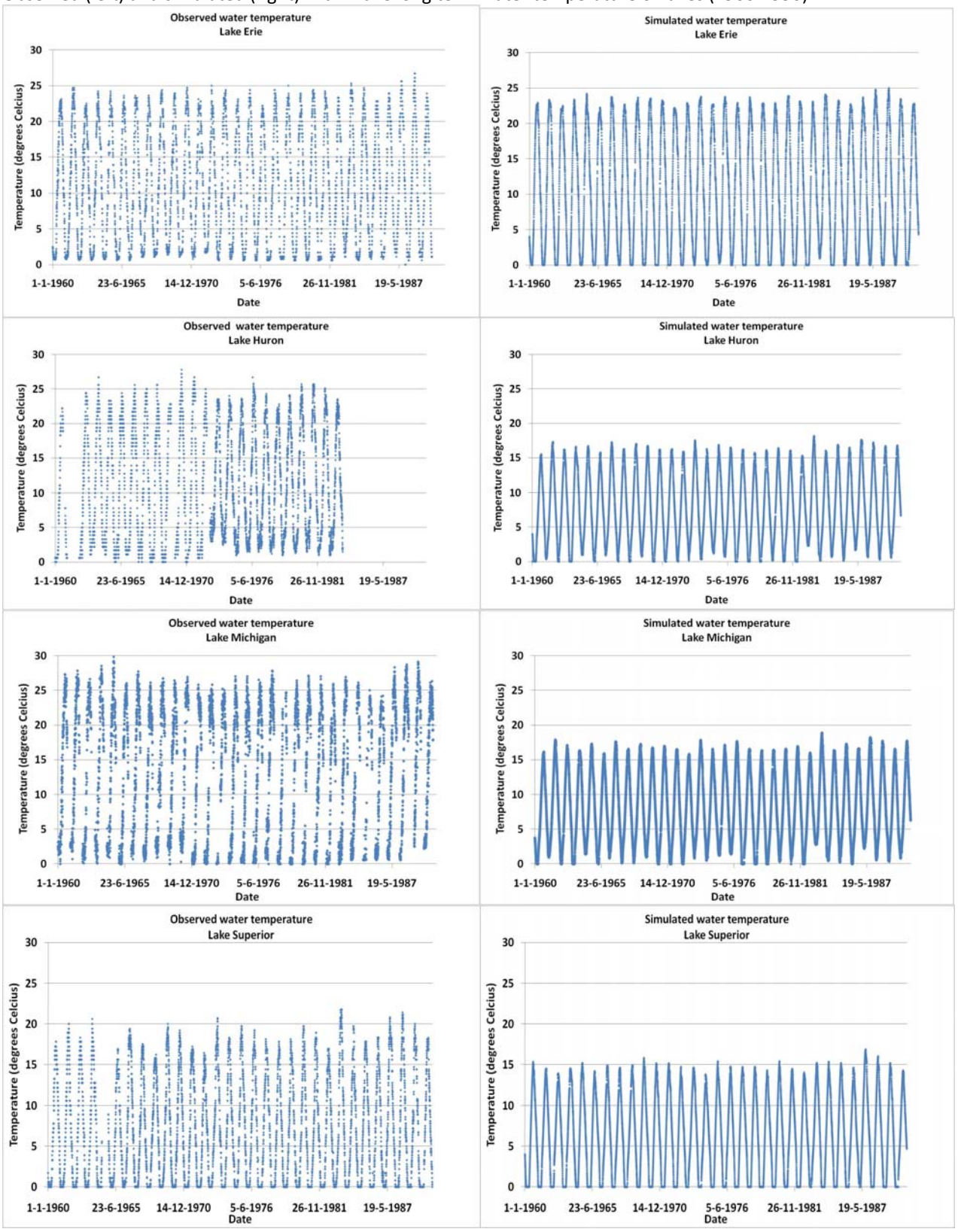

APPENDIX IIA

Observations and simulations of lakes with FLake

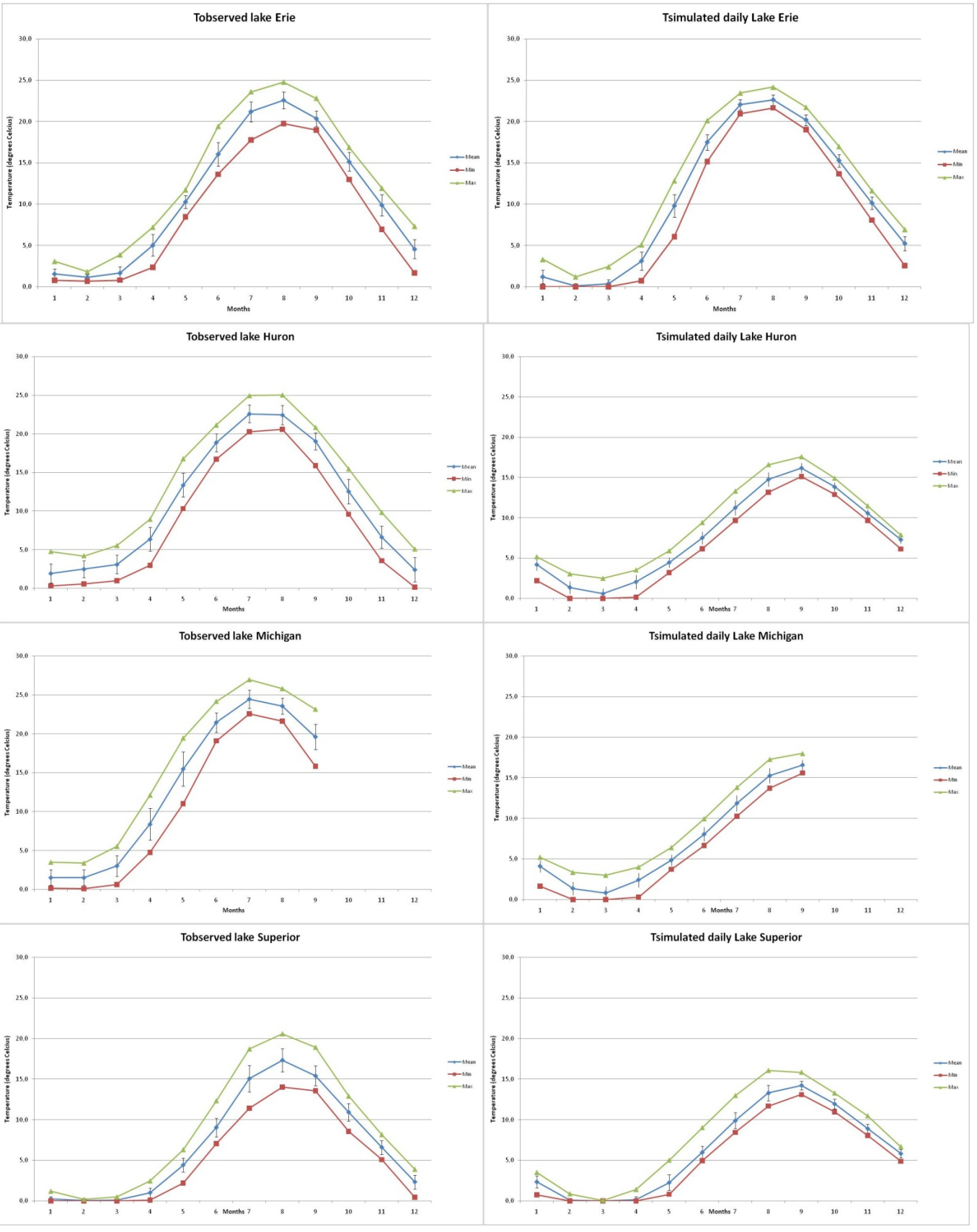

APPENDIX IIB

Simulations of lakes with PCR-GLOBWB

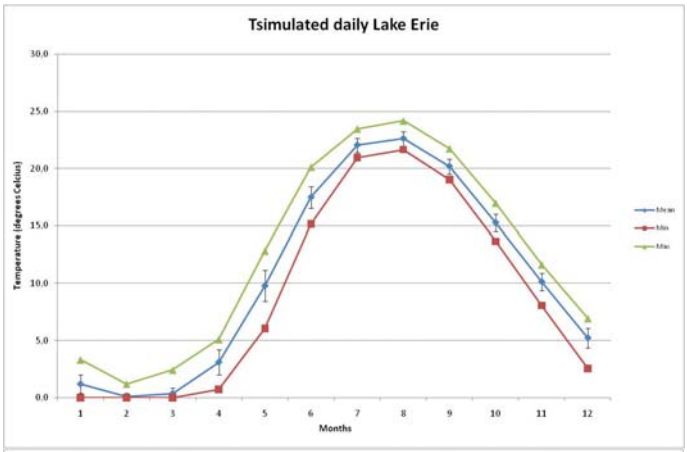

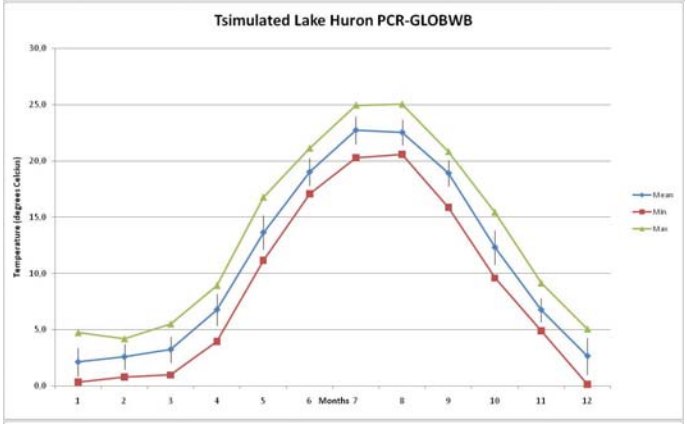

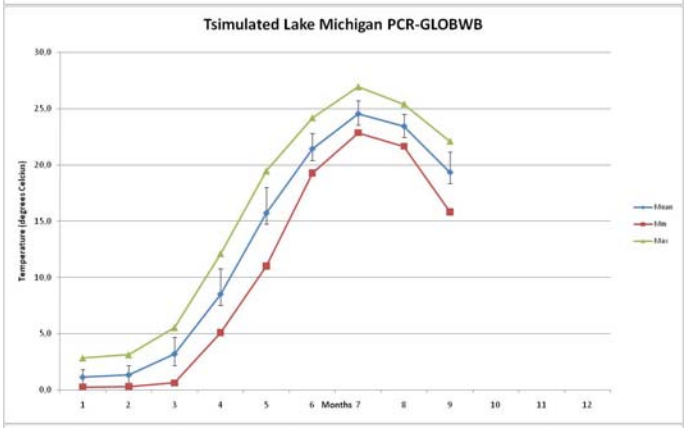

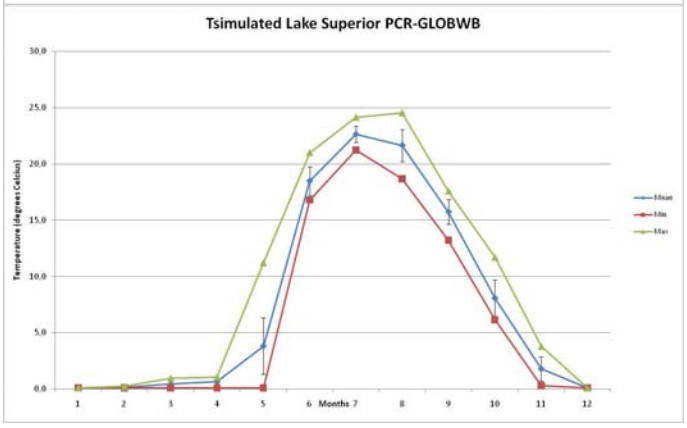

APPENDIX III

Observations and simulations of water temperature for USGS rivers

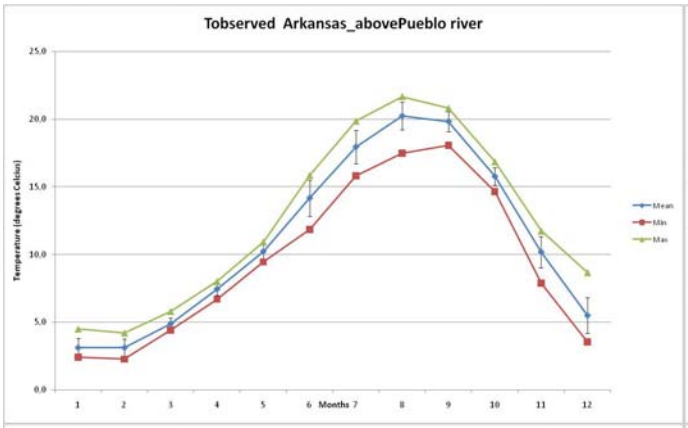

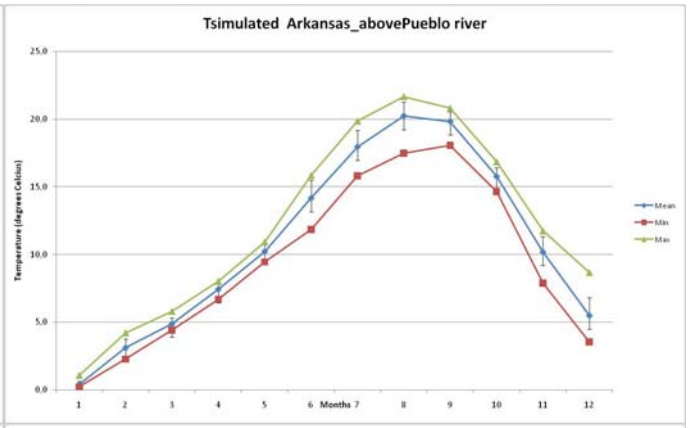

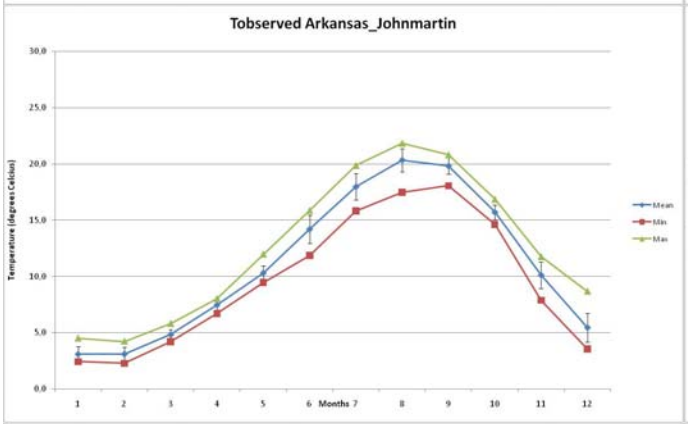

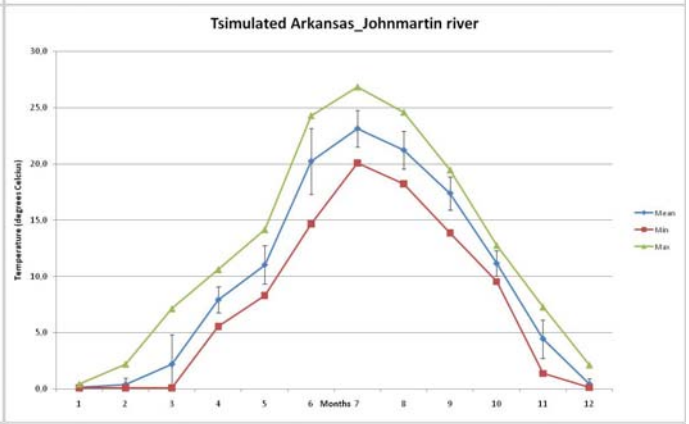

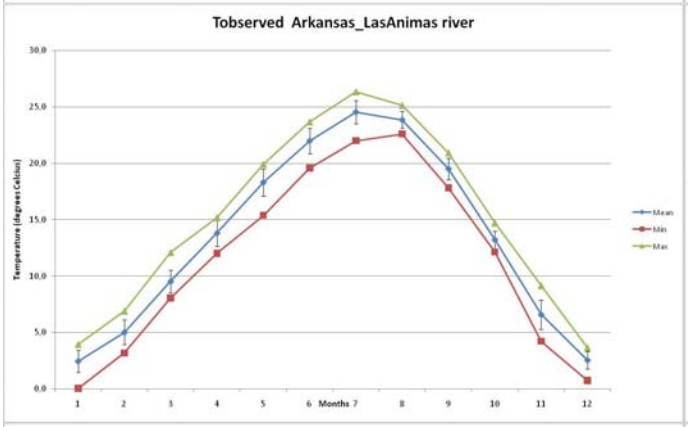

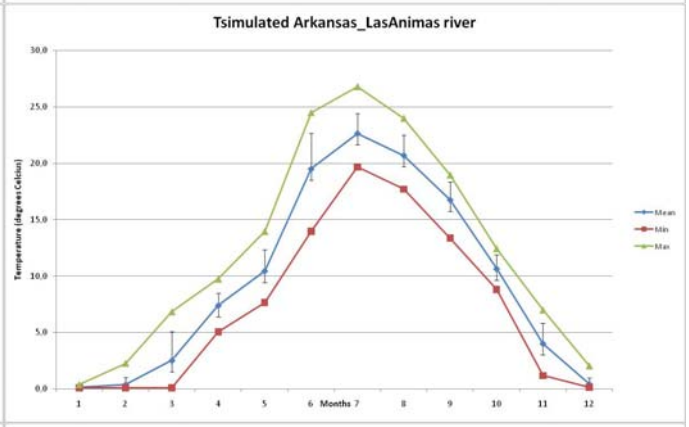

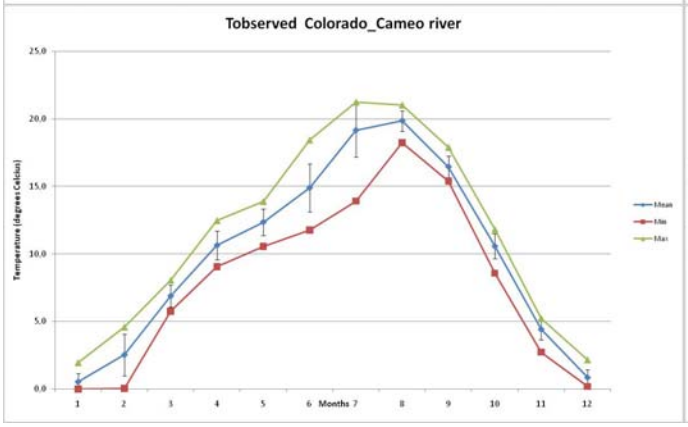

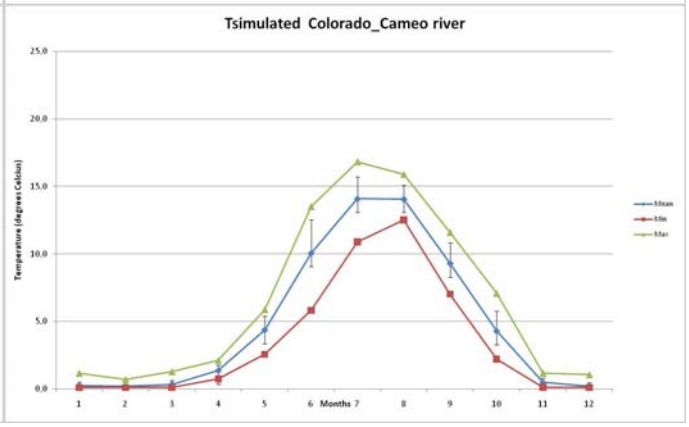

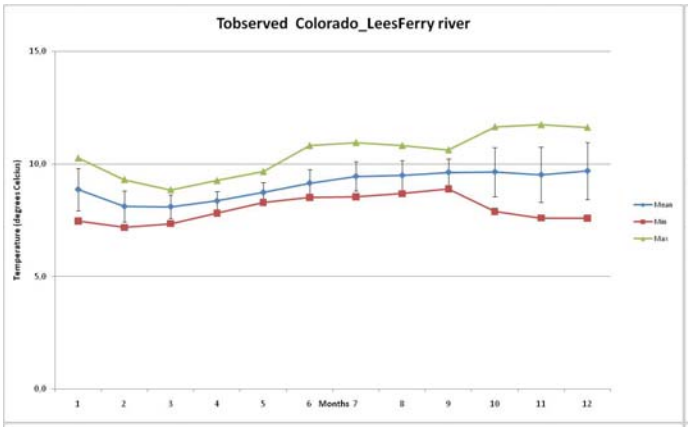
Tobserved Colorado_LeesFerry river
Temperature (degrees Celsius)
Months
Mean
Min
Max

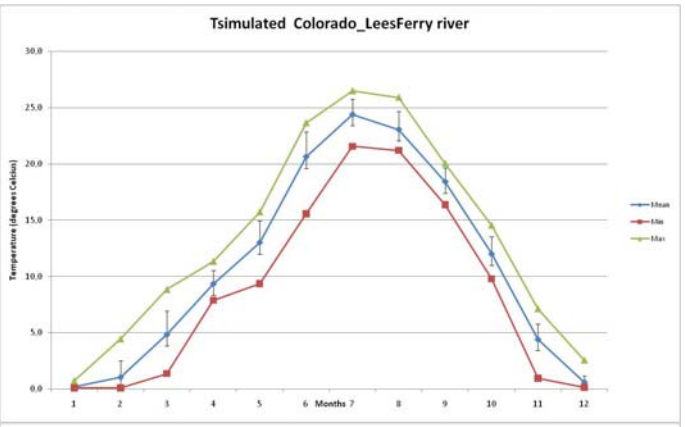
Tsimulated Colorado_LeesFerry river
Temperature (degrees Celsius)
Months
Mean
Min
Max

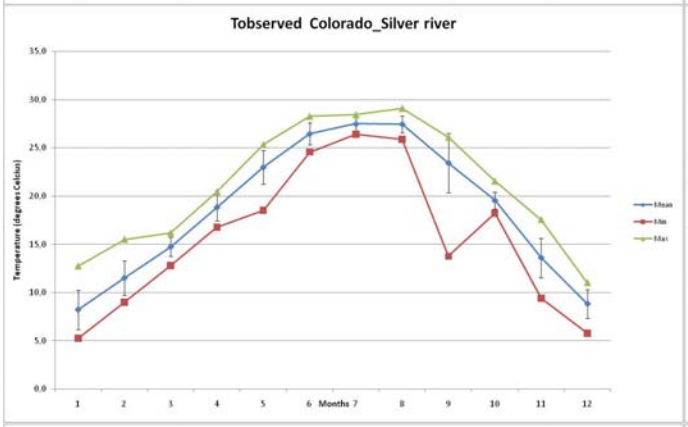
Tobserved Colorado_Silver river
Temperature (degrees Celsius)
Months
Mean
Min
Max

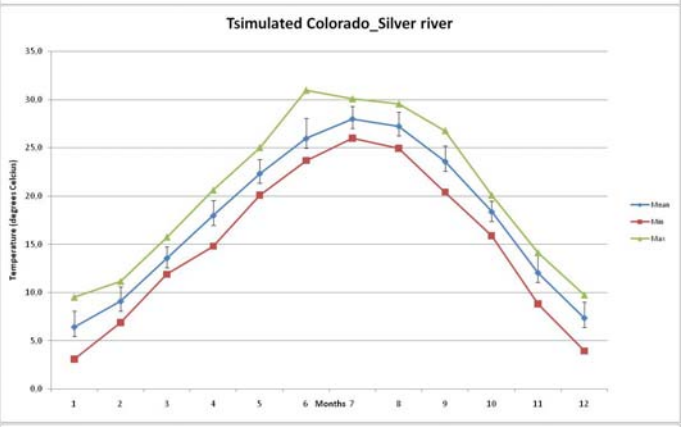
Tsimulated Colorado_Silver river
Temperature (degrees Celsius)
Months
Mean
Min
Max

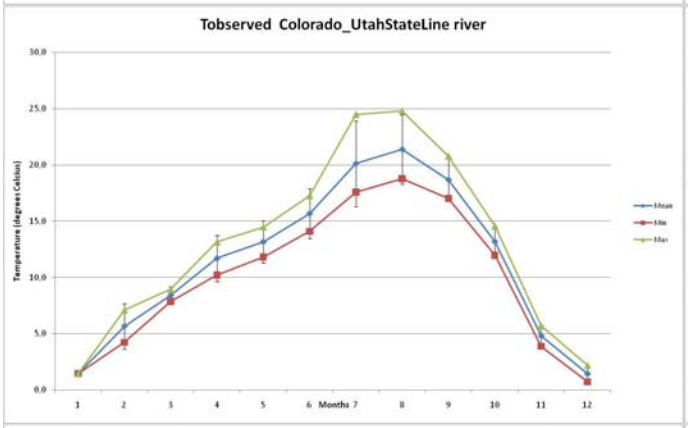
Tobserved Colorado_UtahStateLine river
Temperature (degrees Celsius)
Months
Mean
Min
Max

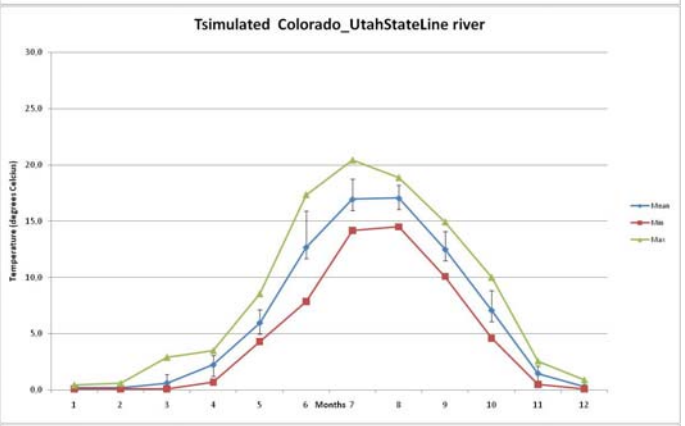
Tsimulated Colorado_UtahStateLine river
Temperature (degrees Celsius)
Months
Mean
Min
Max

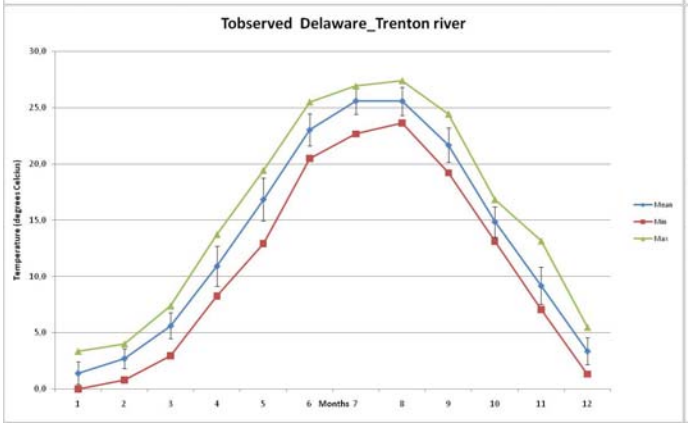
Tobserved Delaware_Trenton river
Temperature (degrees Celsius)
Months
Mean
Min
Max

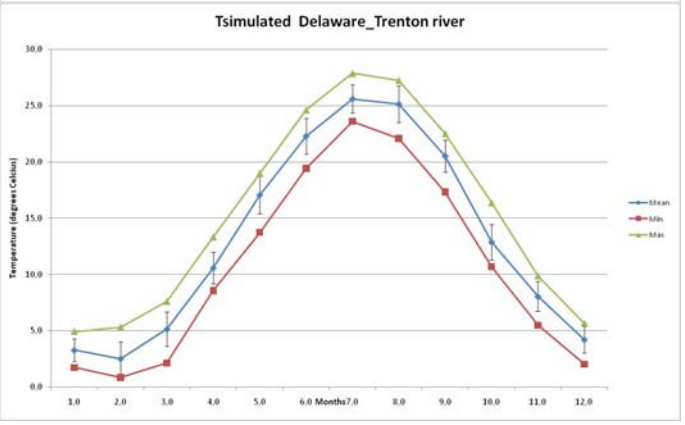
Tsimulated Delaware_Trenton river
Temperature (degrees Celsius)
Months
Mean
Min
Max

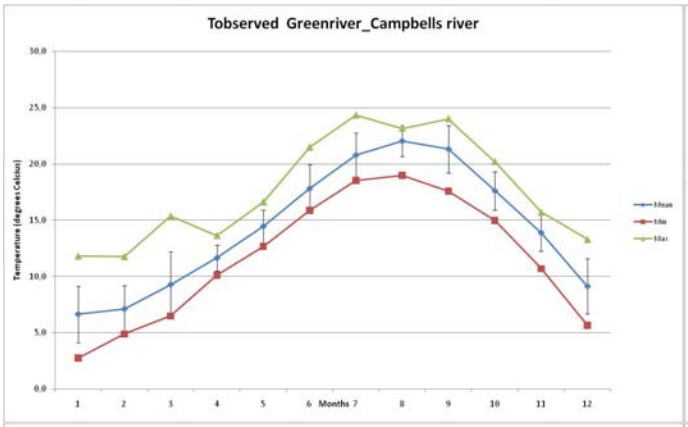
Tobserved Greenriver_Campbells river
Temperature (degrees Celsius)
Months
Mean
Min
Max

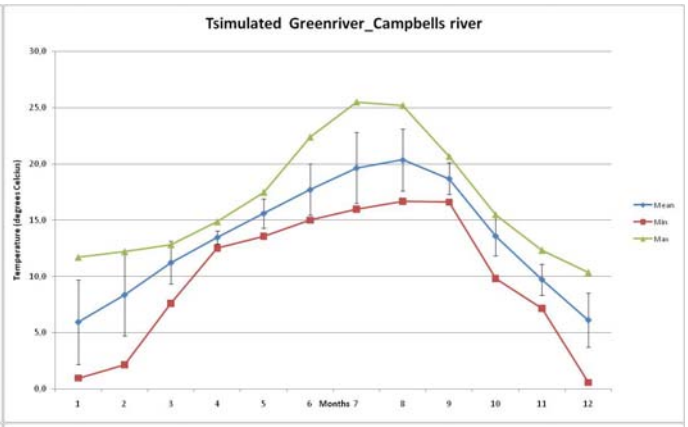
Tsimulated Greenriver_Campbells river
Temperature (degrees Celsius)
Months
Mean
Min
Max

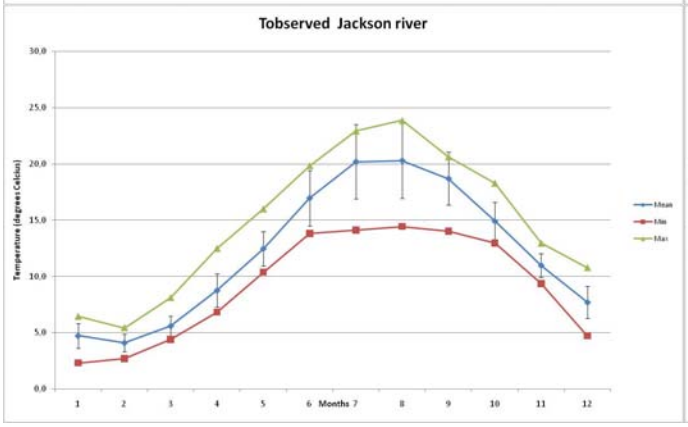
Tobserved Jackson river
Temperature (degrees Celsius)
Months
Mean
Min
Max

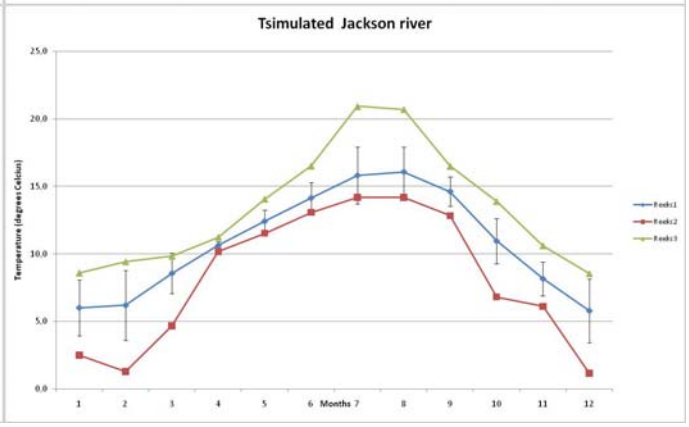
Tsimulated Jackson river
Temperature (degrees Celsius)
Months
Reeks1
Reeks2
Reeks3

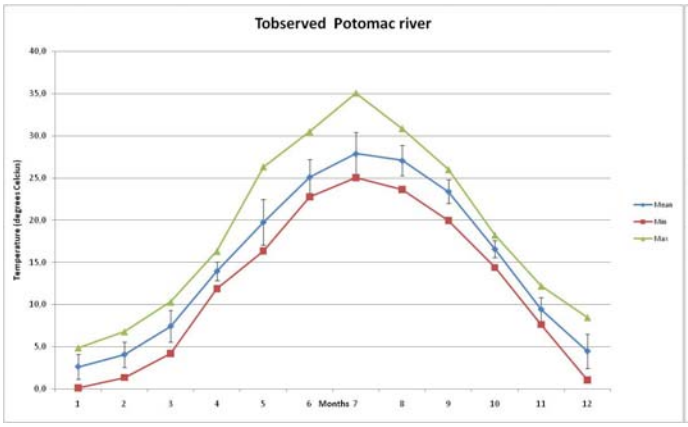
Tobserved Potomac river
Temperature (degrees Celsius)
Months
Mean
Min
Max

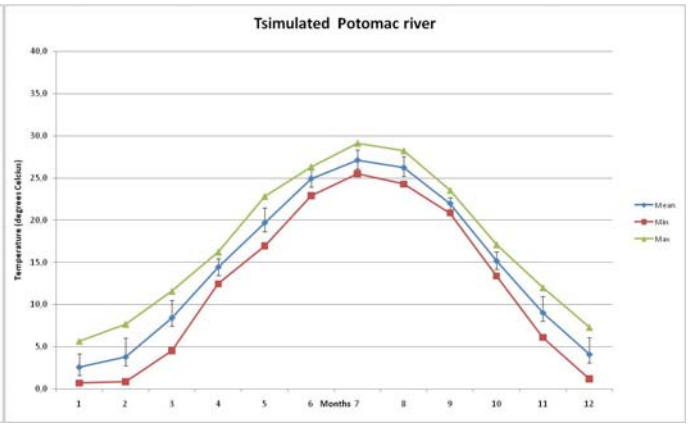
Tsimulated Potomac river
Temperature (degrees Celsius)
Months
Mean
Min
Max

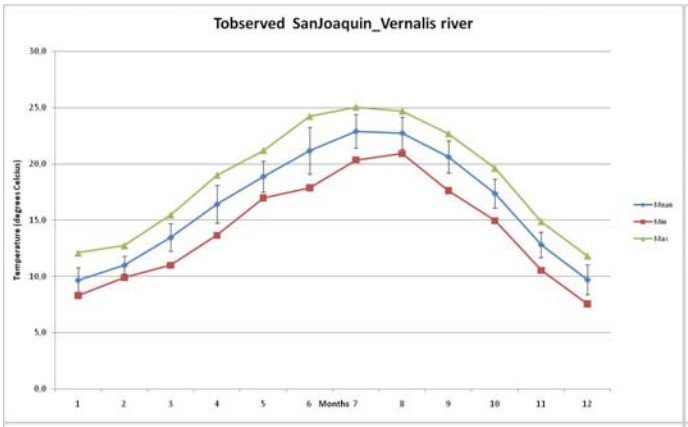
Tobserved SanJoaquin_Vernalis river
Temperature (degrees Celcius)
Months
Mean
Min
Max

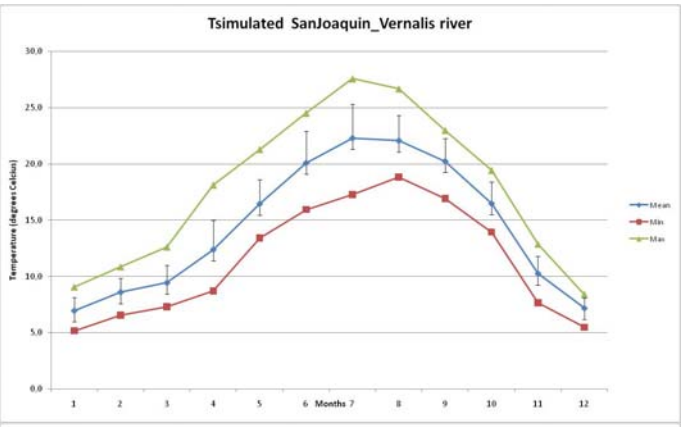
Tsimulated SanJoaquin_Vernalis river
Temperature (degrees Celcius)
Months
Mean
Min
Max

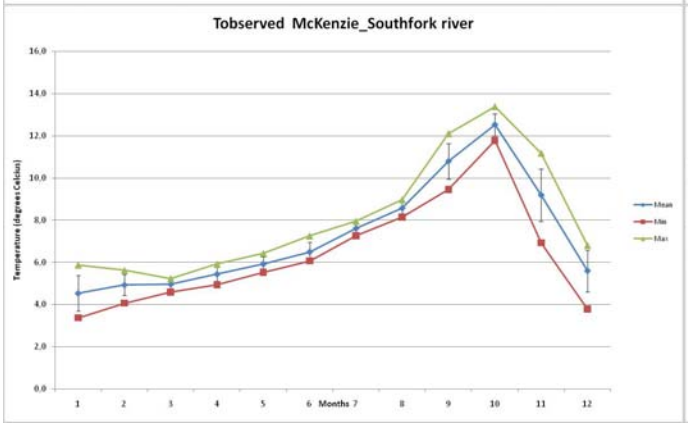
Tobserved McKenzie_Southfork river
Temperature (degrees Celcius)
Months
Mean
Min
Max

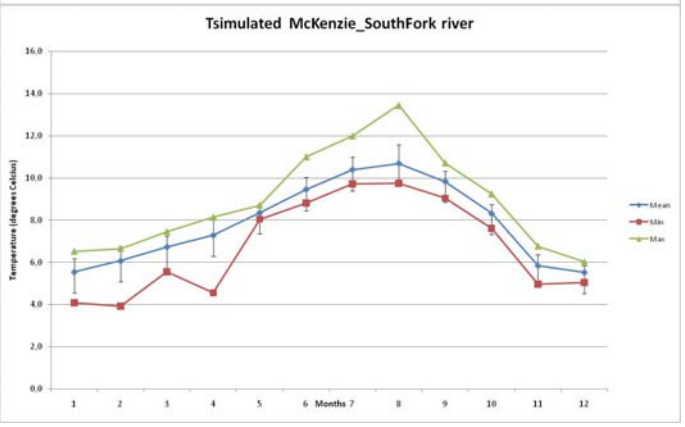
Tsimulated McKenzie_SouthFork river
Temperature (degrees Celcius)
Months
Mean
Min
Max

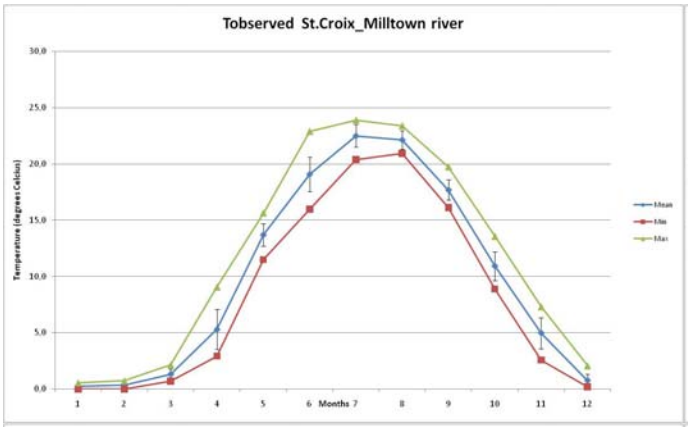
Tobserved St.Croix_Milltown river
Temperature (degrees Celcius)
Months
Mean
Min
Max

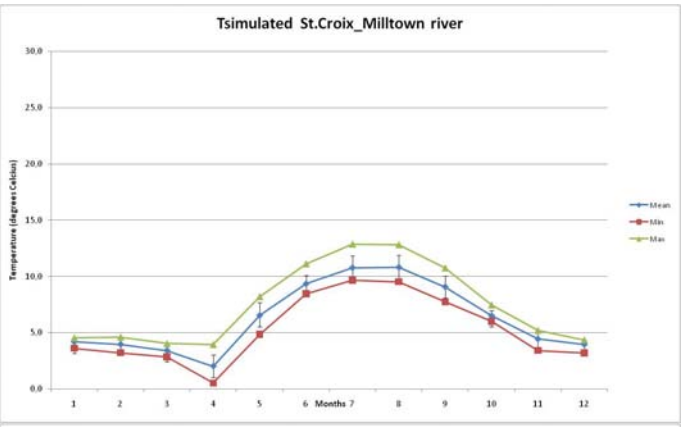
Tsimulated St.Croix_Milltown river
Temperature (degrees Celcius)
Months
Mean
Min
Max

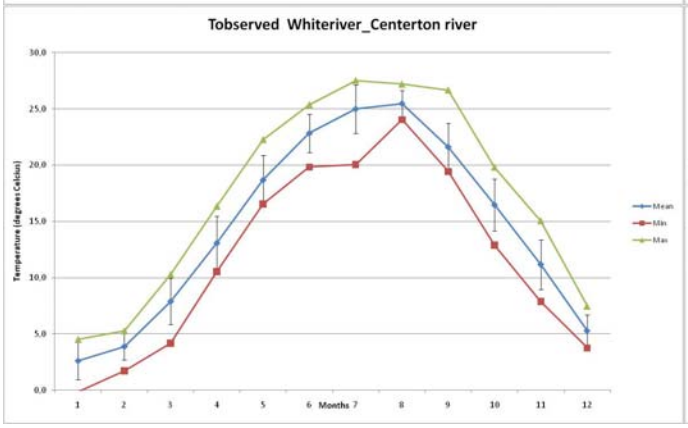
Tobserved Whiteriver_Centerton river
Temperature (degrees Celcius)
Months
Mean
Min
Max

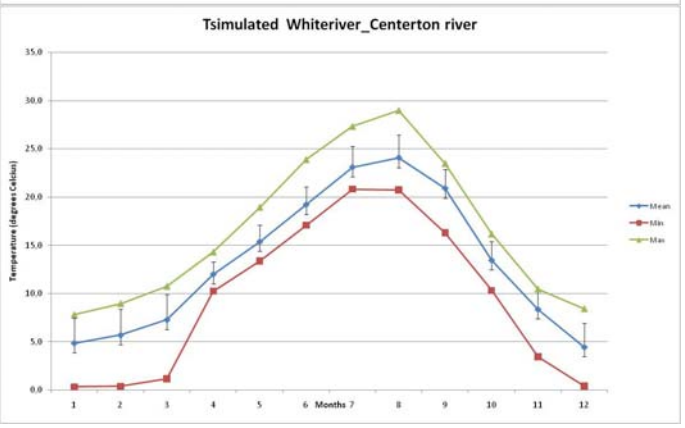
Tsimulated Whiteriver_Centerton river
Temperature (degrees Celcius)
Months
Mean
Min
Max

APPENDIX IV

Results GEMS stations mean temperature sorted by RSE

GEMS ID	Name	Climate	RSE	Ō	SE	R^2	α
26028	Lena River - Stolb	Tundra	1.66	2.61	4.34	0.26	0.44
39101	Alsek River	Tundra	1.39	2.65	3.68	0.17	0.43
26018	Lena River - Kusur	Forest Tundra	1.37	2.86	3.93	0.46	1.05
26010	Yenisey River	Boreal Forest	1.14	4.85	5.52	0.37	0.43
39102	Liard River	Boreal Forest	1.05	6.26	6.57	0.38	0.97
65010	Oulujoki River - at Merikoski 13000	Boreal Forest	1.03	7.41	7.64	0.28	1.10
39099	Nelson River - above Weir River	Boreal Forest	1.01	8.76	8.84	0.08	0.40
65008	Kemijoki River - at Isohaara 14000	Boreal Forest	0.96	7.81	7.46	0.35	0.52
39109	Elk River - Elko	Boreal Forest	0.94	6.73	6.35	0.32	1.28
39021	Skeena River	Forest Tundra	0.91	7.38	6.71	0.23	1.03
26017	Kolyma River	Cold Parklands	0.85	3.08	2.63	0.76	2.29
26009	Amur River	Forest Tundra	0.83	9.97	8.28	0.21	0.37
45002	Glama River - at Haslemoen	Boreal Forest	0.83	7.22	5.99	0.44	1.29
65013	Vuoksi River - at Mansikkakoski 2800	Boreal Forest	0.77	9.12	7.05	0.42	0.70
65002	Kymijoki River - Station 5610	Temperate Forest	0.70	9.25	6.44	0.54	1.09
200005	Rhone River - at Porte du Scex	Tundra	0.67	8.39	5.64	0.02	1.61
39009	Great Bear River	Boreal Forest	0.67	10.45	7.02	0.01	0.30
26011	Ob River	Forest Tundra	0.66	4.93	3.27	0.78	1.28
68002	Adige River - at Trento	Temperate Forest	0.60	9.86	5.92	0.20	2.03
26002	Selenga River	Cold Parklands	0.57	6.82	3.90	0.79	1.01
26020	Dzhida River	Cold Parklands	0.57	5.76	3.30	0.80	1.27
39106	Columbia River - Waneta	Temperate Forest	0.55	10.34	5.72	0.32	1.62
28003	Yukon River	Forest Tundra	0.55	11.10	6.11	0.64	0.59
39004	Saskatchewan River (1) - above Carrot River	Boreal Forest	0.54	11.68	6.34	0.41	1.21
200001	Rhine River - at Diepoldsau	Tundra	0.52	9.03	4.71	0.40	0.55
39002	Nelson River - Kettle Crossing	Boreal Forest	0.52	14.92	7.75	0.07	0.33
68001	Adige River - at Ponte D'Adige	Temperate Forest	0.51	7.45	3.79	0.18	0.38
39110	Fraser River - Red Pass	Forest Tundra	0.49	4.74	2.32	0.70	1.19
65001	Tornionjoki River - Station 14100	Boreal Forest	0.48	6.18	2.94	0.86	0.85
39005	Slave River	Boreal Forest	0.47	6.85	3.24	0.82	0.85
39022	Stikine River	Forest Tundra	0.44	9.10	3.98	0.19	0.56
39006	Roseau River - at Gardenton	Temperate Forest	0.43	9.39	4.06	0.84	1.19
39001	Mackenzie River	Boreal Forest	0.43	10.11	4.33	0.38	1.84
65011	Paatsjoki River - at Virtaniemi 14400	Forest Tundra	0.41	4.08	1.65	0.89	0.87
65007	Iijoki River - at Raasakan	Boreal Forest	0.40	7.51	3.01	0.87	0.79
33002	Mitta Mitta River	Temperate Forest	0.40	13.22	5.26	0.45	1.21
39111	Okanagan River	Boreal Forest	0.39	12.61	4.90	0.67	1.40
67004	Blackwater River - at Killavullen	Temperate Forest	0.38	11.90	4.46	0.40	1.11
65009	Kokemaenjoki River - Kojo 35 Pori-Tre	Temperate Forest	0.37	7.23	2.70	0.89	1.05
67002	Clare River - at Corofin Bridge	Temperate Forest	0.36	11.89	4.24	0.47	1.20
26014	Neva River	Boreal Forest	0.34	7.33	2.50	0.89	0.91
39020	Churchill River	Boreal Forest	0.34	10.92	3.67	0.63	1.21
51036	Dyle River - at Sint-Agatha-Rode	Temperate Forest	0.33	11.88	3.94	0.53	0.97
5005	Liao He River - Liaozhong	Temperate Forest	0.33	11.23	3.67	0.86	1.01
39105	Kicking Horse River	Forest Tundra	0.32	3.71	1.17	0.84	1.06
135009	Weser River - at Hemeln	Temperate Forest	0.31	11.99	3.74	0.75	1.24
150003	Han River - Chungju (South)	Temperate Forest	0.31	13.04	4.01	0.57	0.87
200003	Rhine River - at Basel	Temperate Forest	0.30	13.02	3.84	0.70	1.11
28018	St. Marys River - Lake Superior MI	Temperate Forest	0.28	7.70	2.16	0.96	1.23
26027	Mezen River	Boreal Forest	0.28	5.09	1.40	0.96	0.79
39007	Fraser River - Hope	Forest Tundra	0.27	8.90	2.45	0.83	1.22

28020	Niagara River - Lake Ontario	Temperate Forest	0.27	12.38	3.36	0.84	1.10
75002	Minho River - at Point Mayor Oroza	Temperate Forest	0.27	13.45	3.65	0.55	0.77
135019	Elbe River - at Magdeburg	Temperate Forest	0.26	11.65	3.07	0.86	1.17
28016	Talkeetna River	Boreal Forest	0.26	4.81	1.26	0.92	1.07
45001	Glama River - at Askim	Boreal Forest	0.26	6.48	1.65	0.93	1.07
200002	Rhine River - at Rekingen	Temperate Forest	0.25	11.31	2.85	0.78	0.70
66002	Danube River - at Budapest	Temperate Forest	0.25	11.64	2.90	0.87	1.08
135005	Moselle River - at Koblenz/Moselle	Temperate Forest	0.25	13.23	3.25	0.82	1.23
8003	Gudena River - Tvilum Bro	Temperate Forest	0.24	9.93	2.35	0.85	1.08
28017	Hudson River - Green Island	Temperate Forest	0.23	12.48	2.89	0.93	0.91
28002	Columbia River - Warrendale OR	Temperate Forest	0.23	11.14	2.53	0.87	0.73
39003	St. Lawrence River - Montreal	Temperate Forest	0.23	12.30	2.79	0.92	0.97
200007	Ticino - Riazzino	Warm Temperate Forest	0.22	8.77	1.97	0.72	1.61
135011	Elbe River - at Geesthacht	Temperate Forest	0.22	12.83	2.85	0.85	1.18
39108	Cowichan River	Temperate Forest	0.22	12.42	2.72	0.80	0.67
73003	Minho River - at Valenca	Temperate Forest	0.22	14.74	3.22	0.63	1.01
75009	Douro River - at Puente Pino	Steppe	0.21	15.40	3.30	0.78	1.19
80018	Kyu-Kitakami River - at Kanomata	Temperate Forest	0.21	13.37	2.86	0.90	1.29
28008	Delaware River - Chain Bridge	Temperate Forest	0.21	12.72	2.67	0.92	0.93
30004	Aliakmon River - at Kazani	Chapparal	0.21	14.28	2.94	0.85	1.13
26004	Tom River	Boreal Forest	0.20	6.79	1.35	0.98	0.90
26019	Nimelen River	Boreal Forest	0.20	6.90	1.37	0.96	1.11
135003	Rhine River - at Koblenz/Braubach	Temperate Forest	0.20	14.55	2.87	0.83	1.23
150001	Han River	Temperate Forest	0.20	13.84	2.72	0.91	1.09
28021	St. Lawrence River - Massena NY	Temperate Forest	0.19	11.29	2.20	0.94	0.88
68005	Po River - at Cremona	Temperate Forest	0.19	14.95	2.90	0.84	1.17
68003	Adige River - at Badia Polesine	Chapparal	0.19	11.73	2.27	0.84	2.06
75011	Tejo River - at Aranjuez	Chapparal	0.19	15.89	3.03	0.79	1.03
26003	Belaya River	Steppe	0.19	13.29	2.50	0.86	0.89
73006	Douro River - at Pinhao	Temperate Forest	0.19	15.98	2.96	0.80	1.19
27027	Spey River - Fochabers.	Temperate Forest	0.18	8.38	1.53	0.90	1.19
48013	Santa Lucia River	Warm Temperate Forest	0.18	18.04	3.18	0.74	0.93
73009	Mondego River - Ponte Penacova	Chapparal	0.18	15.98	2.81	0.67	1.05
67003	Barro River - at Grauguenamanagh Bridge	Temperate Forest	0.17	11.17	1.95	0.84	1.10
68008	Po River - at Pontelagoscuro	Chapparal	0.17	15.73	2.73	0.87	1.26
26016	Kuban River	Temperate Forest	0.17	12.62	2.13	0.94	1.10
26015	Don River	Steppe	0.17	11.44	1.92	0.96	1.07
28005	Susquehanna River	Temperate Forest	0.17	14.48	2.43	0.95	0.94
12064	Rhone River - Collonges	Temperate Forest	0.16	11.28	1.86	0.87	0.91
200004	Aare River - at Brugg	Forest Tundra	0.16	11.53	1.85	0.90	1.32
26013	Severnaya Dvina River	Boreal Forest	0.15	6.13	0.92	0.99	0.99
8002	Odense River - Nr Broby	Temperate Forest	0.15	8.97	1.33	0.94	0.97
73010	Tejo River - at Albufeira de Cedilho	Chapparal	0.15	15.30	2.27	0.60	0.90
27015	North Tyne River - Cholleford	Temperate Forest	0.15	9.62	1.42	0.91	1.23
33004	Murray River - Rufus	Chapparal	0.15	18.56	2.72	0.72	0.96
33009	Darling River - Burtundy 425007	Tropical Semi-Arid	0.14	19.34	2.77	0.77	0.93
28525	Mississippi River - St. Francisville	Tropical Seasonal Forest	0.14	19.42	2.71	0.95	1.00
8005	Susa River - Hollose Molle	Temperate Forest	0.14	10.10	1.39	0.96	1.05
135004	Moselle River - at Palzem	Temperate Forest	0.14	13.63	1.85	0.92	1.21
30001	Nestos River - at Drama	Temperate Forest	0.13	12.53	1.69	0.95	1.07
27008	Tweed River above Galafoot	Temperate Forest	0.13	9.14	1.23	0.94	1.10
78002	Blue Nile River - at Khartoum	Hot Desert	0.13	25.79	3.47	0.03	0.88
135012	Danube River - at Jochenstein	Temperate Forest	0.13	10.03	1.35	0.94	1.22
27017	Tyne River - Wylam Bridge	Temperate Forest	0.13	10.71	1.42	0.94	1.44
28004	Missouri River - MO	Temperate Forest	0.13	14.91	1.93	0.96	0.94
28013	Dismal River	Steppe	0.13	14.65	1.89	0.93	1.00

135001	Rhine River - at Maxau	Temperate Forest	0.13	12.76	1.63	0.93	1.09
135008	Ems River - at Herbrum	Temperate Forest	0.13	11.78	1.48	0.94	1.05
28012	Arkansas River	Warm Temperate Forest	0.12	17.73	2.21	0.95	0.98
28007	Potomac River - DC	Warm Temperate Forest	0.12	16.35	1.96	0.95	0.97
66001	Tisza River - at Szolnok	Temperate Forest	0.12	11.30	1.32	0.97	1.07
80014	Ohta River - at Hesaka	Temperate Forest	0.12	15.80	1.84	0.95	0.92
37005	Coatzacoalcos River	Tropical Rain Forest	0.12	22.68	2.63	0.30	0.80
28014	Apalachicola River - Chattahoochee FL	Tropical Seasonal Forest	0.11	20.39	2.34	0.90	1.03
21004	Odra River - Chalupki	Temperate Forest	0.11	10.76	1.23	0.97	1.17
75021	Ebro River - at Tortosa	Chapparal	0.11	18.49	2.11	0.89	1.25
99006	Niger River - at Koulikoro (Campement Somono)	Tropical Dry Forest	0.11	27.50	3.08	0.59	1.14
67001	Boyne River - at Slane Bridge	Temperate Forest	0.11	10.78	1.18	0.94	1.07
73004	Minho River - at Foz do Mouro	Temperate Forest	0.11	13.79	1.50	0.89	1.17
51047	Ourthe River - at Comblain-au-Pont	Temperate Forest	0.11	11.16	1.21	0.94	1.18
135021	Elbe River - at Schmilka	Temperate Forest	0.11	12.21	1.31	0.96	1.18
26012	Pechora River	Forest Tundra	0.11	3.78	0.40	1.00	0.88
51001	Scheldt River - at Bleharies (MRW 360)	Temperate Forest	0.10	12.08	1.25	0.96	1.02
31059	Mahandi River - at Cuttack (Stn 1277)	Tropical Seasonal Forest	0.10	27.59	2.86	0.29	0.99
5001	Yangtze River (Chang Jiang)	Warm Temperate Forest	0.10	17.90	1.85	0.94	0.88
17039	Tukituki River - at Red Bridge	Temperate Forest	0.10	15.96	1.63	0.88	1.57
27024	Ribble River - Samlesbury	Temperate Forest	0.10	10.26	1.05	0.96	1.10
12052	Garonne River - Valence of Agen	Temperate Forest	0.10	13.53	1.38	0.95	0.97
75010	Tejo River - at Trilllo	Steppe	0.10	13.10	1.31	0.94	0.94
73011	Guadiana River - at Rocha da Gale	Chapparal	0.10	18.42	1.83	0.92	1.05
104004	Ruvu River - at Mlandizi	Tropical Dry Forest	0.10	27.06	2.68	0.13	0.99
135010	Weser River - at Intschede	Temperate Forest	0.10	12.75	1.25	0.95	1.19
12162	Rhone River - Lyon (2)	Temperate Forest	0.10	13.08	1.28	0.95	1.01
75012	Tejo River - at Talavera de la Reina	Chapparal	0.10	15.41	1.50	0.95	1.00
73008	Vouga River - at S.Joao de Loure	Warm Temperate Forest	0.10	15.35	1.50	0.90	1.03
21006	Odra River - Krajnik	Temperate Forest	0.10	10.96	1.05	0.98	1.08
27001	Thames River	Temperate Forest	0.10	12.41	1.18	0.96	1.06
12053	Garonne River - Toulouse	Temperate Forest	0.09	13.51	1.26	0.96	0.94
27005	Dee River	Temperate Forest	0.09	10.79	1.00	0.96	1.04
17022	Waikato River - at Reids Farm	Temperate Forest	0.09	14.90	1.38	0.84	1.61
28001	Mississippi River - Vicksburg MS	Tropical Seasonal Forest	0.09	17.66	1.60	0.98	0.99
28011	Sacramento River - Freeport CA	Steppe	0.09	15.05	1.36	0.95	0.87
30006	Acheloos River - at Agrinion	Chapparal	0.09	14.92	1.35	0.93	1.08
80024	Kuma River - at Yokoishi	Warm Temperate Forest	0.09	17.40	1.56	0.93	1.23
75017	Guadalquivir River - at Penaflor	Chapparal	0.09	18.30	1.64	0.91	1.00
75020	Ebro River - at Zaragoza	Chapparal	0.09	15.37	1.37	0.96	1.29
5003	Pearl River (Zhu Jiang)	Tropical Seasonal Forest	0.09	22.20	1.97	0.89	1.02
75013	Tajo River - at Alcantara	Chapparal	0.09	19.98	1.74	0.91	1.22
17037	Motu River - at Houpoto	Warm Temperate Forest	0.09	13.66	1.19	0.91	0.95
27009	Carron River	Boreal Forest	0.09	8.80	0.76	0.97	1.55
54009	Mekong River - Chiang Saen	Tropical Seasonal Forest	0.09	23.26	2.01	0.48	1.10
26005	Irtysh River	Steppe	0.08	12.40	1.05	0.98	1.01
27004	Trent River - Nottingham	Temperate Forest	0.08	12.11	1.02	0.96	1.14
28009	Ohio River - IL	Warm Temperate Forest	0.08	17.03	1.42	0.98	0.97
37016	Grijalva River	Tropical Rain Forest	0.08	27.28	2.28	0.05	1.02
14010	Karun River in Ahwaz City	Hot Desert	0.08	23.59	1.95	0.60	1.34
17058	Hurunui River - at Mandamus	Temperate Forest	0.08	9.69	0.79	0.94	1.28
73013	Douro River - Albufeir Do Focinho	Temperate Forest	0.08	15.64	1.28	0.96	1.17
80023	Chikugo River - at Senoshita	Temperate Forest	0.08	18.44	1.49	0.96	1.23
136002	Lower Ganges River - at Padha	Tropical Dry Forest	0.08	26.48	2.12	0.41	0.93
33003	Yarra River	Chapparal	0.08	14.33	1.14	0.96	1.17
31002	Sabarmati River - in Ahmedabad	Tropical Semi-Arid	0.08	27.60	2.17	0.35	1.01

70003	Mekong River - at Luang Prabang	Tropical Seasonal Forest	0.08	23.82	1.87	0.53	0.96
149002	My Thuan - Mekong River	Tropical Dry Forest	0.08	26.55	2.07	0.12	0.86
17002	Waikato River - at Mercer Bridge	Warm Temperate Forest	0.08	16.34	1.27	0.90	1.09
17075	Clutha River - at Balclutha	Temperate Forest	0.08	11.78	0.91	0.95	1.65
17071	Clutha River - at Millers Flat	Boreal Forest	0.08	11.63	0.89	0.94	1.76
37001	Colorado River	Hot Desert	0.08	16.98	1.30	0.87	0.76
46001	Rhine River - at German Frontier	Temperate Forest	0.08	12.98	0.99	0.98	1.11
303005	Purus River - Labrea	Tropical Rain Forest	0.08	28.65	2.16	0.18	1.05
14006	Zayandeh River in Isfanhan	Hot Desert	0.08	12.21	0.92	0.96	0.83
75018	Guadalquivir River - at Seville	Tropical Dry Forest	0.07	19.76	1.48	0.94	1.08
4002	Maipo River in El Manzano	Tundra	0.07	9.47	0.70	0.85	0.85
28517	Atchafalaya River - Melville	Tropical Seasonal Forest	0.07	23.90	1.77	0.94	0.91
17005	Waipapa River - at Forest Ranger	Warm Temperate Forest	0.07	14.52	1.06	0.91	0.89
31047	Tapti River - at Kathore	Tropical Dry Forest	0.07	27.08	1.93	0.15	0.96
64005	Tonle Sap River - Prek Dam	Tropical Dry Forest	0.07	28.54	2.04	0.02	1.09
31054	Godavari River - at Rajahmundry Downstream	Tropical Dry Forest	0.07	28.33	2.01	0.01	0.95
54002	Chao Phrya River - Nakhon Sawan	Tropical Dry Forest	0.07	29.17	2.04	0.11	1.00
37003	Bravo River	Tropical Semi-Arid	0.07	24.26	1.69	0.88	0.96
54013	Nam Songkhram River - Ban Tha Kok Daeng	Tropical Rain Forest	0.07	28.18	1.96	0.32	0.99
56006	Indus River - at Kotri	Hot Desert	0.07	25.78	1.77	0.85	0.88
17045	Hutt River - at Kaitoke	Temperate Forest	0.07	9.43	0.64	0.93	0.75
75005	Guadiana River - at Point Palmas BA01A	Chapparal	0.07	16.02	1.09	0.97	1.02
37004	Panuco River	Tropical Dry Forest	0.07	21.70	1.47	0.79	0.90
31031	Cauvery River - near Musiri	Tropical Dry Forest	0.07	29.16	1.97	0.05	1.07
17028	Whanganui River - at Paetawa	Warm Temperate Forest	0.07	14.38	0.96	0.96	1.13
64002	Mekong River - at Phnom Penh	Tropical Dry Forest	0.07	27.73	1.83	0.00	1.05
54011	Mekong River - Khong Chiam	Tropical Rain Forest	0.07	26.43	1.73	0.31	0.92
12031	Seine River - Paris	Temperate Forest	0.07	13.63	0.89	0.98	0.98
17029	Rangitikei River - at Mangaweka	Temperate Forest	0.06	10.85	0.70	0.97	0.93
17080	Waiau River - at Tuatapere	Temperate Forest	0.06	11.34	0.73	0.97	1.59
28125	Peace River - FL	Tropical Seasonal Forest	0.06	24.94	1.60	0.82	1.03
17013	Waikato River - at Hamilton Traffic Bridge	Warm Temperate Forest	0.06	16.28	1.04	0.93	1.11
80021	Yoshino River - at Takase	Temperate Forest	0.06	16.11	1.02	0.98	1.02
17044	Hutt River - at Boulcott	Temperate Forest	0.06	11.77	0.73	0.95	0.88
48015	Uruguay River - Salto	Tropical Seasonal Forest	0.06	19.99	1.24	0.93	1.08
31007	Narmada River - near Garudeshwar	Tropical Semi-Arid	0.06	25.99	1.60	0.38	0.93
303012	Amazonas River - Obidos	Tropical Seasonal Forest	0.06	28.11	1.73	0.39	0.93
10004	Nile River - at El Shobak	Hot Desert	0.06	23.75	1.45	0.86	0.91
31014	Godavari River - near Polavaram	Tropical Dry Forest	0.06	27.72	1.62	0.01	0.94
17019	Rangitaiki River - at Murupara	Temperate Forest	0.06	13.14	0.77	0.91	1.15
303010	Madeira River - Porto Velho	Tropical Rain Forest	0.06	26.97	1.56	0.11	1.06
1003	Paraguay River - at Puerto Bermejo	Tropical Seasonal Forest	0.06	24.23	1.40	0.85	1.05
24002	Sakarya River - Adatepe	Steppe	0.06	15.00	0.86	0.98	1.12
10002	Nile River - at Aswan	Hot Desert	0.06	25.10	1.42	0.85	0.88
12041	Loire River - Orleans	Temperate Forest	0.06	13.91	0.78	0.99	1.05
31025	Krishna River - near Vijayawada	Tropical Dry Forest	0.06	28.06	1.58	0.01	0.94
17026	Manganui River - at SH3	Temperate Forest	0.06	10.38	0.58	0.96	0.82
70006	Se Bang River - at Ban Kengdone	Tropical Seasonal Forest	0.06	27.16	1.50	0.67	1.04
31030	Pennar River - near Siddvata	Tropical Dry Forest	0.05	27.94	1.52	0.54	0.96
70005	Se Done River - at Ban Souvannakhili	Tropical Rain Forest	0.05	27.27	1.42	0.21	0.95
77006	Sebou River - at Kenitra	Chapparal	0.05	21.47	1.12	0.95	1.17
70002	Mekong River - at Vientiane	Tropical Seasonal Forest	0.05	25.90	1.35	0.76	0.96
31057	Kathajodi River - at Cuttack (Stn 1301)	Tropical Seasonal Forest	0.05	28.51	1.47	0.89	1.04
73001	Tejo River - at Santarem	Chapparal	0.05	17.17	0.88	0.96	1.05
10003	Nile River - at Assiut	Hot Desert	0.05	24.46	1.26	0.88	0.91
12042	Loire River - Ingrandes	Temperate Forest	0.05	13.77	0.71	0.99	1.01

28010	Rio Grande - Brownsville TX	Tropical Semi-Arid	0.05	25.58	1.31	0.94	1.06
12051	Garonne River - Couthures	Chapparal	0.05	14.18	0.72	0.99	0.95
17054	Buller River -at Te Huha	Boreal Forest	0.05	11.70	0.60	0.98	1.45
81002	Pra River - at Daboase	Tropical Dry Forest	0.05	26.42	1.34	0.31	0.94
70007	Se Bang Fai River - at Se Bang Fai	Tropical Seasonal Forest	0.05	26.03	1.32	0.52	1.05
33001	La Trobe River	Chapparal	0.05	16.34	0.81	0.96	1.17
17052	Wairau River - at Tuamarina	Temperate Forest	0.05	14.43	0.71	0.98	1.24
21002	Vistula River - Warszawa	Temperate Forest	0.05	11.08	0.54	1.00	1.09
28006	Colorado River - Hoover Dam AZ	Hot Desert	0.05	13.30	0.64	0.03	0.70
27003	Exe River	Temperate Forest	0.05	11.02	0.52	0.99	1.11
68006	Po River - at Boretto	Temperate Forest	0.05	14.36	0.68	0.99	1.15
70010	Nam Lik River - at Thalath	Tropical Seasonal Forest	0.05	25.78	1.21	0.44	0.99
136003	Brahmaputra River	Tropical Rain Forest	0.05	27.74	1.29	0.80	1.04
1004	Parana River - at Rosario	Chapparal	0.05	21.47	1.00	0.94	1.05
82006	Kelantan River	Tropical Rain Forest	0.05	27.53	1.28	0.00	1.03
31029	Tungabhadra River - at Ullanuru	Tropical Semi-Arid	0.05	26.53	1.20	0.11	0.93
303011	Madeira River - Fazenda Vista Alegre	Tropical Seasonal Forest	0.04	29.05	1.30	0.02	0.99
31012	Godavari River - near Dhalegaon	Tropical Dry Forest	0.04	25.83	1.14	0.14	0.94
54010	Mekong River - Nakhon Phanom	Tropical Seasonal Forest	0.04	26.77	1.15	0.76	0.95
20003	Pampanga River	Tropical Rain Forest	0.04	29.39	1.25	0.01	0.97
2012	Velhas River - Honorio Bicalho	Tropical Seasonal Forest	0.04	21.71	0.91	0.75	1.07
76006	Kelani River - at Seethawake	Tropical Rain Forest	0.04	26.30	1.10	0.15	1.01
37015	Usumacinta River	Tropical Seasonal Forest	0.04	27.56	1.10	0.73	1.02
17018	Tarawere River - at Awakaponga	Temperate Forest	0.04	16.64	0.65	0.92	1.27
77007	Estruary at the Moulouya River	Chapparal	0.04	19.68	0.75	0.97	0.76
81003	White Volta River - at Nawuni	Tropical Dry Forest	0.04	29.68	1.12	0.52	0.95
31049	Subarnerekha River - at Mango Bridge	Tropical Dry Forest	0.04	28.88	1.09	0.90	1.08
21003	Vistula River - Kiezmark	Temperate Forest	0.04	10.43	0.39	1.00	1.02
56005	Lower Chenab River - Gujra Branch	Hot Desert	0.04	18.91	0.70	0.96	0.68
70009	Nam Lik River - at Nam Ngum below Dam	Tropical Seasonal Forest	0.03	25.41	0.88	0.32	1.09
31011	Wainganga River - near Ashti	Tropical Dry Forest	0.03	25.08	0.84	0.81	0.89
31004	Mahi River - near Sevalia	Tropical Semi-Arid	0.03	26.87	0.86	0.89	1.00
70004	Se Done River - at Se Done Dam Site	Tropical Rain Forest	0.03	27.58	0.84	0.79	0.95
82001	Klang River	Tropical Rain Forest	0.03	26.27	0.79	0.02	1.02
1002	Parana River - at Corrientes	Tropical Seasonal Forest	0.03	22.93	0.67	0.97	0.93
64001	Mekong River - near Luang	Tropical Seasonal Forest	0.03	28.74	0.81	0.36	1.03
2008	Jacui River - JA 042	Tropical Seasonal Forest	0.03	21.34	0.59	0.99	1.01
54012	Nam Mae Kok River - Chiang Rai	Tropical Seasonal Forest	0.03	25.37	0.70	0.94	1.02
31013	Godavari River - near Mancherial	Tropical Dry Forest	0.03	28.14	0.76	0.71	0.99
31028	Bhima River - near Takali	Tropical Semi-Arid	0.02	27.27	0.64	0.83	1.00
149005	Chau Doc - Mekong River	Tropical Seasonal Forest	0.02	29.36	0.66	0.77	0.96
64003	Mekong River - at Kam Pong Cham	Tropical Dry Forest	0.02	28.54	0.60	0.68	1.01
2009	Capibaribe River	Tropical Seasonal Forest	0.02	27.35	0.57	0.80	1.12
31033	Cauvery River - downstream K.R.S. Reservoir	Tropical Semi-Arid	0.02	26.22	0.51	0.59	1.06
104003	Kagera River - at Nyakanyasi	Tropical Seasonal Forest	0.02	24.43	0.46	0.19	0.93
127001	Waimanu River - XF 53 05	Tropical Seasonal Forest	0.01	24.70	0.32	0.92	1.00
31018	Periyar River - near Kalady	Tropical Seasonal Forest	0.01	27.95	0.33	0.92	1.07
82005	Muda River	Tropical Rain Forest	0.01	26.79	0.14	0.33	1.01
		Min	0.01	2.61	0.14	0.00	0.30
		Max	1.66	29.68	8.84	1.00	2.29

APPENDIX V

Results GEMS stations mean discharge sorted by RSE

GEMS ID	Name	Climate	RSE	Ō	SE	R^2	α
51036	Dyle River - at Sint-Agatha-Rode	Temperate Forest	1.65	8.88	14.64	0.23	0.45
31030	Pennar River - near Siddvata	Tropical Dry Forest	1.53	70.33	107.35	0.28	0.24
20003	Pampanga River	Tropical Rain Forest	1.22	211.42	258.75	0.09	0.62
70004	Se Done River - at Se Done Dam Site	Tropical Rain Forest	1.16	60.88	70.69	0.28	0.01
31029	Tungabhadra River - at Ullanuru	Tropical Semi-Arid	1.08	155.19	167.72	0.43	0.43
70006	Se Bang River - at Ban Kengdone	Tropical Seasonal Forest	1.05	413.83	434.15	0.41	1.14
31025	Krishna River - near Vijayawada	Tropical Dry Forest	1.04	1020.76	1061.25	0.60	0.72
2009	Capibaribe River	Tropical Seasonal Forest	0.96	42.01	40.23	0.63	0.89
31028	Bhima River - near Takali	Tropical Semi-Arid	0.90	254.72	229.13	0.67	1.53
39110	Fraser River - Red Pass	Forest Tundra	0.84	44.98	37.57	0.48	1.00
39101	Alsek River	Tundra	0.80	223.68	178.86	0.54	1.65
56006	Indus River - at Kotri	Hot Desert	0.77	2278.20	1750.68	0.73	0.71
31033	Cauvery River - downstream K.R.S. Reservoir	Tropical Semi-Arid	0.77	151.02	115.76	0.73	0.37
99006	Niger River - at Koulikoro (Campement Somono)	Tropical Dry Forest	0.76	1021.53	777.50	0.62	0.47
73006	Douro River - at Pinhao	Temperate Forest	0.72	168.42	122.02	0.15	0.41
31031	Cauvery River - near Musiri	Tropical Dry Forest	0.72	239.62	171.87	0.29	0.21
73011	Guadiana River - at Rocha da Gale	Chapparal	0.71	117.95	84.24	0.56	1.43
26004	Tom River	Boreal Forest	0.69	1032.33	714.98	0.71	5.31
39021	Skeena River	Forest Tundra	0.68	897.82	606.60	0.52	2.09
75005	Guadiana River - at Point Palmas BA01A	Chapparal	0.65	51.22	33.25	0.47	0.78
31012	Godavari River - near Dhalegaon	Tropical Dry Forest	0.63	98.40	62.31	0.80	0.54
26013	Severnaya Dvina River	Boreal Forest	0.63	3266.48	2043.44	0.73	2.19
39105	Kicking Horse River	Forest Tundra	0.62	40.23	25.00	0.71	0.90
26019	Nimelen River	Boreal Forest	0.61	114.33	69.70	0.62	4.87
39109	Elk River - Elko	Boreal Forest	0.60	45.27	27.37	0.67	0.92
39007	Fraser River - Hope	Forest Tundra	0.58	2676.68	1542.62	0.44	1.19
54013	Nam Songkhram River - Ban Tha Kok Daeng	Tropical Rain Forest	0.57	150.93	85.82	0.88	1.40
39022	Stikine River	Forest Tundra	0.56	651.95	367.90	0.70	1.97
26010	Yenisey River	Boreal Forest	0.56	19113.19	10701.84	0.72	1.30
56005	Lower Chenab River - Gujra Branch	Hot Desert	0.54	1482.52	807.60	0.81	1.97
70005	Se Done River - at Ban Souvannakhili	Tropical Rain Forest	0.52	164.26	85.94	0.87	1.52
31018	Periyar River - near Kalady	Tropical Seasonal Forest	0.52	199.83	103.90	0.80	1.34
1003	Paraguay River - at Puerto Bermejo	Tropical Seasonal Forest	0.51	422.24	215.93	0.76	2.38
73008	Vouga River - at S.Joao de Loure	Warm Temperate Forest	0.51	11.28	5.76	0.66	0.50
26027	Mezen River	Boreal Forest	0.50	76.68	38.61	0.85	2.60
39102	Liard River	Boreal Forest	0.50	357.52	179.97	0.75	2.36
5005	Liao He River - Liaozhong	Temperate Forest	0.49	54.98	27.14	0.82	0.27
65007	Iijoki River - at Raasakan	Boreal Forest	0.49	166.88	80.96	0.64	2.31
26018	Lena River - Kusur	Forest Tundra	0.48	17096.35	8255.77	0.87	1.17
73009	Mondego River - Ponte Penacova	Chapparal	0.48	125.79	60.61	0.72	2.50
54005	Mun River	Tropical Seasonal Forest	0.48	648.45	311.10	0.82	0.41
80021	Yoshino River - at Takase	Temperate Forest	0.48	121.26	57.86	0.56	4.44
77007	Estruary at the Moulouya River	Chapparal	0.46	13.82	6.40	0.64	2.65
81003	White Volta River - at Nawuni	Tropical Dry Forest	0.44	234.51	103.66	0.92	2.01
26011	Ob River	Forest Tundra	0.44	13083.76	5761.20	0.73	1.12
31047	Tapti River - at Kathore	Tropical Dry Forest	0.43	467.69	203.34	0.75	0.73
31002	Sabarmati River - in Ahmedabad	Tropical Semi-Arid	0.43	49.19	21.20	0.90	0.82
28094	Tar River - NC	Warm Temperate Forest	0.43	65.13	28.00	0.46	2.41
150003	Han River - Chungju (South)	Temperate Forest	0.43	257.69	110.40	0.77	0.87

104005	Ruvu River - at Rufiji Stiglers Gorge	Tropical Semi-Arid	0.43	667.06	284.37	0.72	0.32
37005	Coatzacoalcos River	Tropical Rain Forest	0.42	458.45	191.57	0.70	2.48
28016	Talkeetna River	Boreal Forest	0.42	113.35	47.15	0.84	2.25
26028	Lena River - Stolb	Tundra	0.42	15693.45	6521.16	0.90	1.05
51047	Ourthe River - at Comblain-au-Pont	Temperate Forest	0.41	27.20	11.28	0.61	1.02
31013	Godavari River - near Mancherial	Tropical Dry Forest	0.41	377.47	156.46	0.92	0.69
65008	Kemijoki River - at Isohaara 14000	Boreal Forest	0.41	562.59	230.68	0.63	3.84
12031	Seine River - Paris	Temperate Forest	0.41	320.63	130.29	0.67	0.87
28102	Contentnea Creek - NC	Tropical Seasonal Forest	0.41	22.79	9.26	0.36	1.56
33008	Murrumbidgee River - Burrinjuck 410008	Chapparal	0.40	40.54	16.42	0.20	0.24
127001	Waimanu River - XF 53 05	Tropical Seasonal Forest	0.40	58.45	23.61	0.57	1.30
2008	Jacui River - JA 042	Tropical Seasonal Forest	0.40	1629.38	647.33	0.66	0.99
104004	Ruvu River - at Mlandizi	Tropical Dry Forest	0.39	51.35	20.13	0.79	0.28
26020	Dzhida River	Cold Parklands	0.39	36.53	14.27	0.89	0.71
78002	Blue Nile River - at Khartoum	Hot Desert	0.38	1175.24	450.27	0.93	0.51
28120	Kissimmee River - FL	Tropical Seasonal Forest	0.38	39.28	14.92	0.22	0.86
75020	Ebro River - at Zaragoza	Chapparal	0.38	273.98	104.06	0.56	1.92
31004	Mahi River - near Sevalia	Tropical Semi-Arid	0.38	501.29	189.10	0.96	4.05
8002	Odense River - Nr Broby	Temperate Forest	0.38	3.03	1.14	0.68	0.28
77006	Sebou River - at Kenitra	Chapparal	0.37	37.14	13.84	0.39	0.21
26016	Kuban River	Temperate Forest	0.37	340.32	126.07	0.06	0.43
67003	Barro River - at Grauguenamanagh Bridge	Temperate Forest	0.37	38.70	14.17	0.52	0.84
39001	Mackenzie River	Boreal Forest	0.36	8930.13	3221.05	0.74	1.34
39006	Roseau River - at Gardenton	Temperate Forest	0.36	12.39	4.42	0.89	0.89
30006	Acheloos River - at Agrinion	Chapparal	0.35	52.48	18.18	0.77	1.62
73001	Tejo River - at Santarem	Chapparal	0.34	347.40	119.76	0.76	1.61
45002	Glama River - at Haslemoen	Boreal Forest	0.34	251.38	86.06	0.72	1.68
135021	Elbe River - at Schmilka	Temperate Forest	0.34	340.90	116.64	0.07	0.73
26002	Selenga River	Cold Parklands	0.34	931.06	316.40	0.85	0.33
150001	Han River	Temperate Forest	0.34	385.00	130.44	0.87	0.70
200005	Rhone River - at Porte du Scex	Tundra	0.33	190.23	63.47	0.47	0.79
135019	Elbe River - at Magdeburg	Temperate Forest	0.33	568.61	189.20	0.14	0.72
26003	Belaya River	Steppe	0.33	798.13	265.22	0.88	2.65
17039	Tukituki River - at Red Bridge	Temperate Forest	0.33	869.81	288.59	0.85	9.89
31011	Wainganga River - near Ashti	Tropical Dry Forest	0.33	739.01	245.04	0.96	1.02
26005	Irtysh River	Steppe	0.33	795.91	263.70	0.70	0.85
33004	Murray River - Rufus	Chapparal	0.33	214.40	70.57	0.73	0.11
48013	Santa Lucia River	Warm Temperate Forest	0.33	59.83	19.68	0.62	0.32
28012	Arkansas River	Warm Temperate Forest	0.33	605.63	198.81	0.78	0.34
30004	Aliakmon River - at Kazani	Chapparal	0.33	43.16	14.07	0.82	1.27
26017	Kolyma River	Cold Parklands	0.32	3255.14	1049.48	0.95	1.20
31007	Narmada River - near Garudeshwar	Tropical Semi-Arid	0.32	1251.65	398.62	0.96	1.31
75010	Tejo River - at Trilllo	Steppe	0.31	16.61	5.21	0.66	5.43
14006	Zayandeh River in Isfanhan	Hot Desert	0.30	17.50	5.26	0.00	0.36
12162	Rhone River - Lyon (2)	Temperate Forest	0.30	1111.35	332.62	0.59	1.35
135011	Elbe River - at Geesthacht	Temperate Forest	0.30	710.32	210.68	0.36	0.62
27009	Carron River	Boreal Forest	0.29	10.78	3.15	0.55	0.09
12051	Garonne River - Couthures	Chapparal	0.29	693.67	202.34	0.67	2.37
27015	North Tyne River - Chollefor d	Temperate Forest	0.29	46.59	13.31	0.71	1.26
66001	Tisza River - at Szolnok	Temperate Forest	0.28	579.23	162.37	0.59	0.89
49001	Daule River	Tropical Dry Forest	0.28	291.48	81.29	0.88	0.88
51001	Scheldt River - at Bleharies (MRW 360)	Temperate Forest	0.28	19.86	5.52	0.49	0.36
21004	Odra River - Chalupki	Temperate Forest	0.27	42.72	11.63	0.20	0.77
26012	Pechora River	Forest Tundra	0.27	4708.03	1271.71	0.95	1.95

303011	Madeira River - Fazenda Vista Alegre	Tropical Seasonal Forest	0.27	26651.64	7150.84	0.76	1.30
28145	Alabama River - AL	Tropical Seasonal Forest	0.27	1106.62	295.45	0.86	1.79
54010	Mekong River - Nakhon Phanom	Tropical Seasonal Forest	0.27	6403.53	1707.49	0.92	1.29
39108	Cowichan River	Temperate Forest	0.27	9.46	2.51	0.92	0.09
27001	Thames River	Temperate Forest	0.27	76.77	20.37	0.80	0.69
70010	Nam Lik River - at Thalath	Tropical Seasonal Forest	0.26	400.58	105.12	0.89	1.03
54012	Nam Mae Kok River - Chiang Rai	Tropical Seasonal Forest	0.26	106.15	27.52	0.88	0.78
4002	Maipo River in El Manzano	Tundra	0.26	177.64	45.85	0.53	1.26
14010	Karun River in Ahwaz City	Hot Desert	0.26	701.33	180.63	0.65	2.28
82005	Muda River	Tropical Rain Forest	0.26	24.18	6.16	0.86	0.20
73003	Minho River - at Valenca	Temperate Forest	0.25	315.20	80.12	0.83	4.24
200007	Ticino - Riazzino	Warm Temperate Forest	0.25	68.55	17.36	0.71	0.65
75013	Tajo River - at Alcantara	Chapparal	0.25	209.82	53.10	0.80	1.96
33002	Mitta Mitta River	Temperate Forest	0.25	12.94	3.27	0.89	0.35
31014	Godavari River - near Polavaram	Tropical Dry Forest	0.25	3034.71	764.84	0.97	1.12
12042	Loire River - Ingrandes	Temperate Forest	0.25	1082.99	271.48	0.86	1.09
76006	Kelani River - at Seethawake	Tropical Rain Forest	0.25	140.37	34.86	0.77	0.84
65010	Oulujoki River - at Merikoski 13000	Boreal Forest	0.25	259.75	64.47	0.00	2.99
54011	Mekong River - Khong Chiam	Tropical Rain Forest	0.25	9281.12	2282.70	0.94	1.50
75009	Douro River - at Puente Pino	Steppe	0.24	230.93	55.74	0.84	0.68
303005	Purus River - Labrea	Tropical Rain Forest	0.24	5567.71	1330.27	0.90	0.82
135004	Moselle River - at Palzem	Temperate Forest	0.24	160.92	38.31	0.85	0.97
81002	Pra River - at Daboase	Tropical Dry Forest	0.23	184.66	43.35	0.85	1.44
67001	Boyne River - at Slane Bridge	Temperate Forest	0.23	32.71	7.66	0.91	0.99
26009	Amur River	Forest Tundra	0.23	9522.53	2225.35	0.91	1.00
70002	Mekong River - at Vientiane	Tropical Seasonal Forest	0.23	4219.93	980.75	0.92	1.32
135005	Moselle River - at Koblenz/Moselle	Temperate Forest	0.23	351.68	80.48	0.85	0.97
28009	Ohio River - IL	Warm Temperate Forest	0.23	8382.42	1917.63	0.78	1.50
5003	Pearl River (Zhu Jiang)	Tropical Seasonal Forest	0.23	6590.63	1507.14	0.89	1.04
30001	Nestos River - at Drama	Temperate Forest	0.23	39.04	8.83	0.83	2.51
10002	Nile River - at Aswan	Hot Desert	0.22	1821.38	404.80	0.00	0.23
10003	Nile River - at Assiut	Hot Desert	0.22	1186.90	260.14	0.00	0.15
28125	Peace River - FL	Tropical Seasonal Forest	0.22	25.74	5.64	0.88	1.20
82006	Kelantan River	Tropical Rain Forest	0.22	519.14	113.74	0.87	0.68
33001	La Trobe River	Chapparal	0.22	7.14	1.56	0.76	1.02
75012	Tejo River - at Talavera de la Reina	Chapparal	0.22	73.01	15.76	0.85	1.05
82007	Kinta River	Tropical Rain Forest	0.21	75.82	16.12	0.70	0.14
28003	Yukon River	Forest Tundra	0.21	6407.42	1347.88	0.94	4.17
28007	Potomac River - DC	Warm Temperate Forest	0.21	375.38	78.94	0.85	2.25
48015	Uruguay River - Salto	Tropical Seasonal Forest	0.21	5179.63	1089.06	0.45	0.82
70003	Mekong River - at Luang Prabang	Tropical Seasonal Forest	0.21	3740.38	786.03	0.93	1.30
28525	Mississippi River - St. Francisville	Tropical Seasonal Forest	0.21	15504.21	3250.88	0.77	0.82
65009	Kokemaenjoki River - Kojo 35 Pori-Tre	Temperate Forest	0.21	247.59	51.79	0.06	2.66
80018	Kyu-Kitakami River - at Kanomata	Temperate Forest	0.21	327.37	68.03	0.59	1.52
68005	Po River - at Cremona	Temperate Forest	0.20	1107.25	226.66	0.63	1.09
28001	Mississippi River - Vicksburg MS	Tropical Seasonal Forest	0.20	18581.27	3802.26	0.69	1.08
135009	Weser River - at Hemeln	Temperate Forest	0.20	123.03	25.00	0.78	2.04
67004	Blackwater River - at Killavullen	Temperate Forest	0.20	35.06	7.11	0.88	0.76
37015	Usumacinta River	Tropical Seasonal Forest	0.20	2063.72	414.29	0.87	0.72
39111	Okanagan River	Boreal Forest	0.20	19.66	3.94	0.80	0.37
12053	Garonne River - Toulouse	Temperate Forest	0.20	0.75	0.15	0.92	0.09
37004	Panuco River	Tropical Dry Forest	0.19	380.27	73.65	0.95	0.64
21003	Vistula River - Kiezmark	Temperate Forest	0.19	1080.88	205.32	0.61	0.97
26015	Don River	Steppe	0.19	692.10	131.23	0.63	0.27

12064	Rhone River - Collonges	Temperate Forest	0.19	362.01	68.26	0.39	0.99
17005	Waipapa River - at Forest Ranger	Warm Temperate Forest	0.19	4.61	0.87	0.76	0.05
10004	Nile River - at El Shobak	Hot Desert	0.19	1269.94	235.27	0.00	0.17
28063	Delaware River - Port Jervis NY	Temperate Forest	0.18	158.61	28.98	0.84	0.99
37003	Bravo River	Tropical Semi-Arid	0.18	24.83	4.54	0.78	0.05
75002	Minho River - at Point Mayor Oroza	Temperate Forest	0.18	233.17	42.53	0.90	0.93
27008	Tweed River above Galafoot	Temperate Forest	0.18	37.83	6.88	0.86	1.50
303010	Madeira River - Porto Velho	Tropical Rain Forest	0.18	19071.57	3423.95	0.92	1.38
33009	Darling River - Burtundy 425007	Tropical Semi-Arid	0.18	42.78	7.53	0.13	0.04
21006	Odra River - Krajnik	Temperate Forest	0.17	545.88	94.26	0.57	0.76
27003	Exe River	Temperate Forest	0.17	16.26	2.79	0.93	0.27
80014	Ohta River - at Hesaka	Temperate Forest	0.17	79.87	13.61	0.87	1.62
80024	Kuma River - at Yokoishi	Warm Temperate Forest	0.17	117.83	19.56	0.97	0.84
39004	Saskatchewan River (1) - above Carrot River	Boreal Forest	0.17	514.82	85.23	0.76	0.39
21002	Vistula River - Warszawa	Temperate Forest	0.16	570.50	94.08	0.55	0.87
68008	Po River - at Pontelagoscuro	Chapparal	0.16	1584.53	260.43	0.61	0.87
54002	Chao Phrya River - Nakhon Sawan	Tropical Dry Forest	0.16	651.68	106.76	0.91	0.52
28005	Susquehanna River	Temperate Forest	0.16	1009.18	161.73	0.91	1.47
24002	Sakarya River - Adatepe	Steppe	0.16	185.58	29.27	0.85	0.77
68006	Po River - at Boretto	Temperate Forest	0.16	1425.03	223.07	0.71	1.00
28017	Hudson River - Green Island	Temperate Forest	0.16	439.53	68.65	0.90	1.57
70007	Se Bang Fai River - at Se Bang Fai	Tropical Seasonal Forest	0.15	365.10	56.44	0.99	1.21
28469	Yakima River - WA	Steppe	0.15	94.32	14.52	0.85	0.49
303004	Amazonas River - Tabatinga	Tropical Rain Forest	0.15	7034.57	1072.93	0.49	0.31
75011	Tejo River - at Aranjuez	Chapparal	0.15	34.28	5.22	0.93	1.70
17058	Hurunui River - at Mandamus	Temperate Forest	0.15	56.18	8.47	0.67	0.52
27027	Spey River - Fochabers.	Temperate Forest	0.15	67.22	9.98	0.78	1.42
303012	Amazonas River - Obidos	Tropical Seasonal Forest	0.15	170712.52	24975.15	0.74	1.29
200004	Aare River - at Brugg	Forest Tundra	0.14	328.26	46.93	0.42	0.82
28006	Colorado River - Hoover Dam AZ	Hot Desert	0.14	414.14	59.17	0.48	0.63
136003	Brahmaputra River	Tropical Rain Forest	0.14	22547.41	3221.35	0.97	1.66
135008	Ems River - at Herbrum	Temperate Forest	0.14	83.76	11.95	0.93	0.63
75021	Ebro River - at Tortosa	Chapparal	0.14	338.80	47.17	0.89	0.66
5001	Yangtze River (Chang Jiang)	Warm Temperate Forest	0.14	13588.75	1874.86	0.97	0.84
27024	Ribble River - Samlesbury	Temperate Forest	0.14	32.83	4.48	0.93	0.58
39106	Columbia River - Waneta	Temperate Forest	0.14	2753.15	374.02	0.65	0.97
54009	Mekong River - Chiang Saen	Tropical Seasonal Forest	0.13	2522.58	337.47	0.96	1.35
46001	Rhine River - at German Frontier	Temperate Forest	0.13	2332.57	307.97	0.67	0.92
17071	Clutha River - at Millers Flat	Boreal Forest	0.13	525.69	69.12	0.04	0.69
17080	Waiau River - at Tuatapere	Temperate Forest	0.13	470.18	60.98	0.19	1.39
28008	Delaware River - Chain Bridge	Temperate Forest	0.13	342.57	43.47	0.90	1.20
200003	Rhine River - at Basel	Temperate Forest	0.13	1139.93	144.38	0.65	1.07
45001	Glama River - at Askim	Boreal Forest	0.13	681.19	86.27	0.92	1.41
17075	Clutha River - at Balclutha	Temperate Forest	0.13	600.19	75.90	0.13	0.72
28004	Missouri River - MO	Temperate Forest	0.13	2594.72	326.65	0.81	0.65
17019	Rangitaiki River - at Murupara	Temperate Forest	0.12	20.75	2.58	0.04	0.21
17054	Buller River -at Te Huha	Boreal Forest	0.12	448.68	55.72	0.73	1.27
200001	Rhine River - at Diepoldsau	Tundra	0.12	241.99	29.62	0.95	0.65
68002	Adige River - at Trento	Temperate Forest	0.12	234.64	28.59	0.93	0.52
136002	Lower Ganges River - at Padha	Tropical Dry Forest	0.12	11024.33	1333.21	0.99	1.10
27005	Dee River	Temperate Forest	0.12	31.12	3.71	0.95	0.96
17044	Hutt River - at Boulcott	Temperate Forest	0.12	22.60	2.64	0.88	1.01
28529	Missouri River - Garrison Dam	Steppe	0.12	649.78	75.54	0.01	0.72
28011	Sacramento River - Freeport CA	Steppe	0.12	652.03	75.45	0.92	0.58

28517	Atchafalaya River - Melville	Tropical Seasonal Forest	0.11	3721.49	423.94	0.87	0.20
26014	Neva River	Boreal Forest	0.11	2462.53	278.38	0.81	1.85
75017	Guadalquivir River - at Penaflor	Chapparal	0.11	9.20	1.03	0.00	0.60
17045	Hutt River - at Kaitoke	Temperate Forest	0.11	8.16	0.90	0.83	0.10
17022	Waikato River - at Reids Farm	Temperate Forest	0.11	155.44	16.54	0.24	0.97
33003	Yarra River	Chapparal	0.10	1.48	0.15	0.91	0.04
28002	Columbia River - Warrendale OR	Temperate Forest	0.10	5023.97	512.74	0.89	1.14
65001	Tornionjoki River - Station 14100	Boreal Forest	0.10	298.09	29.81	0.04	0.94
135010	Weser River - at Intschede	Temperate Forest	0.10	299.17	29.75	0.93	0.76
135003	Rhine River - at Koblenz/Braubach	Temperate Forest	0.10	1761.73	172.80	0.61	0.99
28014	Apalachicola River - Chattahoochee FL	Tropical Seasonal Forest	0.10	611.12	59.52	0.95	1.39
37016	Grijalva River	Tropical Rain Forest	0.10	147.84	14.20	0.25	0.10
37001	Colorado River	Hot Desert	0.10	176.04	16.89	0.03	0.23
17037	Motu River - at Houpoto	Warm Temperate Forest	0.10	90.72	8.66	0.92	1.78
68003	Adige River - at Badia Polesine	Chapparal	0.09	208.18	19.58	0.94	0.41
68001	Adige River - at Ponte D'Adige	Temperate Forest	0.09	146.36	13.66	0.97	0.72
17026	Manganui River - at SH3	Temperate Forest	0.09	1.56	0.14	0.81	0.01
200002	Rhine River - at Rekingen	Temperate Forest	0.09	457.89	41.30	0.88	1.14
17052	Wairau River - at Tuamarina	Temperate Forest	0.09	117.23	10.11	0.95	1.75
17029	Rangitikei River - at Mangaweka	Temperate Forest	0.09	62.93	5.41	0.96	1.43
1002	Parana River - at Corrientes	Tropical Seasonal Forest	0.08	20457.06	1644.74	0.73	0.73
82001	Klang River	Tropical Rain Forest	0.08	22.87	1.82	0.60	0.15
80023	Chikugo River - at Senoshita	Temperate Forest	0.08	118.63	9.15	0.99	1.15
8003	Gudena River - Tvilum Bro	Temperate Forest	0.08	17.21	1.30	0.94	0.76
67002	Clare River - at Corofin Bridge	Temperate Forest	0.08	15.43	1.16	0.99	0.29
135001	Rhine River - at Maxau	Temperate Forest	0.07	1293.94	93.01	0.80	1.03
17002	Waikato River - at Mercer Bridge	Warm Temperate Forest	0.07	343.27	23.72	0.91	0.57
39003	St. Lawrence River - Montreal	Temperate Forest	0.07	8757.29	576.95	0.29	2.21
27004	Trent River - Nottingham	Temperate Forest	0.07	84.94	5.57	0.98	0.76
17028	Whanganui River - at Paetawa	Warm Temperate Forest	0.06	215.68	13.30	0.97	1.00
66002	Danube River - at Budapest	Temperate Forest	0.06	2274.42	127.38	0.93	0.85
135012	Danube River - at Jochenstein	Temperate Forest	0.06	1452.79	80.94	0.93	0.97
17018	Tarawere River - at Awakaponga	Temperate Forest	0.05	26.85	1.29	0.62	0.15
1004	Parana River - at Rosario	Chapparal	0.04	18350.70	817.33	0.58	0.59
39005	Slave River	Boreal Forest	0.04	3351.48	130.66	0.98	1.04
39002	Nelson River - Kettle Crossing	Boreal Forest	0.04	3017.45	117.12	0.01	0.65
28021	St. Lawrence River - Massena NY	Temperate Forest	0.04	7800.63	300.47	0.60	4.38
39009	Great Bear River	Boreal Forest	0.04	513.39	18.73	0.61	5.99
28018	St. Marys River - Lake Superior MI	Temperate Forest	0.03	2191.26	71.79	0.80	0.81
65013	Vuoksi River - at Mansikkakoski 2800	Boreal Forest	0.03	608.35	17.94	0.32	2.23
39020	Churchill River	Boreal Forest	0.02	683.28	16.44	0.26	0.46
28020	Niagara River - Lake Ontario	Temperate Forest	0.02	6187.57	143.01	0.49	1.66
		Min	0.02	0.75	0.14	0.00	0.01
		Max	1.65	170712.52	24975.15	0.99	9.89

APPENDIX VI

Comparison of observed and simulated temperature for each month for all GEMS stations with different climates.

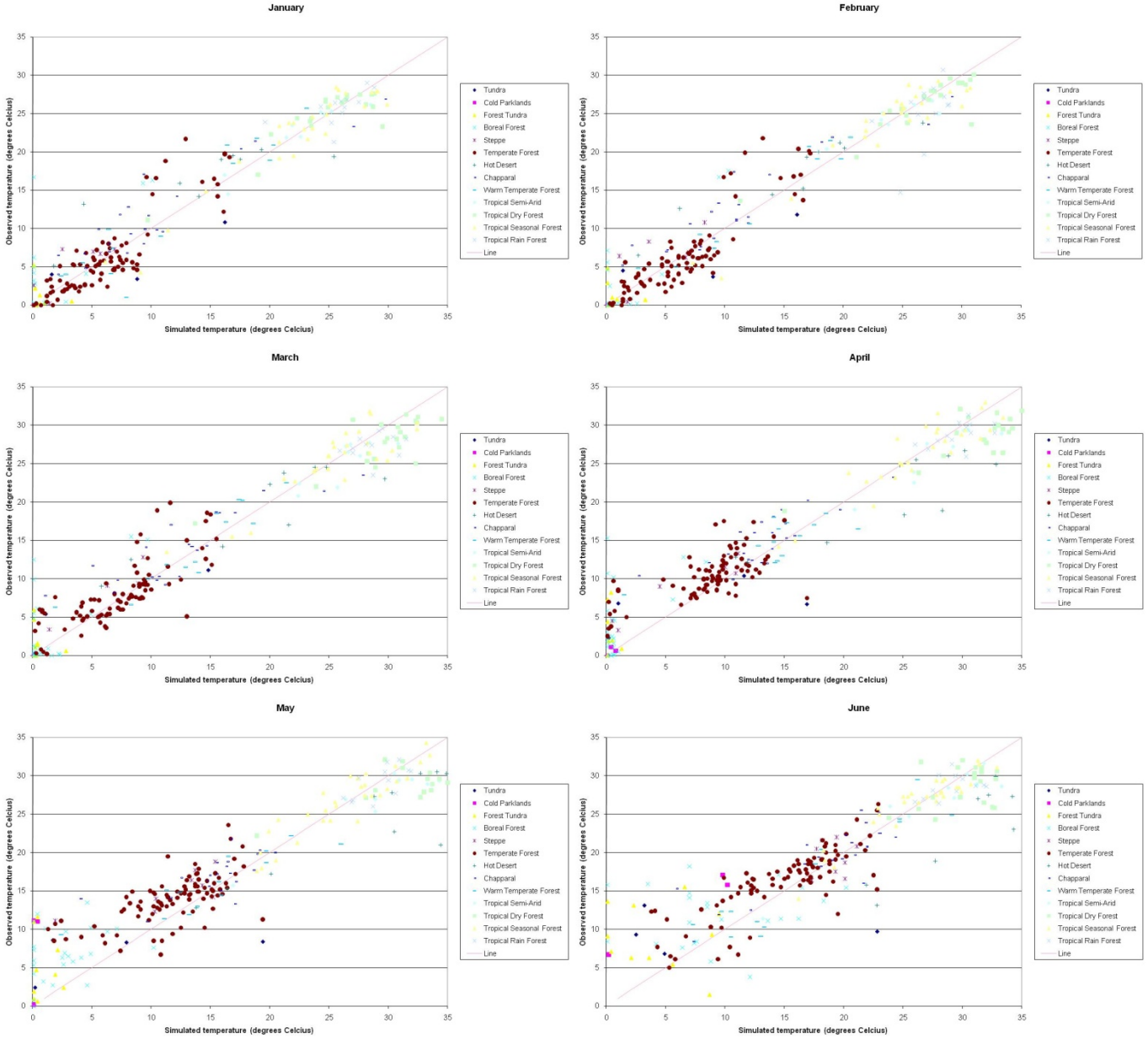

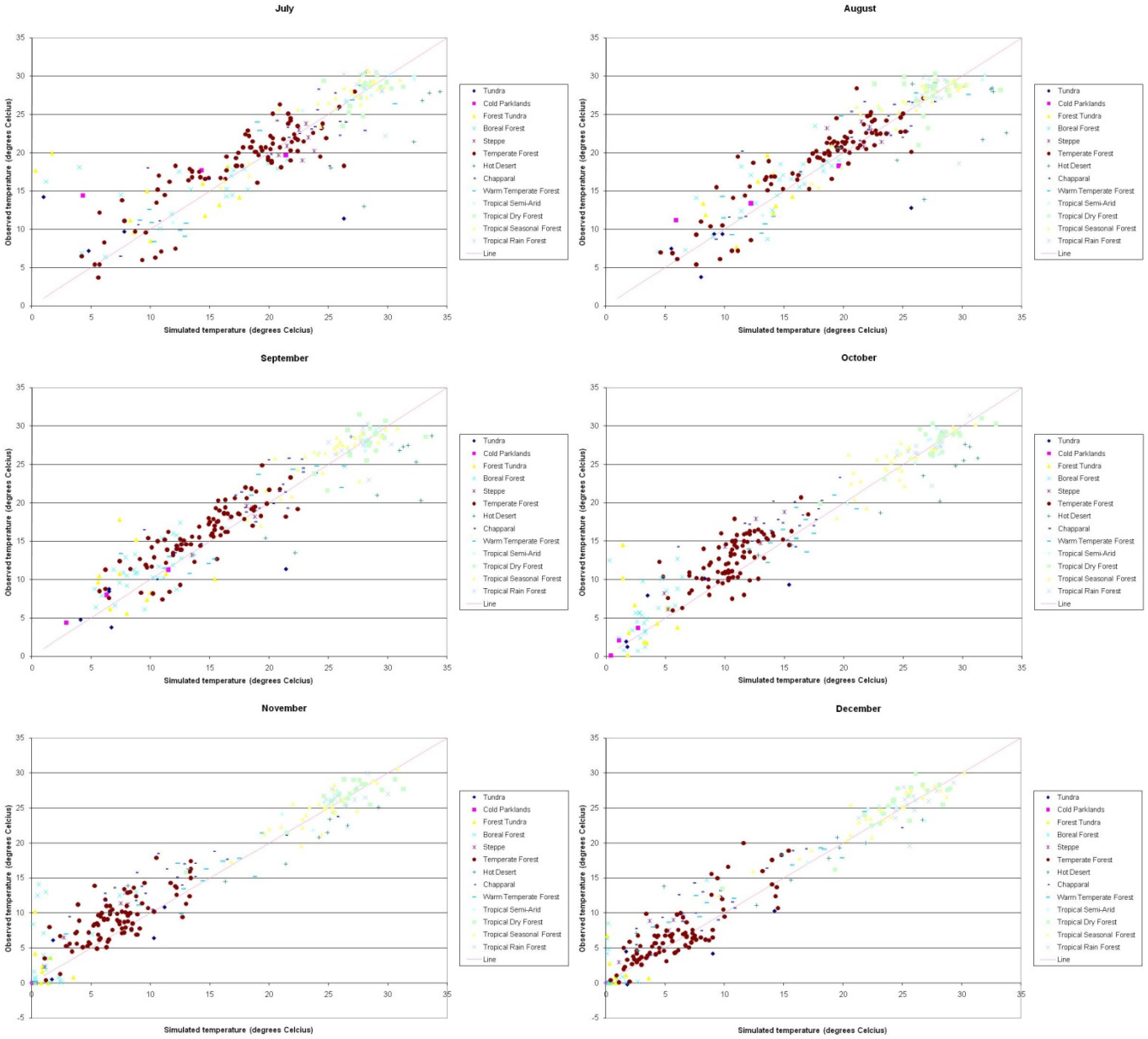
July
August
September
October
November
December
Observed temperature (degrees Celcius)
Simulated temperature (degrees Celcius)
Tundra
Cold Parklands
Forest Tundra
Boreal Forest
Steppe
Temperate Forest
Hot Desert
Chapparal
Warm Temperate Forest
Tropical Semi-Arid
Tropical Dry Forest
Tropical Seasonal Forest
Tropical Rain Forest
Line

APPENDIX VII

Comparison of observed and simulated discharge for each month for all GEMS stations with different climates.

January

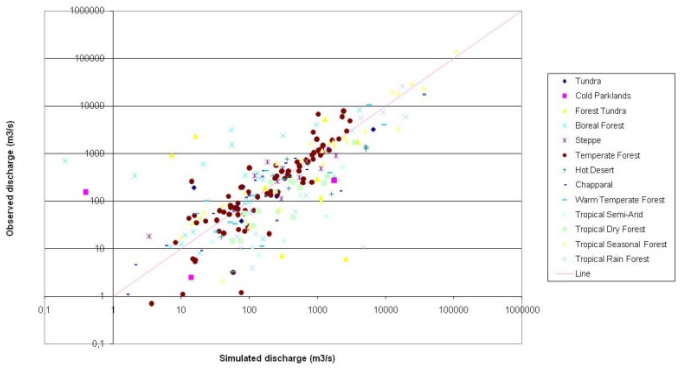

February

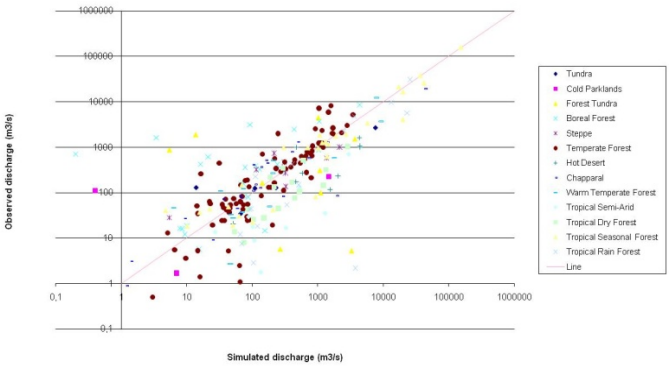

March

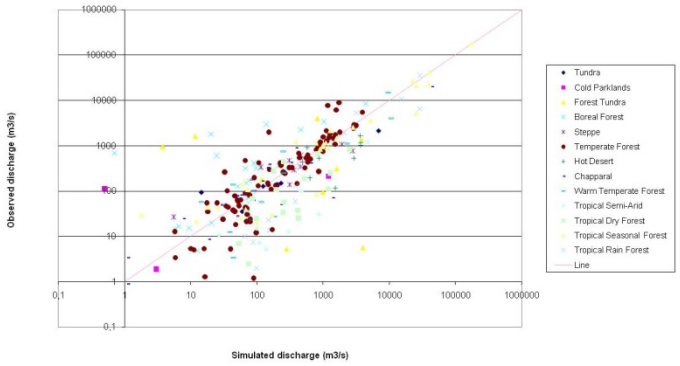

April

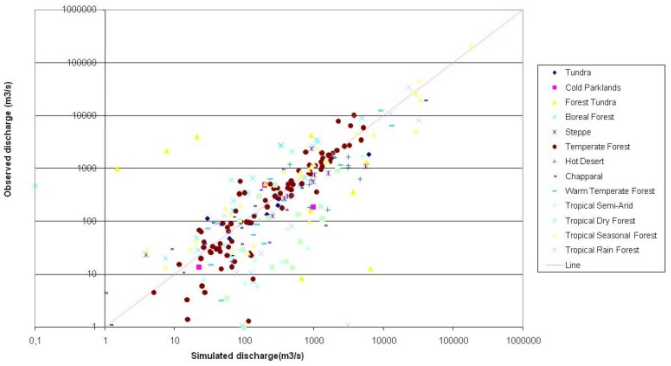

May

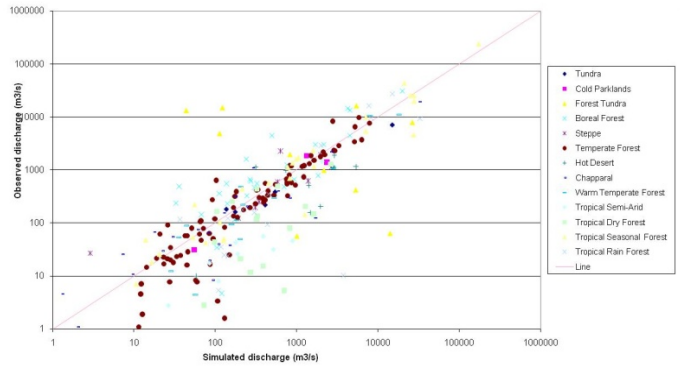

June

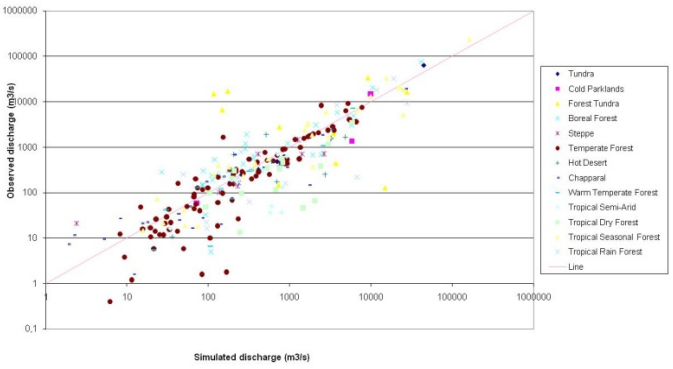

July

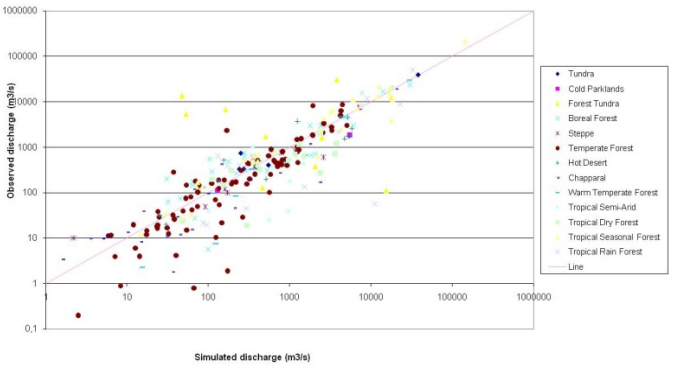

August

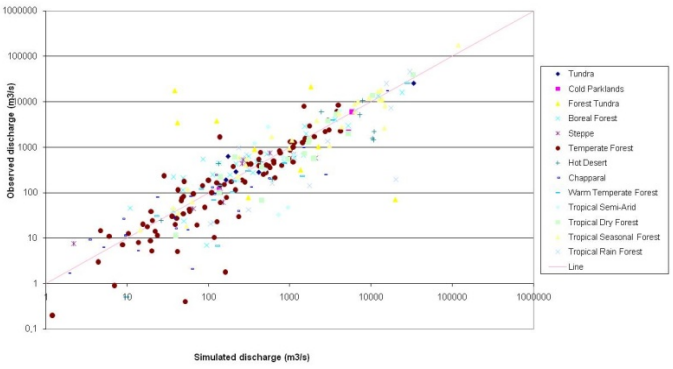

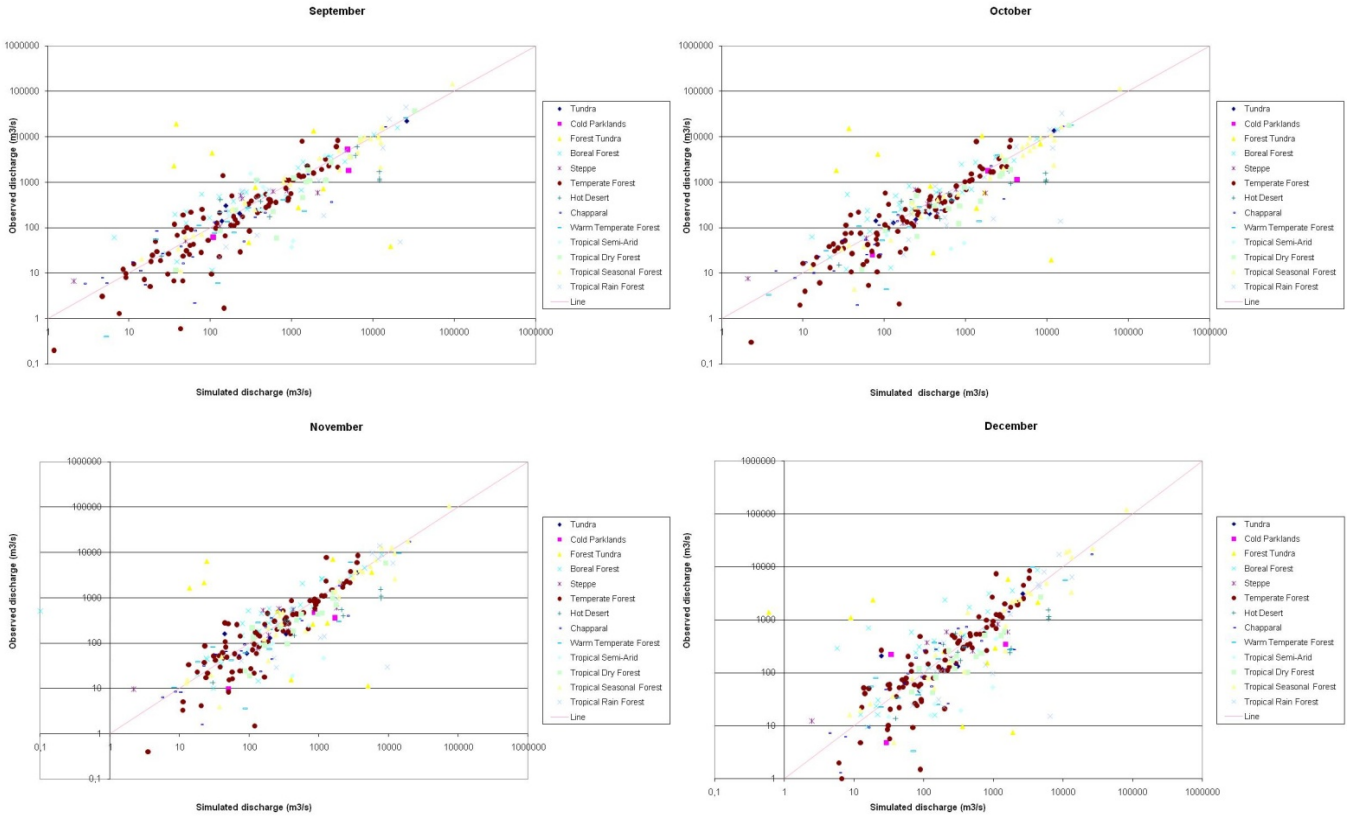
September
October
November
December
Observed discharge (m3/s)
Simulated discharge (m3/s)
Tundra
Cold Parklands
Forest Tundra
Boreal Forest
Steppe
Temperate Forest
Hot Desert
Chapparal
Warm Temperate Forest
Tropical Semi-Arid
Tropical Dry Forest
Tropical Seasonal Forest
Tropical Rain Forest
Line

APPENDIX VIII

ILEC lakes with transparency

ILEC ID	Lake Name	Lake Area (m^2)	Longitude	Latitude	Extinction coefficient	Transparency
I124	Lake Tahoe	499000000	-120.10	39.10	0.06	27.60
I89	Lake Hubsugul	2770000000	101.03	51.00	0.07	25.14
I150	Mashu-ko (Lake Mashu)	19100000	144.07	43.05	0.07	23.50
I178	Shikotsu-ko (Lake Shikotsu)	78800000	141.02	42.08	0.09	18.08
I213	Issyk-kool, lake	6236000000	77.02	42.08	0.11	16.00
I112	Lake Rara	9800000	82.02	29.03	0.11	15.55
I166	Ozero Baykal (Lake Baikal)	31500000000	106.07	53.07	0.11	15.00
I126	Lake Taupo	616000000	175.08	-38.08	0.11	15.33
I56	Lago Lacar (Lake Lacar)	55000000	-71.07	-40.02	0.13	12.97
I90	Lake Huron	59570000000	-82.03	44.07	0.13	13.00
I125	Lake Tanganyika	32000000000	30.02	-6.00	0.13	13.35
I192	Towada-ko (Lake Towada)	59000000	140.08	40.05	0.14	12.25
I193	Toya-ko (Lake Toya)	70400000	140.08	42.07	0.14	12.50
I132	Lake Vattern	1856000000	14.07	58.03	0.16	10.48
I181	Shuswap Lake	310000000	-119.02	51.00	0.16	10.61
I59	Lago Todos Los Santos	178500000	-72.02	-41.02	0.17	10.20
I147	Lunzer See	680000	15.02	47.08	0.17	10.00
I210	Great Central lake	51000000	-125.03	49.03	0.17	9.97
I57	Lago Maggiore (Lake Maggiore)	212500000	8.07	45.10	0.17	10.00
I163	Okanagan Lake	351000000	-119.05	49.08	0.18	9.68
I19	Chuzenji-ko (Lake Chuzenji)	12000000	139.03	36.07	0.18	9.60
I200	Western Brook Pond	22800000	-57.08	49.07	0.19	8.77
I6	Attersee	46000000	13.07	47.08	0.20	8.50
I130	Lake Uvildy	60600000	60.07	55.07	0.20	8.40
I186	Starnberger See	56000000	11.03	47.08	0.20	8.58
I9	Bodensee (Lake Constance)	539000000	9.03	47.07	0.20	8.58
I45	Kootenay Lake	389000000	-116.08	49.03	0.21	8.04
I140	Loch Morar	27000000	-5.07	56.10	0.21	7.98
I34	Inawashiro-ko (Lake Inawashiro)	104800000	140.02	37.05	0.21	8.09
I55	Lago d'Orta (Lake Orta)	18200000	8.03	45.08	0.21	8.00
I100	Lake Michigan	58016000000	-86.02	43.08	0.21	8.00
I121	Lake Stechlin	4300000	13.02	53.02	0.22	7.70
I58	Lago Titicaca (Lake Titicaca)	8372000000	-69.07	-15.07	0.23	7.36
I12	Buttle Lake	35300000	-125.05	49.08	0.23	7.29
I103	Lake Naroch	79600000	26.07	54.08	0.23	7.27
I33	Ikeda-ko (Lake Ikeda)	10950000	130.07	31.02	0.23	7.47
I41	Keuka Lake	47000000	-77.10	42.07	0.24	7.00
I91	Lake Inari	1050000000	27.75	69.00	0.26	6.43
I142	Loch Shiel	20000000	-5.07	56.08	0.26	6.55
I69	Lake Balkhash	18200000000	76.03	45.07	0.26	6.62
I80	Lake Druksiai	49000000	26.07	55.07	0.26	6.43
I8	Biwa-ko (Lake Biwa)	674000000	136.02	35.02	0.27	6.36
I203	Wood Lake	9300000	-119.03	50.10	0.28	6.02
I136	Lake Washington	87600000	-122.02	47.07	0.29	5.84
I26	Garrow Lake	4000000	-96.08	75.03	0.30	5.67
I149	Manicouagan Reservoir	1950000000	-68.07	50.07	0.30	5.70
I176	Saroma-ko (Lake Saroma)	150300000	143.07	44.03	0.30	5.63

I43	Kizaki-ko (Lake Kizaki)	1400000	137.08	36.05	0.31	5.56
I122	Lake Superior	82367000000	-88.03	47.05	0.31	5.40
I139	Loch Lomond	71000000	-4.07	56.00	0.31	5.48
I27	Hachiro-gata (Lake Hachirogata)	45600000	139.08	39.08	0.31	5.50
I28	Hamana-ko (Lake Hamana)	69000000	137.07	34.08	0.31	5.50
I98	Lake Memphremagog	102000000	-72.02	45.10	0.32	5.38
I92	Lake Kariba	5400000000	27.08	-17.03	0.32	5.28
I206	Zurichsee	65100000	8.07	47.03	0.33	5.10
I211	Hazen Lake	542000000	-70.00	81.08	0.34	5.00
I180	Shumarinai-ko (Lake Shumarinai)	23700000	142.02	44.03	0.34	5.00
I207	Bratskoye Reservoir	5478000000	102.02	54.07	0.34	5.00
I14	Canandaigua Lake	42300000	-77.03	42.08	0.34	5.00
I49	Lac Leman (Lake Of Geneva)	584000000	6.07	46.03	0.34	5.00
I155	Muskoka Lake	89400000	-79.03	45.00	0.35	4.90
I182	Skaha Lake	20100000	-119.07	49.03	0.36	4.70
I131	Lake Vanern	5648000000	13.02	58.08	0.36	4.73
I151	Massawippi Lake	17900000	-72.00	45.02	0.36	4.67
I66	Lake Ammersee	46600000	11.02	47.10	0.38	4.50
I158	Nojiri-ko (Lake Nojiri)	4556000	138.02	36.08	0.38	4.47
I116	Lake Simcoe	725000000	-79.03	44.03	0.39	4.40
I4	Amisk Lake	5200000	-112.07	54.07	0.40	4.29
I78	Lake Dillon	13350000	-106.10	39.07	0.41	4.15
I194	Twin Lakes	11200000	-106.03	39.10	0.41	4.17
I141	Loch Ness	56000000	-4.07	57.03	0.41	4.10
I77	Lake Diefenbaker	430000000	-107.03	51.00	0.41	4.15
I73	Lake Champlain	1130000000	-73.03	43.07	0.41	4.10
I106	Lake Ontario	19009000000	-78.00	43.07	0.41	4.10
I29	Harveys Lake	2660000	-76.10	41.03	0.42	4.09
I101	Lake Mjosa	365000000	11.02	60.08	0.43	4.00
I117	Lake Skadar	372300000	19.03	42.02	0.43	4.00
I199	Webster Lake	2500000	-71.07	43.05	0.43	3.94
I165	Oze-numa (Lake Oze)	1700000	139.03	36.10	0.44	3.87
I161	Ogochi-damu-ko (Okutama Reservoir)	4250000	139.02	35.08	0.44	3.83
I108	Lake Paanajarvi	23600000	30.02	66.03	0.45	3.75
I148	Manasbal Lake	2810000	74.07	34.03	0.47	3.64
I160	Ogawara-ko (Lake Ogawara)	62300000	141.03	40.08	0.47	3.62
I177	Seneca Lake	175400000	-76.08	42.08	0.47	3.60
I105	Lake Onego	9890000000	35.03	61.08	0.48	3.55
I152	Miquelon Lake	8720000	-112.08	53.03	0.48	3.51
I20	Conesus Lake	12900000	-77.07	42.08	0.48	3.53
I15	Caniapiscau Reservoir	2892500000	-69.03	54.03	0.49	3.50
I168	Pyramid Lake	453000000	-119.07	40.00	0.49	3.50
I3	Akan-ko (Lake Akan)	13000000	144.02	43.05	0.50	3.43
I195	Ust-Ilimskoye Reservoir	1920000000	102.07	57.02	0.50	3.40
I46	Krasnoyarskoye Reservoir	2000000000	91.07	54.08	0.51	3.31
I201	Williston Lake	1779000000	-123.07	56.00	0.51	3.33
I60	Lago Trasimeno (Lake Trasimeno)	124000000	12.02	43.02	0.52	3.27
I208	Lake Buhi	16500000	123.02	13.00	0.52	3.29
I138	Loch Awe	39000000	-5.02	56.03	0.53	3.20
I24	Estany de Banyoles (Lake Banyoles)	1120000	2.07	42.02	0.53	3.21
I94	Lake Ladoga	18135000000	31.03	60.08	0.54	3.12
I95	Lake Lukomskoje	36700000	29.02	54.07	0.54	3.18
I159	Northwood Lake	2600000	-71.03	43.02	0.54	3.12
I39	Kawaguchi-ko (Lake Kawaguchi)	5960000	138.07	35.05	0.57	2.98

I30	Hemlock Lake	7200000	-77.07	42.08	0.57	3.00
I31	Honeoye Lake	7050000	-77.05	42.08	0.57	3.00
I99	Lake Mendota	39400000	-89.03	43.10	0.57	3.00
I109	Lake Paijanne	1100000000	25.07	61.07	0.58	2.93
I111	Lake Pielinen	867000000	29.07	63.02	0.62	2.73
I198	Wabamun Lake	81800000	-114.07	53.07	0.63	2.70
I82	Lake Erie	25821000000	-81.10	41.07	0.65	2.62
I88	Lake Hjalmaren	478000000	15.07	59.02	0.65	2.61
I96	Lake Malaren	1140000000	17.02	59.05	0.65	2.61
I119	Lake Sniardwy	110000000	21.07	53.08	0.65	2.62
I1	Abashiri-ko (Lake Abashiri)	32500000	144.02	43.10	0.68	2.50
I79	Lake Driyviaty	36100000	27.02	55.07	0.68	2.50
I183	Smith Mountain Lake	80900000	-79.07	37.10	0.69	2.45
I145	Lough Ree (Lake Ree)	105000000	-7.08	53.05	0.71	2.39
I156	Nagase-damu-ko (Nagase Reservoir)	2000000	133.08	33.07	0.71	2.40
I81	Lake Edward	2325000000	29.07	0.08	0.71	2.40
I113	Lake Rotorua	79780000	176.02	-38.00	0.72	2.38
I162	Oguta Lake	2150000	6.07	5.07	0.74	2.30
I2	Aishihik Lake	146000000	-137.03	61.03	0.77	2.22
I35	Kamafusa damu-ko	3900000	140.07	39.02	0.78	2.19
I110	Lake Phewa	5000000	83.08	28.02	0.78	2.17
I17	Changshou-hu (Lake Changshou)	60000000	107.03	30.00	0.81	2.10
I7	Baptiste Lake	9810000	-113.07	54.08	0.83	2.06
I184	Sobradinho Reservoir	4220000000	-40.08	-9.05	0.83	2.05
I169	Qionghai-hu (Lake Qionghai)	31000000	102.03	27.08	0.84	2.02
I118	Lake Slapy	13000000	14.03	49.07	0.85	2.00
I164	Owasco Lake	26700000	-76.05	42.08	0.85	2.00
I42	Kezar Lake	1400000	-71.08	43.03	0.88	1.93
I189	Tasek Bera (Swamp Lake Tasek Bera)	61500000	102.07	3.00	0.88	1.94
I173	Sagami-ko (Sagami Reservoir)	3260000	139.02	35.07	0.89	1.90
I197	Volta Lake	8502000000	1.00	7.07	0.89	1.91
I47	La Grande 2 Reservoir	2485500000	-76.00	53.08	0.91	1.88
I153	Miyun Reservoir	188000000	117.02	40.07	0.92	1.85
I40	Kejimkujik Lake	26300000	-65.03	44.03	0.93	1.82
I97	Lake McIlwaine	26000000	30.08	-17.08	0.94	1.80
I170	Represa do Lobo (Broa Reservoir)	6800000	-47.08	-22.02	0.95	1.79
I51	Lago de Amatitilan	15200000	-90.07	14.05	0.97	1.75
I143	Lough Derg (Lake Derg)	118000000	-8.03	52.10	0.99	1.72
I71	Lake Burley Griffin	7100000	149.02	-35.03	1.00	1.70
I54	Lago de Valencia (Lake Valencia)	350000000	-67.07	10.02	1.00	1.70
I22	Dong-hu (Lake Dong)	27900000	114.03	30.05	1.01	1.69
I85	Lake G. Dimitrov	11000000	25.03	42.07	1.05	1.62
I134	Lake Volvi	67000000	23.03	40.07	1.06	1.60
I172	Reservoir Voronegskoe	70000000	39.02	54.07	1.10	1.55
I129	Lake Turkana	6750000000	36.02	3.05	1.13	1.50
I13	Cabora Bassa Reservoir	2739000000	31.07	-15.07	1.15	1.48
I114	Lake Saguling	53400000	107.03	-6.08	1.17	1.45
I174	San Roque Reservoir	16500000	-64.07	-31.03	1.21	1.40
I64	Laguna de Rocha	72000000	-54.02	-34.07	1.21	1.40
I67	Lake Ba Be	4500000	105.07	22.03	1.21	1.40
I11	Bung Boraphet (Boraped Reservoir)	106400000	100.02	15.08	1.27	1.34
I171	Reservoir Kujbyshevskoe	5900000000	49.07	54.08	1.30	1.30
I10	Buffalo Pound Lake	29500000	-105.02	50.03	1.31	1.30
I21	Dal Lake	21200000	75.07	34.03	1.37	1.24

I179	Shinji-ko (Lake Shinji)	80300000	132.08	35.05	1.40	1.22
I137	Lake Winnipeg	23750000000	-97.08	52.10	1.45	1.18
I187	Suwa-ko (Lake Suwa)	13300000	138.02	36.00	1.50	1.14
I144	Lough Neagh	385000000	-6.07	54.07	1.53	1.11
I175	Sancha-hu (Lake Sancha)	27300000	104.02	30.03	1.55	1.10
I133	Lake Victoria	68800000000	33.02	-1.07	1.60	1.06
I185	Southern Indian Lake	2391000000	-98.08	57.10	1.70	1.00
I5	Aswan High Dam Reservoir	6000000000	31.07	22.02	1.70	1.00
I135	Lake Vortsjarv	270700000	25.07	58.03	1.76	0.96
I214	Kyoga Lake	1720000000	33.02	1.07	1.89	0.90
I38	Kasumigaura (Lake Kasumigaura)	220000000	140.03	36.02	1.92	0.88
I84	Lake Fateh Sagar	4000000	73.07	24.05	2.63	0.65
I37	Kanhargaov Reservoir	6100000	78.07	22.00	2.65	0.64
I146	Lower Lake	1300000	77.03	23.03	2.66	0.64
I74	Lake Chervonoje	40000000	27.08	52.03	2.68	0.63
I52	Lago de Chapala (Lake Chapala)	1112000000	-103.10	20.02	2.83	0.60
I188	Tai-hu	2427800000	120.02	31.03	2.96	0.58
I120	Lake Songkhla	1082000000	100.03	7.05	3.19	0.53
I128	Lake Trummen	1000000	14.08	56.08	3.40	0.50
I191	Tjeukemeer	21000000	5.08	52.08	3.40	0.50
I44	Kojima-ko (Lake Kojima)	10880000	133.08	34.05	3.58	0.48
I68	Lake Balaton	593000000	17.07	46.08	3.61	0.47
I204	Xi-hu (The West Lake)	5600000	120.02	30.03	3.86	0.44
I72	Lake Chad	1540000000	14.02	13.03	4.25	0.40
I86	Lake George	250000000	30.02	0.00	4.25	0.40
I16	Cayuga Lake	172100000	-76.07	42.07	4.26	0.40
I75	Lake Chicot	17200000	-91.02	33.02	4.32	0.39
I53	Lago de Salto Grande (Lake Salto G	783000000	-57.07	-30.05	4.43	0.38
I63	Laguna de Bay (Lake Bay)	900000000	121.02	14.00	4.56	0.37
I87	Lake Guiers	227500000	-15.08	16.02	5.67	0.30
I93	Lake Kinneret (Sea of Galilee)	170000000	35.07	32.08	5.67	0.30
I70	Lake Balta Alba	10500000	27.03	45.03	5.70	0.30
I61	Lago Xolotlan (Lake Managua)	1016000000	-86.08	12.05	5.96	0.29
I205	Zeekoevlei	2560000	18.07	-34.00	6.56	0.26
I32	Ho-Tay (West Lake)	4130000	105.08	21.00	7.34	0.23
I23	Dongting-hu (Lake Dongting)	2740000000	112.03	29.03	8.24	0.21
I102	Lake Nakuru	40000000	36.02	-0.03	8.72	0.20
I196	Varna Lake	17000000	27.07	43.02	8.81	0.19
I18	Chao-hu (Lake Chao)	756200000	117.07	31.00	10.54	0.16
I62	Lago Ypacarai	59600000	-57.03	-25.03	18.38	0.09
I76	Lake Chilwa	1750000000	35.07	-15.03	24.29	0.07